

Durability and Mechanical Properties of Portland Cement
Concrete That Utilizes Crumb Rubber as an Alternative Fine
Aggregate

By
Andrew Olesen, B.Eng

Thesis
Presented to Lakehead University in Fulfilment of
the Thesis/Research Writing Requirements of
the Master of Science (Civil Engineering) Degree

Thunder Bay, ON, Canada
© Andrew Olesen, 2018

Abstract

This research project investigated in an intensive experimental program the influence of using crumb rubber in the mechanical properties and durability of Portland cement concrete mixtures. Crumb rubber is produced from waste tires which pose significant problems in the waste management sector. The incorporation of crumb rubber in some concrete infrastructure will help reduce the number of tires stockpiled annually.

Two rounds of batching and testing were undergone. One round occurred over the summer of 2017 and the other in the spring of 2018. The water cement ratio used in all mixes containing crumb rubber was 0.45. One mix with a water cement ratio of 0.4 was also prepared to give comparative values as to what would be obtained in a pavement structure designed meeting MTO criteria. Crumb rubber replaced a percent volume of the fine aggregate. Batches with crumb rubber substitution in amounts of 0 % to 25 %, in 5 % increments were prepared.

Each mix was tested for 28-day compressive strength, flexural strength, splitting tensile strength, bulk resistivity, surface resistivity, rapid chloride penetration and freeze-thaw testing (ASTMC39, ASTM C78, ASTM C496, ASTM C1202, ASTM C666, respectively). The 28-day compressive strength, flexural strength and splitting tensile strength were all observed to decrease with the increase in crumb rubber.

It was found that a 25 MPa 28 day compressive strengths are possible with crumb rubber replacing as much as 15% of the fine aggregate. The corresponding modulus of rupture of the mixture was 5.2 MPa compared to 5.9 MPa in a similar concrete mixture but without crumb rubber. The splitting tensile strength for the mixture containing 15 % of the fine aggregate crumb rubber was 2.9 MPa which is 90 % of the splitting tensile strength of a similar concrete mixture but with no rubber.

Bulk resistivity, and surface resistivity as a function of the rubber content and the effect of the freeze freeze-thaw durability all improved, however the improvement was not statistically significant. The bulk resistivity was found to be 6.0 kΩcm for the mixture with 15 % of the fine

aggregate crumb rubber and 5.9 kΩcm for the mixture containing no crumb rubber. Similarly, for surface resistivity the values were 17.4 kΩcm and 17.1 kΩcm for the 15 % and 0 % crumb rubber contents, respectively.

The rapid chloride penetration values did improve, but again not significantly. In fact, the classification according to ASTM C1202 did not change. All samples were of moderate penetrability.

For every 5 % increase in rubber as a portion of fine aggregate, it was found that the plastic air content increased 0.5 % above the measured mechanically entrapped air.

Durability factors were not able to be calculated from freeze-thaw tests due to low fundamental frequency readings before any cycles. However, a plot of the relative dynamic moduli shows that the introduction of crumb rubber did significantly improve the durability of the concrete mixture. After 300 cycles the relative dynamic moduli of the mix with a 0.4 water cement ratio and no crumb rubber was 483, whereas a mix with a 0.45 water cement ratio and 15 % crumb rubber had a relative dynamic modulus of 773.

I. Table of Contents

ABSTRACT	I
I. TABLE OF CONTENTS	III
II. TABLE OF FIGURES	VIII
III. TABLE OF TABLES	IX
IV. LIST OF SYMBOLS AND ABBREVIATIONS.....	XII
1. INTRODUCTION.....	1
1.1. Research Motivation	1
1.2. Overview.....	1
1.3. Hypothesis	1
1.4. Document layout	2
2. LITERATURE REVIEW	3
2.1. Background	3
2.2. Crumb Rubber	5
2.2.1. Tire Composition	5
2.2.2. Crumb Rubber Manufacture	6
2.3. Mechanical and other Intrinsic Properties of Concrete that Contains Crumb Rubber	8
2.3.1. Compressive Strength.....	8
2.3.2. Flexural Strength	10
2.3.3. Tensile Strength.....	11
2.3.4. Noise Damping and Resistance to Dynamic Loading.....	13
2.3.5. Toughness.....	14

2.3.6.	Electrical Conductivity	15
2.3.7.	Air Entrainment	16
2.3.8.	Durability	17
3.	RESEARCH OBJECTIVES AND METHODOLOGY	20
4.	MATERIALS	22
4.1.	Coarse Aggregate	23
4.2.	Fine Aggregate	26
4.3.	Crumb Rubber	29
4.4.	Portland Cement	35
5.	MIX DESIGN	36
6.	PROCEDURES	40
6.1.	Mixing	40
6.2.	Casting and Curing	42
6.3.	Electrical Resistivity (Bulk and Surface)	43
6.4.	Rapid Chloride Penetration Test.....	45
6.5.	Compressive Strength	47
6.6.	Flexural Strength.....	48
6.7.	Splitting Tensile Strength	49
6.8.	Freeze-Thaw Test	50
7.	RESULTS.....	52
7.1	Compressive Strength	52

7.2. Splitting Tensile Strength	54
7.3. Flexural Strength.....	57
7.4. Bulk Resistivity.....	59
7.5. Surface Resistivity	60
7.6. Rapid Chloride Penetration	62
7.7. Air Entrainment	62
7.8. Freeze Thaw.....	64
8. DISCUSSION	65
8.1. Compressive Strength	65
8.2. Splitting Tensile Strength	66
8.3. Flexural Strength.....	66
8.4. Bulk Resistivity and Surface Resistivity	67
8.5. Rapid Chloride Penetration	67
8.6. Air Entrainment	67
8.7. Freeze-Thaw.....	67
9. CONCLUSION	69
10. RECOMMENDATIONS FOR FUTURE STUDY	71
11. ACKNOWLEDGEMENTS.....	72
12. REFERENCES	73
APPENDIX A. DATA RELATING TO AGGREGATE PROPERTIES	78

12.3.	Coarse Aggregate Sieve Analyses and Bulk Density Calculation	79
12.4.	Fine Aggregate Gradations and Fineness Modulus Calculations	83
12.5.	Crumb Rubber Gradings and Relative Density Data.....	86
APPENDIX B. MIX DESIGNS.....		89
APPENDIX C. LAB RESULT DATA SHEETS.....		94
12.6.	MTO Comparison Mix	94
12.7.	0.45WCM00AE00CR	95
12.8.	0.45WCM00AE05CR	96
12.9.	0.45WCM00AE10CR	97
12.10.	0.45WCM00AE15CR.....	98
12.11.	0.45WCM00AE20CR.....	99
12.12.	0.45WCM00AE25CR.....	100
12.13.	CM1 Repeat.....	101
12.14.	0.45WCM00AE00CR Repeat.....	102
12.15.	0.45WCM00AE05CR Repeat.....	103
12.16.	0.45WCM00AE10CR Repeat.....	104
12.17.	0.45WCM00AE15CR Repeat.....	105
12.18.	0.45WCM00AE20CR Repeat.....	106
12.19.	0.45WCM00AE25CR Repeat.....	107
APPENDIX D. RAPID CHLORIDE PENETRATION RESULTS		108

APPENDIX E. FREEZE THAW DATA.....	122
APPENDIX F. COMPUTER CODES.....	126
12.20. RCP Data Logger	126
12.21. MATLAB Fundamental Frequency Calculator	129

II. Table of Figures

FIGURE 2-2-1 TIRE FIBRES [24].....	6
FIGURE 2-2 TYPICAL AMBIENT GRINDING SYSTEM, ADAPTED FROM [22]	7
FIGURE 2-3 TYPICAL CRYOGENIC GRINDING SYSTEM, ADAPTED FROM [22]	7
FIGURE 2-4 MAGNIFIED IMAGES OF CRUMB RUBBER PARTICLES (SCALE: 1 UNIT=0.50 MM) [21].....	8
FIGURE 2-5 MICROSTRUCTURE OF CONCRETE WITH RUBBER; (A) CEMENT MATRIX WITH RUBBER PARTICLE; (B) INTERFACE RUBBER/CONCRETE (SEM) [27]	9
FIGURE 2-6 COMPRESSIVE STRENGTH V. RUBBER CONTENT FOR 3 DIFFERENT TYPES OF RUBBER AS ADAPTED FROM [29]	10
FIGURE 2-7 FLEXURAL STRENGTH V. TOTAL RUBBER CONTENT FOR 3 DIFFERENT TYPES OF RUBBER [29]	11
FIGURE 2-8 STRESSES ASSOCIATED WITH A SPLITTING TENSILE TEST [16]	12
FIGURE 2-9 SPLITTING TENSILE STRENGTH V. CRUMB RUBBER REPLACEMENT OF FINE AGGREGATE VOLUME ADAPTED FROM ELDIN AND SENOUCCI [30]	13
FIGURE 2-10 LOAD DISPLACEMENT CURVES FOR ORDINARY CONCRETE AND RUBBERIZED CONCRETE [24]	15
FIGURE 4-1 COARSE AGGREGATE GRADATION	25
FIGURE 4-2 FINE AGGREGATE AVERAGE GRADING	28
FIGURE 4-3 CRUMB RUBBER GRADING CURVE 10-20 SIZE.....	30
FIGURE 4-4 CRUMB RUBBER GRADING CURVE 30- SIZE.....	30
FIGURE 4-5 COMBINED GRADING OF TWO CRUMB RUBBER SIZES BASED ON LABORATORY RESULTS	33
FIGURE 4-6 FINE AGGREGATE AND COMBINED RUBBER GRADING CURVES	34
FIGURE 6-1 CONCRETE MIXER SOURCE: PRIMARY	41
FIGURE 6-6-2 AIR METER, SOURCE: PRIMARY	42
FIGURE 6-3 RCP EXCEL SHEET, SOURCE: PRIMARY	47
FIGURE 6-6-4 SPLITTING TENSILE JIG, SOURCE: PRIMARY.....	49
FIGURE 6-5 EXAMPLE FREQUENCY PLOT, SOURCE: PRIMARY.....	51
FIGURE 7-1 CRUMB RUBBER V. 28 DAY COMPRESSIVE STRENGTH.....	54
FIGURE 7-2 SPLITTING TENSILE STRENGTH V. CRUMB RUBBER	56
FIGURE 7-3 MODULUS OF RUPTURE V. CRUMB RUBBER.....	58
FIGURE 7-4 BULK RESISTIVITY V. CRUMB RUBBER	60
FIGURE 7-5 SURFACE RESISTIVITY V. CRUMB RUBBER	61
FIGURE 7-6 RCP TEST RESULTS V. CRUMB RUBBER.....	62
FIGURE 7-7 AIR CONTENT V. CRUMB RUBBER.....	63
FIGURE 7-8 RELATIVE DYNAMIC MODULI V. FREEZE THAW CYCLES	64
FIGURE 8-1 FAILED COMPRESSIVE STRENGTH SPECIMEN, SOURCE: PRIMARY	66

FIGURE 8-2 SAMPLE CONTAINING 0 % OF THE FINE AGGREGATE AS CRUMB RUBBER AFTER 300 CYCLES OF FREEZE THAW	68
FIGURE 8-3 SAMPLE CONTAINING 15 % OF THE FINE AGGREGATE AS CRUMB RUBBER AFTER 300 CYCLES OF FREEZE/THAW	68
FIGURE 12-1 COARSE AGGREGATE GRADATION TRIAL 1	79
FIGURE 12-2 COARSE AGGREGATE GRADATION TRIAL 2	80
FIGURE 12-3 COARSE AGGREGATE GRADATION TRIAL 3	81
FIGURE 12-4 FINE AGGREGATE GRADING TRIAL 1	83
FIGURE 12-5 FINE AGGREGATE GRADING TRIAL 2	84
FIGURE 12-6 FINE AGGREGATE GRADATION TRIAL 3	85
FIGURE 12-7 0.40WCM5.7AE00CR SAMPLE 4 RCP RESULT	108
FIGURE 12-8 0.40WCM5.7AE00CR SAMPLE 5 RCP RESULT	109
FIGURE 12-9 0.45WCM00AE00CR SAMPLE 4 RCP RESULT	110
FIGURE 12-10 0.45WCM00AE00CR SAMPLE 5 RCP RESULT	111
FIGURE 12-11 0.45WCM00AE05CR SAMPLE 4 RCP RESULT	112
FIGURE 12-12 0.45WCM00AE05CR SAMPLE 5 RCP RESULT	113
FIGURE 12-13 0.45WCM00AE10CR SAMPLE 4 RCP RESULT	114
FIGURE 12-14 0.45WCM00AE10CR SAMPLE 5 RCP RESULT	115
FIGURE 12-15 0.45WCM00AE15CR SAMPLE 4 RCP RESULT	116
FIGURE 12-16 0.45WCM00AE15CR SAMPLE 5 RCP RESULT	117
FIGURE 12-17 0.45WCM00AE20CR SAMPLE 4 RCP RESULT	118
FIGURE 12-18 0.45WCM00AE20CR RCP RESULT	119
FIGURE 12-19 0.45WCM00AE25CR RCP RESULT	120
FIGURE 12-20 0.45WCM00AE25CR SAMPLE 5 RCP RESULT	121

III. Table of Tables

TABLE 2-1 PROPERTIES OF CRUMB RUBBER CONCRETE	5
TABLE 4-1 COARSE AGGREGATE PROPERTIES	24
TABLE 4-2 CSA GRADING LIMITS FOR COARSE AGGREGATES USED IN OPC [36]	26
TABLE 4-3 AVERAGE GRADING AND USCS CLASSIFICATION CRITERIA	26
TABLE 4-4 FINE AGGREGATE PROPERTIES	27
TABLE 4-5 FINE AGGREGATE AVERAGE GRADING	29
TABLE 4-6 CSA GRADATION LIMITS FOR FINE AGGREGATES.....	29
TABLE 4-7 COMBINED GRADING OF 10-20 AND 30- CRUMB RUBBER FROM MANUFACTURERS DATA	31

TABLE 4-8 COMBINED GRADING OF 10-20 AND 30- CRUMB RUBBER FROM MANUFACTURERS DATA CONT'D	31
TABLE 4-9 COMBINED CRUMB RUBBER GRADING FROM LABORATORY SIEVING	32
TABLE 4-10 COMBINED CRUMB RUBBER GRADING FROM LABORATORY SIEVING CONT'D	32
TABLE 4-11 PORTLAND CEMENT COMPOSITION	35
TABLE 5-1 SAMPLE MIX DESIGN	37
TABLE 5-2 MIX DESIGN FORMULAE	38
TABLE 7-1 COMPRESSIVE STRENGTH RESULT.....	52
TABLE 7-2 COMPRESSIVE STRENGTH RESULTS FOR REPEATED MIXES.....	53
TABLE 7-3 SRF MODEL PARAMETERS FOR COMPRESSIVE STRENGTH.....	53
TABLE 7-4 SPLITTING TENSILE STRENGTH RESULTS.....	55
TABLE 7-5 SPLITTING TENSILE STRENGTH RESULTS FOR REPEATED MIXES.....	55
TABLE 7-6 SRF MODEL PARAMETERS FOR SPLITTING TENSILE STRENGTH	56
TABLE 7-7 FLEXURAL STRENGTH RESULTS.....	57
TABLE 7-8 FLEXURAL STRENGTH RESULTS FOR REPEATED TESTS	57
TABLE 7-9 SRF MODEL PARAMETERS FOR FLEXURAL STRENGTH.....	57
TABLE 7-10 ALPHA FACTOR IN ACI MODULUS OF RUPTURE EQUATION.....	58
TABLE 7-11 BULK RESISTIVITY RESULTS	59
TABLE 7-12 BULK RESISTIVITY RESULTS FOR REPEATED MIXES	59
TABLE 7-13 SURFACE RESISTIVITY RESULTS.....	61
TABLE 7-14 SURFACE RESISTIVITY RESULTS FOR REPEATED MIXES.....	61
TABLE 7-15 AIR CONTENT RESULTS	62
TABLE 7-16 AIR CONTENT RESULTS FOR REPEATED MIXES	62
TABLE 12-1 COARSE AGGREGATE GRADATION TRIAL 1	79
TABLE 12-2 COARSE AGGREGATE GRADATION TRIAL 2	80
TABLE 12-3 COARSE AGGREGATE GRADATION TRIAL 3	81
TABLE 12-4 BULK DENSITY OF COARSE AGGREGATE CALCULATION	82
TABLE 12-5 FINE AGGREGATE GRADATION TRIAL 1 DATA	83
TABLE 12-6 FINE AGGREGATE GRADATION TRIAL 2 DATA	84
TABLE 12-7 FINE AGGREGATE GRADATION TRIAL 3 DATA	85
TABLE 12-8 MANUFACTURER GRADING OF CRUMB RUBBER #6-#10 MESH.....	86
TABLE 12-9 MANUFACTURER GRADING OF CRUMB RUBBER #10-#20 MESH.....	86
TABLE 12-10 MANUFACTURER GRADING OF CRUMB RUBBER NOR 20 SIZE	86
TABLE 12-11 MANUFACTURER GRADING OF CRUMB RUBBER #30- MESH.....	87
TABLE 12-12 RELATIVE DENSITY OF CRUMB RUBBER TRIAL 1.....	87
TABLE 12-13 RELATIVE DENSITY OF CRUMB RUBBER TRIAL 2.....	87

TABLE 12-14 RELATIVE DENSITY OF CRUMB RUBBER TRIAL 3.....	88
TABLE 12-15 RELATIVE DENSITY OF CRUMB RUBBER TRIAL 4.....	88
TABLE 12-16 CONTROL MIX 1 0.4WCM3.5AE00CR 85 L MIX DESIGN	89
TABLE 12-17 0.45WCM00AE00CR 85 L MIX DESIGN	89
TABLE 12-18 0.45WCM00AE20CR 85 L MIX DESIGN	89
TABLE 12-19 0.40WCM00AR15CR 85 L MIX DESIGN	90
TABLE 12-20 0.45WCM00AE15CR 85 L MIX DESIGN	90
TABLE 12-21 0.45WCM00AE10CR 85L MIX DESIGN	90
TABLE 12-22 0.45WCM00AE25CR	90
TABLE 12-23 0.45WCM00AE05CR 85 L MIX DESIGN	91
TABLE 12-24 CM1R 0.40WCM00AE00CR 55 L MIX DESIGN.....	91
TABLE 12-25 R-0.45WCM00AE00CR 46 L MIX	91
TABLE 12-26 R-0.45WCM00AE05CR 51 L MIX DESIGN	92
TABLE 12-27 R-45WCM00AE10CR 51 L MIX DESIGN	92
TABLE 12-28 R-0.45WCM00AE15CR 33 L MIX DESIGN	92
TABLE 12-29 R- 0.45WCM00AE20CR 96 L MIX DESIGN	92
TABLE 12-30 R-0.45WCM00AE25CR 46 L MIX DESIGN	93
TABLE 12-31 0.40WCM5.7AE00CR SAMPLE 4 RCP TABLE	108
TABLE 12-32 0.40WCM5.7AE00CR SAMPLE 5 RCP TABLE	109
TABLE 12-33 0.45WCM00AE00CR SAMPLE 4 RCP TABLE	110
TABLE 12-34 0.45WCM00AE00CR SAMPLE 5 RCP TABLE	111
TABLE 12-35 0.45WCM00AE05CR SAMPLE 4 RCP TABLE	112
TABLE 12-36 0.45WCM00AE05CR SAMPLE 5 RCP TABLE	113
TABLE 12-37 0.45WCM00AE10CR SAMPLE 4 RCP TABLE	114
TABLE 12-38 0.45WCM00AE10CR SAMPLE 5 RCP TABLE	115
TABLE 12-39 0.45WCM00AE15CR SAMPLE 4 RCP RESULT	116
TABLE 12-40 0.45WCM00AE15CR SAMPLE 5 RCP RESULT	117
TABLE 12-41 0.45WCM00AE20CR SAMPLE 4 RCP TABLE	118
TABLE 12-42 0.45WCM00AE20CR RCP TABLE	119
TABLE 12-43 0.45WCM00AE25CR RCP TABLE	120
TABLE 12-44 0.45WCM00AE25CR SAMPLE 5 RCP TABLE	121
TABLE 12-45 COMPREHENSIVE FREEZE THAW DATA	122

IV. List of Symbols and Abbreviations

- a: SRF model parameter
- AAR: Alkali aggregate reactivity
- ACI: American Concrete Institute
- ACR: Alkali carbonate reactivity
- AE: Air entrainment
- ASR: Alkali silicate reactivity
- ASTM: American society for testing and materials
- b: SRF model parameter
- BR: Bulk resistivity
- c: Number of freeze thaw cycles a test corresponds to
- CA: Coarse aggregate
- C_c : Coefficient of curvature
- CO₂: Carbon dioxide
- CR: Crumb rubber
- CSA: Canadian standards association
- CSH: Calcium silicate hydrate
- C_u : Coefficient of Uniformity
- D: Diameter of a specimen
- d: Depth of a specimen
- DAQ: Data acquisition system
- DF: Durability factor
- E: Elastic Modulus
- FA: Fine Aggregate
- f'_c : 28-day compressive strength
- f_{cm} : Compressive strength of a given sample
- fft: Fast Fourier transform
- f_n : Fundamental frequency
- f'_r : Modulus of rupture
- hrs: Hours

Hz: Unit of frequency, one cycle per second
I: Moment of inertia
kg: Kilograms
L: Span of beam in 3rd point load test
l: Length of a sample
m: metres, SRF model parameter
M: Number of cycles at which freeze thaw test is to be terminated
m³: Cubic metres
MC: Moisture Content
mm: millimetres
MPa: Megapascals
MTO: Ministry of Transportation, Ontario
n: Fundamental frequency before freezing
n_f: Fundamental frequency after l cycles of freezing and thawing
OD: Oven dry
OPC: Ordinary Portland Cement concrete
P_c: Relative dynamic modulus of elasticity
P_{max}: Maximum load on a sample
R: Rubber content as a decimal in SRF Model, as a prefix signals a repeated mix
RCP: Rapid Chloride Penetration
RD: Relative Density
s: Sample number
SCPI: Standard commands for programmable instruments
SEM: Scanning electron microscope
SRF: Strength reduction factor
SSD: Saturated surface dry
SSW: Saturated surface wet
T: Splitting tensile strength
USCS: United soils classification system
VOC: Volatile organic compounds

WCM: Water to cementing materials ratio

α : Factor to relate modulus of rupture to the square root of 28-day compressive strength

k Ω cm: Unit of resistivity, Kilo-ohm centimetres

ν : Poisson's ratio

1. Introduction

1.1. Research Motivation

Discarded tires have been a problem in the waste management sector for several decades. Tires are often stockpiled outside of landfills, posing a fire hazard, threatening surface and ground water quality and making ideal mosquito breeders. This has prompted researchers to investigate alternative uses for discarded tires. One promising application is in the use of waste tires as a concrete aggregate. All the main components of a tire can be incorporated into a concrete mixture, including the rubber, the steel wires and the textile weave.

1.2. Overview

A study was carried out at Lakehead University to investigate the mechanical and durability effects of incorporating reclaimed tire rubber in a Portland cement concrete mixture. This study focused solely on the use of crumb rubber as previous research efforts had found coarse rubber particles were too detrimental to the mechanical properties of a concrete mixture [1]. ASTM testing methods were used and followed for the following parameters:

- Compressive Strength
- Flexural Strength
- Splitting Tensile Strength
- Rapid Chloride Penetration
- Freeze/Thaw Durability
- Air Entrainment

Bulk resistivity and surface resistivity were also tested, but ASTM standards did not exist for these tests at the time of the study.

1.3. Hypothesis

The following hypotheses were made prior to the study:

1. The compressive strength will decrease with the addition of a rubber phase to a Portland cement concrete mixture, this will be due to the low compressive strength of the rubber itself. Weak interface bonds between the cement paste and rubber particles are also suspected to play a role in the reduction of compressive strength.

2. The air content of a concrete mixture containing rubber particles will increase, this will be due to the hydrophobic nature of rubber causing repulsion forces between the rubber and the cement paste, mainly the hydrates in the calcium silicate hydrate (CSH) gel.
3. The freeze/thaw durability will increase due to the increased air entrainment.

1.4. Document layout

The subsequent literature review chapter of this document gives detailed motivation for this research topic. It also provides specific details on tire composition and crumb rubber manufacture. Finally, the current state of research and theory of the influence of a rubber phase on a concrete mixture is discussed.

The research objectives and methodology chapter describes how results from the tests were interpreted to confirm or dismiss the preceding hypotheses. Afterwards, the materials chapter describes the properties of the aggregates and crumb rubber that was used in the testing for future researchers to compare to. Also, it describes the alpha-numeric code that was used to differentiate between different mixes within the testing regime.

The mix design chapter presents the absolute volume method of mix proportioning that was used to prepare the various batches of concrete. Spreadsheets with equations are also included to aid in any future research. The procedures chapter explains all the ASTM tests that were performed in details with any significant deviations from the standards noted.

The results chapter gives a quick overview of the results that were found in the testing program. This chapter is separate from the discussion chapter for convenience to the reader, the intent is to save the reader the tedious task of looking up values in the associated appendices. The discussion chapter then takes all of the results and compares them against the above hypotheses.

In the conclusion chapter, a summary of the results is given along with recommendations for the implementation of crumb rubber as an alternative aggregate. The recommendations for future research highlights current gaps in the body of knowledge available to the academy and what should be confirmed in this study by third party laboratories.

2. Literature Review

2.1. Background

Concrete is the most used construction material worldwide and as such, has a large ecological footprint. This includes the total greenhouse gas emissions from the harvesting of raw materials to placement of the finished product, diminishing aggregate resources, and solid waste streams. The greenhouse gas emissions are mostly from the production of Portland Cement (about one tonne of CO₂ is emitted for every tonne of Portland Cement produced) [2]. Global population growth, 83 million annually, is resulting in a larger demand for infrastructure and consequently concrete. Since the materials used in concrete are non-renewable, the world's aggregate and mineral supplies will only be exploited further to keep up with demand. For example, "...approximately 109 million tonnes of construction and demolition residues are generated in the UK; around 60 million tonnes of this is derived from concrete." [3]. Similar numbers on a per capita basis are reported for other countries in the literature.

The Portland Cement industry is taking large strides towards reducing its carbon footprint through the burning of alternate fuels, carbon capture and storage technologies, and using alternate raw materials. The concrete industry is also readily looking for ways to reduce the amount of Portland Cement in concrete mixtures by using supplementary cementing materials in partial replacement of the cement [2, 4-7]. A detailed literature review of alternative fuels and supplementary cementing materials is beyond the scope of this work.

Demand for concrete is increasing, and with it so does the demand for virgin aggregate. To alleviate this problem many alternate aggregates are being extensively studied to evaluate their potential to substitute raw materials. Some of these are crushed glass, shredded bottles and other plastics, recycled concrete and rubber from tires. Each alternate aggregate comes with its own challenges when introducing the new aggregate to the mix design, as well as a lack of industry confidence. The focus of this literature review will be on the use of rubber from tires as an alternate aggregate [2-4,6,8-11].

Each year approximately 300 hundred million scrap tires are stock piled in the United States, along with other developed nations that report similar numbers per capita [12]. These tires can't

be buried and landfilled due to the risk of contaminating the groundwater. To make matters worse, these stockpiles collect rain water and organic matter making them ideal mosquito breeders. It has been found that the primary carrier of West Nile virus, the northern house mosquito, is the most common larvae found in scrap tires [12]. The stockpiles can also catch fire, which in turn releases harmful volatile organics (VOC's) in to the atmosphere. One such fire happened in Hagersville Ontario in February of 1990, 4,000 residents were evacuated from their homes while the fire raged for 17 days [13].

A proposed solution to both the problem of stock piled scrap tires and the over utilization of virgin aggregates is to use the waste tires as concrete aggregate. This idea is not new but has gained recent popularity with new research on the topic that has been regularly published in the last few years. The mechanical and intrinsic properties of a concrete containing non-mineral aggregates will be different than that of one containing pure mineral aggregates [14]. Details on how these properties change in correspondence to the volumetric content of the rubber and the size of the rubber particles used are provided in the subsequent section. Table 2-1 summarizes how each property changes with respect to the addition of rubber. Rubberized concrete may not be ideal for all concrete structures, but there are many structures that would benefit from the modified properties of a concrete containing rubber particles.

Table 2-1 Properties of Crumb Rubber Concrete

Mechanical or Intrinsic Property	Rubberized particles effect on the property
Compressive Strength	Decreases [15]
Flexural Strength	Decreases [15]
Damping	Improves [16]
Abrasion Resistance	Improves [17]
Toughness	Improves [18]
Electrical Conductivity	Less conductive [19]
Durability	Improves [20]
Air Entrainment	Improves [21]

2.2. Crumb Rubber

2.2.1. Tire Composition

“A tire is a composite of complex elastomer formulations, fibers and steel/fiber cord. Tires are made of plies of reinforcing cords extending transversely from bead to bead, on top of which is a belt located below the tread [8]”. The typical materials used in manufacturing a tire are synthetic and natural rubber, sulfuric compounds, phenolic resins, oils (aromatic, naphthenic, and paraffinic), polyester, nylon, petroleum waxes, pigments carbon black, other inert materials and steel wires [8].

According to the Recycling Research Institute, a typical scrap tire contains (by weight): 70 % recoverable rubber, 15 % steel, 3 % fibre and 12 % extraneous inert materials [22]. Before a scrap tire is used as an aggregate, it is processed in to an appropriate sizes. The smaller sizes fit into four categories; tire shreds, tire chips, tire fibres¹ and crumb rubber. Tire shreds are generally 50-305 mm in size and have basic geometric shapes, and tire chips are 12-50 mm and with most of the wire removed [23]. Tire fibres are typically smaller than chips in two dimensions but longer in one dimension. A picture of tire fibres is shown in Figure 2-2-1. Crumb rubber is granulated rubber particles and typically smaller than 5 mm and larger than 450 µm.

¹ Tire fibre is also a term used to refer to reclaimed textile fibres in the recycling process. For the sake of this discussion tire fibre refers to the type of particle shown in Figure 2-2-1

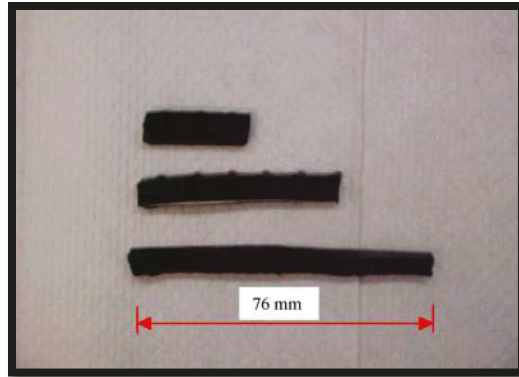


Figure 2-2-1 Tire Fibres [24]

Of the four types of tire particles listed, both crumb rubber and tire fibres are promising alternative aggregates for Portland Cement concrete. Crumb rubber has the advantage of already being mass-produced for use in asphalt concretes and athletic surfaces, whereas tire fibres have only ever been produced for research purposes. Regardless of the shape of the particle, it has been found that coarser crumb rubber particles have greater detrimental effects on the mechanical properties of concrete and offer little to no additional benefit over the use of finer particles [1, 21,24-26].

2.2.2. Crumb Rubber Manufacture

In order to produce crumb rubber, waste tires are shredded into smaller pieces and then subjected to an electromagnetic process to remove as much steel wire and textile as possible and then finally granulated [25]. Two different procedures are known for granulating tires, namely, ambient and cryogenic. The ambient process is purely mechanical in that after the tires are initially shredded, the shred pieces are milled in a granulator to the desired size. In the cryogenic process the tire shreds are frozen to a temperature below $-66.2\text{ }^{\circ}\text{C}$ after which the shreds are granulated. Freezing the tires at such a low temperature that surpasses the glass transition temperature² of the rubber making it more brittle and requiring less mechanical energy to granulate. Figure 2-2 and Figure 2-3 show process diagrams for the ambient method and the cryogenic method respectively.

² The glass transition temperature is the temperature that when cooled below, the amorphous regions of a polymer or semi-crystalline material behave as a brittle material as opposed to a ductile material.

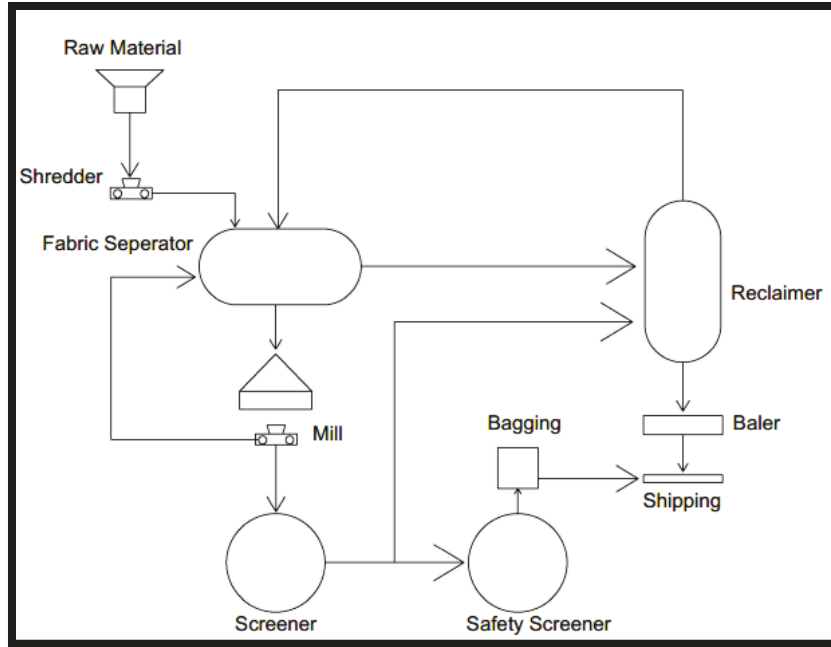


Figure 2-2 Typical Ambient Grinding System, Adapted from [22]

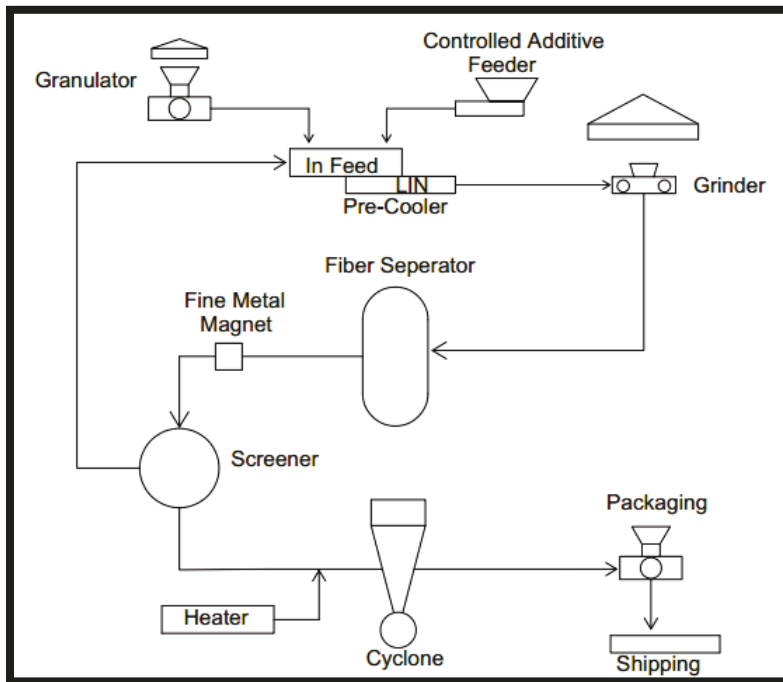


Figure 2-3 Typical Cryogenic Grinding System, Adapted from [22]

The ambient process produces crumb rubber with highly textured surfaces and the particles are generally considered angular. The cryogenic process produces particles with smooth and glossy surfaces [21]. Figure 2-4 shows photographs of the two different types of rubber.

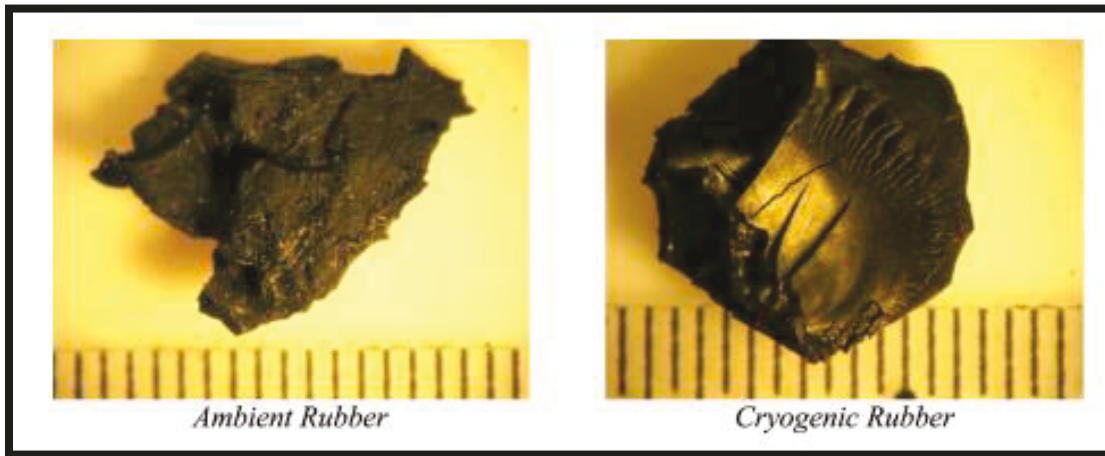


Figure 2-4 Magnified Images of Crumb Rubber Particles (Scale: 1 unit=0.50 mm) [21]

2.3. Mechanical and other Intrinsic Properties of Concrete that Contains Crumb Rubber

2.3.1. Compressive Strength

As would be expected, Portland Cement concrete made with crumb rubber replacing part of the aggregates has a lower compressive strength than concrete with pure mineral aggregate. This is due to weak interfacial bonds between crumb rubber particles and cement paste [1]. Pelisser et al [27] provided scanning electron microscope (SEM) microstructural analyses for concrete with rubber as shown in Figure 2-5. In the figure, it is quite clear that there is an empty space between the cement paste and the rubber particles. In terms of compressive strength analyses, the rubber particles are considered additional void spaces in the concrete mix as the rubber debonds from the cement matrix [28]. It has been found that coarse rubber shreds have a larger detriment on the compressive strength than finer crumb rubber particles or tire fibres [1, 24, 25, 28]

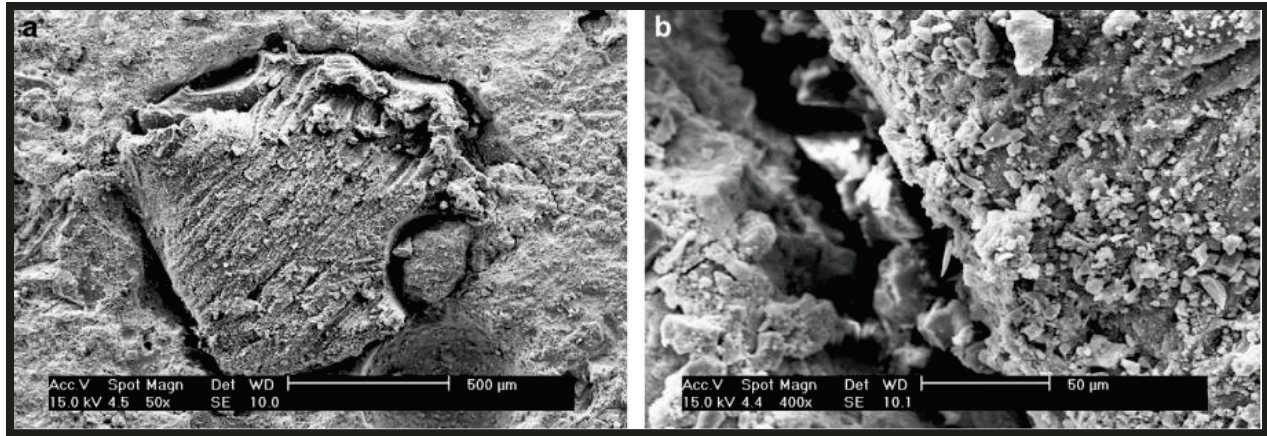


Figure 2-5 Microstructure of concrete with rubber; (a) cement matrix with rubber particle; (b) interface rubber/concrete (SEM) [27]

While a lower compressive strength is not ideal, there are many non-structural applications of concrete in which compressive strength is not a governing design criterion. An example is pavements where flexural strength is the governing parameter. Other examples include jersey barriers, noise barriers and sidewalks, where the durability of concrete is important.

The loss of compressive strength in relation to the amount of crumb rubber added is not a linear trend as shown in Figure 2-6. Khatib and Bayomy [29] developed a strength reduction factor model of the form:

$$SRF = a + b(1 - R)^m$$

Where: a , b and m are function parameters

$$a = 1 - b$$

R = Rubber Content as Volumetric Ratio in decimal form

SRF = Strength Reduction Factor (0-1)

Since the SRF must equal unity at zero rubber content, b must be less than one and likewise a . The parameter m controls the curvature of the model and can be considered as a sensitivity parameter, with higher values of m indicating greater sensitivity of the mix to rubber replacement. Values as high as 17 were found by Khatib and Bayomy [29]. In an analysis they performed on Eldin and Senoucci's data [30], they found the value of m to be 7 for 28-day compressive strength. For mix

design purposes, Khatib and Bayomy [22, 23] suggested using 0.1 for a and 5 for m , for a mix with rubber volume \leq to 20 % of the aggregate.

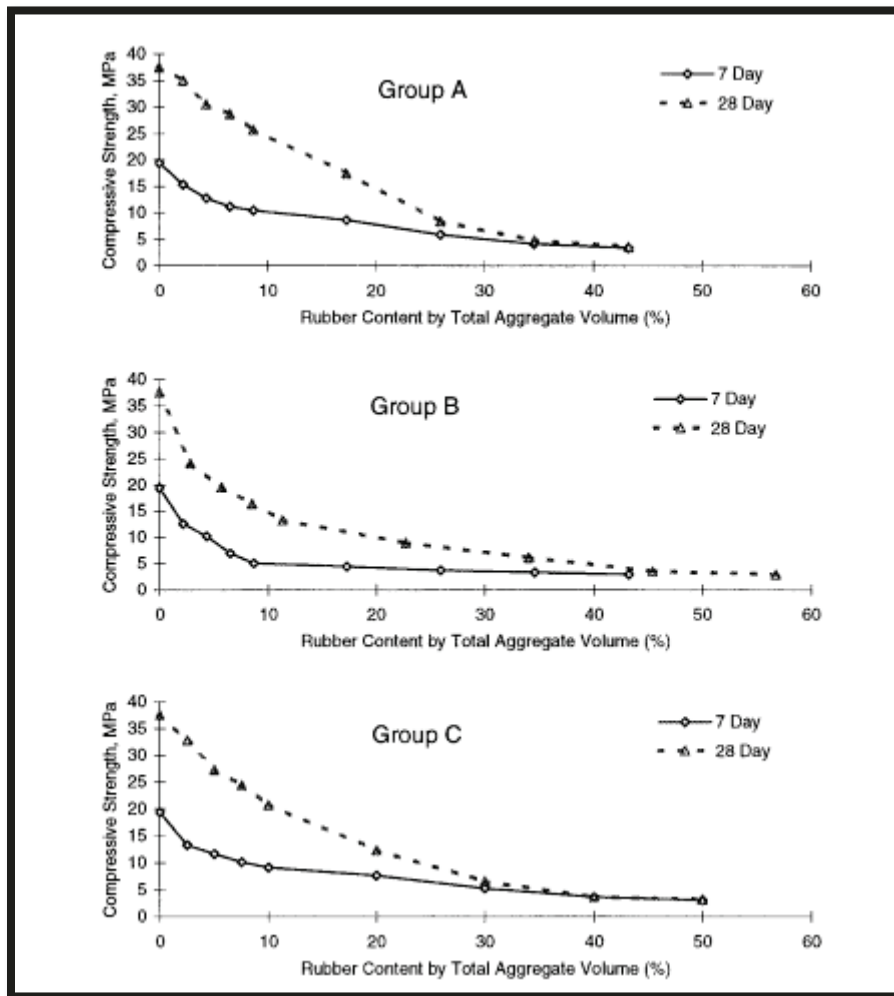


Figure 2-6 Compressive Strength v. Rubber Content for 3 different types of Rubber as adapted from [29]

A practical limit of 20 % replacement of fine aggregate has been reported in literature [31] Larger amounts of crumb rubber replacement lead to the detrimental effects outweighing the benefits.

2.3.2. Flexural Strength

Flexural strength is also reported to decrease with the addition of rubber to a concrete mix [15, 25, 29]. Toutanji [15] found that the decrease in flexural strength wasn't as large as the decrease in compressive strength. Siringi et al. [20] suggested that this decrease could also be related to the weak interfacial bonds, and that effects would be more pronounced in tension than compression.

The American Concrete Institute provides the following proportionality relationship between flexural strength f'_r [MPa] and compressive strength f'_c [MPa] [20].

$$f'_r = \alpha \sqrt{f'_c}$$

These researchers also found α to be between 0.58 and 0.83 for a concrete with flexural strength between 3.45 MPa and 4.48 MPa. Figure 2-7 shows that the decrease in flexural strength occurs at very low rubber contents.

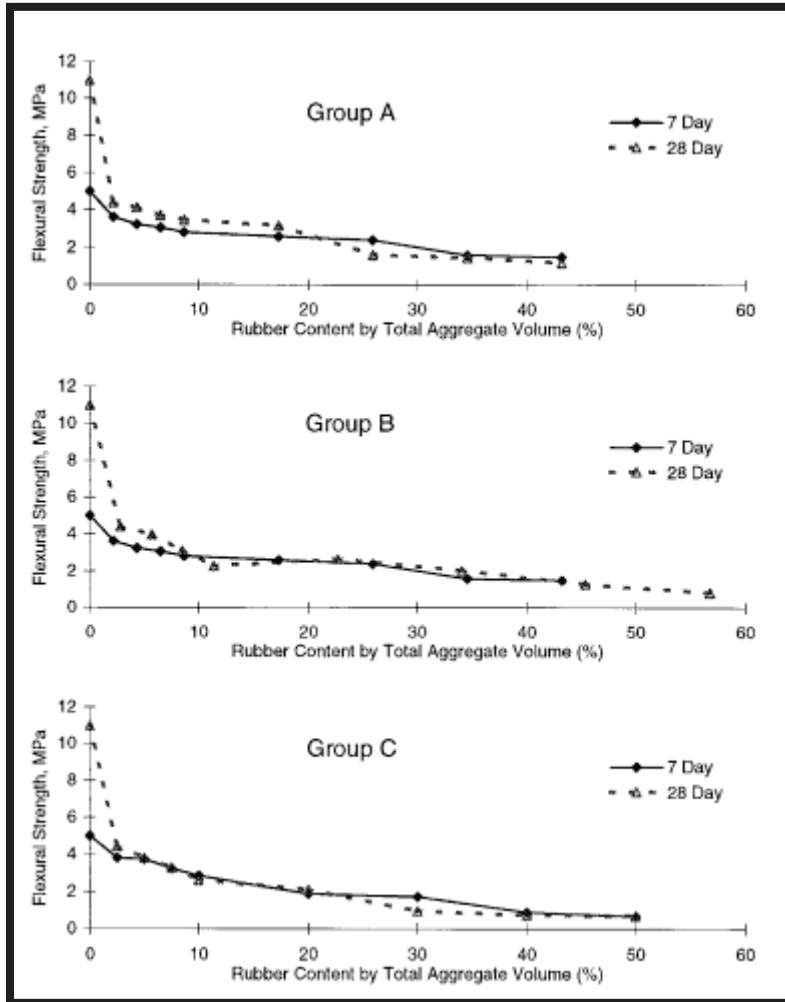


Figure 2-7 Flexural Strength v. Total Rubber Content for 3 different types of rubber [29]

2.3.3. Tensile Strength

The splitting tensile strength of rubberized concrete has been assessed in several research studies [1, 7, 20, 26, 28, 32]. A general decrease in splitting tensile strength was observed in the studies. This is partially attributed to the weak bonding between cement particles and the particles acting as stress concentrators. Since rubber has such a high Poisson's ratio ($\nu \sim 0.5$), when a force is

applied to it almost all the strain energy is redistributed into the plane perpendicular to the applied force. In the splitting tensile test this is the plane perpendicular to the failure surface, and as can be seen in Figure 6 2-8 adds to the stress causing failure rather than opposing it.

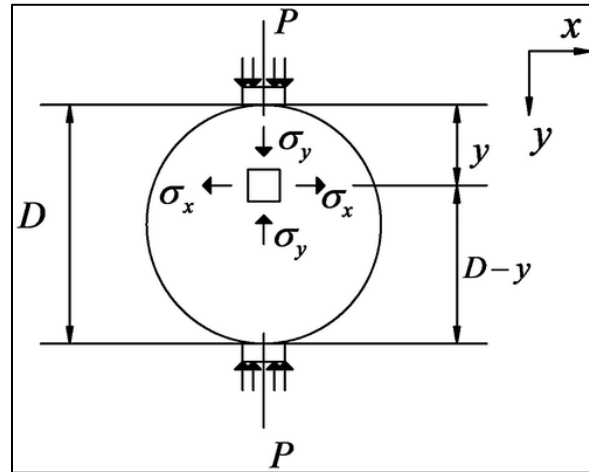


Figure 2-8 Stresses associated with a splitting tensile test [16]

Thakur and Singh [32] found the 28-day splitting tensile strength of concrete to decrease by 50 % at 18 % rubber replacement by natural aggregate volume. Eldin and Senoucci [26] found similar results and noted that less of a decrease in both compressive and tensile strength was seen in mixes that contained higher proportions of crumb rubber than rubber chips. Li et al. [28] found smaller tensile strength decreases in rubberized concrete that used tire fibre. Li et al. [24] used COSMOS/M to develop a finite element model of a rubberized concrete specimen under splitting tensile load to compare rubber chips to tire fibre. These researchers also found that using stiffer rubber (i.e. from truck tires with the steel belt remaining) could significantly improve the post fracture tensile strength. It was noted however that before fracture the positive benefits are not realized.

Snelson et al. [7] showed that the decrease in tensile strength is dependent on both the amount of rubber and supplementary cementing materials used (pulverized fuel ash in this study). Siringi et al. [20] found that while the splitting tensile strength decreased with additional rubber content the ratio of compressive strength to splitting tensile strength remained constant.

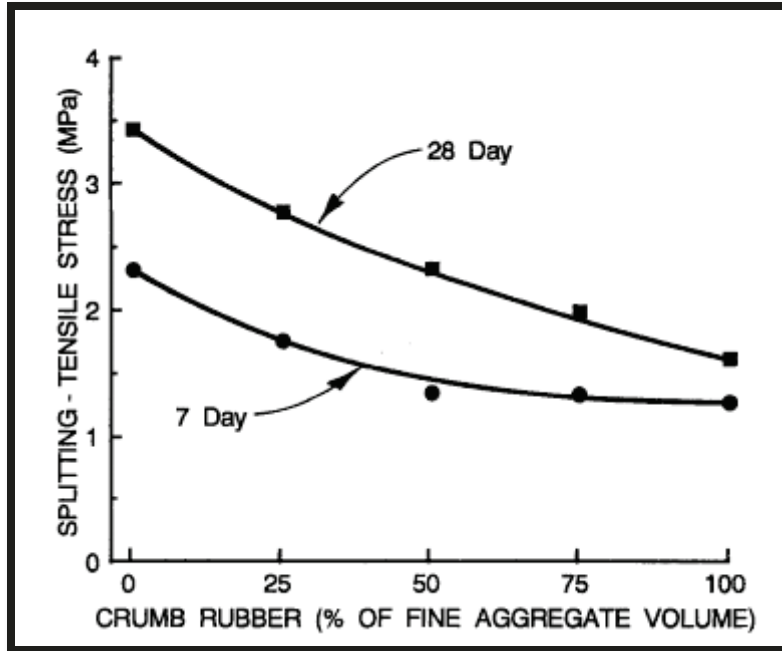


Figure 2-9 Splitting Tensile Strength v. Crumb Rubber Replacement of Fine Aggregate Volume Adapted from Eldin and Senoucci [30]

2.3.4. Noise Damping and Resistance to Dynamic Loading

Noise and dynamic loading are caused by two different mechanisms. However, a material's resistance to both is governed by the same properties, namely; natural frequency, damping ratio and stiffness. For a simply supported beam subjected to flexural free vibration the natural frequency can be calculated as [33]:

$$f_n = \frac{n^2 \pi}{2} \sqrt{\frac{EI}{ml^4}}$$

Where f_n : Natural Frequency of the n^{th} mode (For the fundamental $n=1$, Hz)

E : Dynamic modulus of elasticity (MPa)

I : Moment of inertia (mm^4)

l : Length of the beam (mm)

m : Mass of the beam in unit length (kg/mm)

The dynamic modulus of elasticity is determined as:

$$E = \frac{4mf^2l^4}{\pi^2n^4}$$

Where f is the fundamental frequency

While it may seem at first counter intuitive that the resistance to dynamic loading improves, since the stiffness of a concrete with rubber in it would be lower, the opposite is true. This is due in part to the "...reversible elasticity properties of the rubberized material... [33]". Hernandez-Olivares et al. [34] performed dynamic load tests on rubberized concrete in the viscoelastic range (< 30 % of the compressive elastic limit) and found that specific energy dissipated was between 23 and 30 %. Zheng et al. [33] used ultrasound transducers to measure P-wave and S-wave velocities through rubberized concrete specimens. These researchers also found frequencies by impacting a beam specimen on a rigid foundation with an impulse load (hammer) and using a modal analyzer to obtain the natural frequency via fast Fourier transform. In this study it was found that the damping ratio of rubberized concrete containing ground rubber could be as high as 75.3 %. Coarser particles were found to have a greater effect on both static and dynamic properties. It was also found that the relationship between damping ratio and rubber content is not linear, though no model was suggested.

Kahloo et al. [18] used ultrasonic echo technique to quantify sound absorption. It was found that the ultrasonic moduli of the concrete decreased significantly with increasing rubber content.

2.3.5. Toughness

Toughness, defined as the after-fracture strength, and calculated as the integral of the stress/strain curve between no loading and ultimate failure, has been reported to drastically increase [15, 18, 20, 24-26].

"At 7.5 % replacement, crumb rubber improved the modulus of toughness by 54 %, whereas at 15 % the modulus of toughness for crumb rubber concrete was 15 % greater than that of the control concrete" – Siringi et al. [20].

This is due to the ductile nature of the rubber in the concrete and its high deformability. The high deformability of the rubber allows the rubber to stay intact long after cracks have developed and become quite wide.

Li et al. [24] plotted load displacement curves for both ordinary concrete and rubberized concrete (Figure 2-10). The area between the curves and the abscissa is the energy absorbed by the specimen. This energy is proportional to the toughness. Toutanji [15] plotted load displacement

curves for flexural tests performed on rubberized concretes using tire chips to replace the mineral aggregates. It was found that at high replacement levels of rubber, toughness does not appear to increase further. Topcu [1] drew stress strain curves for cylindrical specimens of rubberized concrete under compressive load which allowed for direct calculation of the toughness. It was observed in this study that the ultimate strain of the rubberized concrete could reach 0.007 and 0.008 in comparison to 0.002 of the control mix.

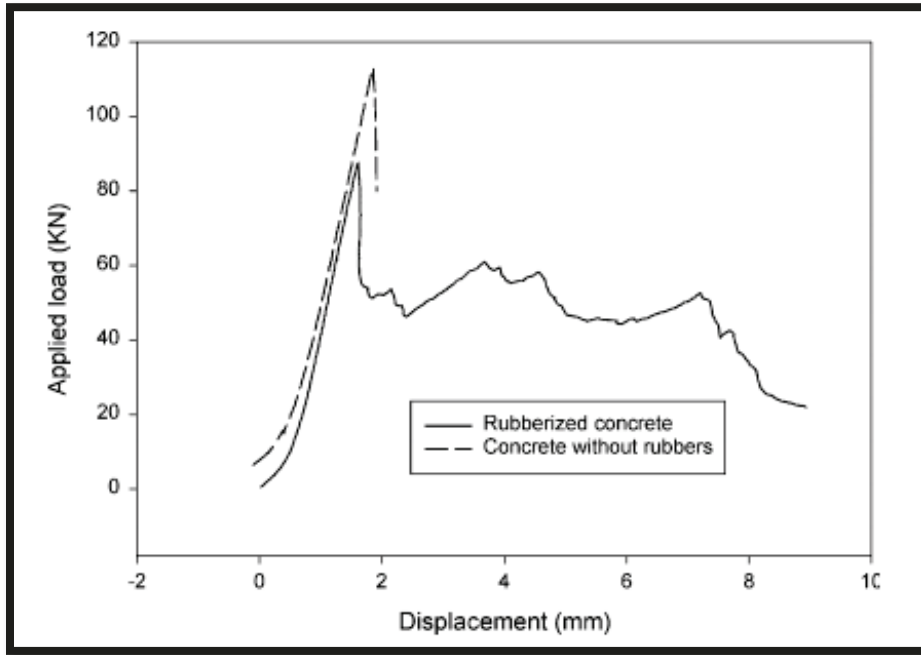


Figure 2-10 Load Displacement Curves for Ordinary Concrete and Rubberized Concrete [24]

2.3.6. Electrical Conductivity

Electrical conductivity of a concrete is proportional to its permeability. Permeability is one of the most important parameters regarding corrosion of rebar. The more permeable a concrete structure, the more readily pore fluid can move through it. The pore fluid acts as conduits for electrons and anions, such as chlorides and sulfates to move through the medium, a transport mechanism known as mechanical dispersion. If a low permeability concrete is placed in an environment with a high concentration of chloride, such as at sea, the transport of the chloride ions will be diffusive and slow, ultimately protecting the reinforcement from corrosion. If a higher permeability concrete is placed in the same environment the mechanical dispersion of the chloride ions will accelerate the transport of the chloride ions, resulting in corrosion of the reinforcement. When the reinforcement

corrodes not only does it lose some of its tensile strength, but the bars also expand resulting in internal stresses like that of freezing water.

The rapid chloride penetration (RCP) test³, is typically used to validate a given concrete's susceptibility to chloride ingress, which is a measurement of conductivity. Recently devices have emerged to market to measure the resistivity of a given concrete sample. Since the resistivity is the mathematical inverse of conductivity, there exists inverse relationships between these devices readings and RCP test data. The advantage of these new devices over the traditional RCP test is that they present a lower cost and tests can be performed much quicker.

Issa and Salem [19] performed a simple conductivity test on rubberized concrete samples and found that the conductivity does decrease. This indicates that rubberized concrete has a lower permeability and chloride ion penetration potential. This decrease may be attributed to different factors. First rubber has good electrical resistance properties. Second, the hydrophobic nature of rubber entrains more air during mixing, and dry air also acts as a good insulator. Since the pore spaces of concrete are relatively small it is safe to assume that any water in the pores will be in the liquid phase, and that the gas phase would be dry air.

2.3.7. Air Entrainment

Air pockets increase concrete resistance to freeze and thaw cycles by creating void spaces for water to expand in when it freezes. Thus, preventing the internal stresses due to crystallization from being fully realized in the solid. Due to the hydrophobic nature of crumb rubber, air pockets are naturally entrained during the mixing process. It has also been suggested due to the rough surface nature of crumb rubber particles, additional air is entrapped on the particle surface [18]. Since this is the case, crumb rubber concretes designed for external use in cold climates can use less to no air entraining agent, allowing the engineers and technicians better control of the mix by removing the uncertainty associated with the performance of different air entraining agents.

Gadkar and Rangaraju found that

³ ASTM C1202

“...addition of rubber to a cement matrix increased the porosity of the matrix and greater air entrainment was observed with smaller rubber particle sizes. [21]”

In this study, it was found that replacement of fine aggregate with crumb rubber produced using the ambient method could perform as well as air entrained concrete with respect to freeze-thaw cycles. The authors also suggested that the rubber particles could arrest more crack development in the concrete matrix further improving the freeze-thaw resistance of the concrete. Khatib and Bayomy [29] found that finer particles entrained more air than coarser particles, but assumed this was due to differences in preparation between the two materials.

2.3.8. Durability

Durability is the ability of a material to withstand the forces it is subject to for long periods of time. The durability of a given concrete structure is a function of, mainly permeability, resistance to dynamic loading, chemical composition of aggregates, pore fluid chemistry, and air entrainment. If all these properties are improved, it is expected that the overall durability of the concrete would improve. It should be noted that designing for durability is not a substitute for maintenance, however it should prevent major repair or replacement of the structure before its life span is reached. The effect of crumb rubber on dynamic loading and air entrainment were discussed in previous sections and will not be repeated here.

Permeability and porosity are not the same parameter. Permeability is the ability of a material to allow fluid to pass through it, whereas porosity is the volume of voids of a given material normalized to the materials' constituent volume. Porosity is necessary for permeability however high porosity does not always result in high permeability as the voids need to be interconnected to facilitate fluid flow. Correlations have been developed to relate the porosity, or pore sizes of a given concrete or mortar to its permeability. Four types of voids exist in concrete, in order of largest to smallest; entrapped air (also referred to as mechanically entrained air), entrained air, capillary pores, and gel pores. As much entrapped air as practical is removed through different methods of consolidation (i.e. vibration, roller compaction) and is of little concern to the mix designer if good concrete placement practices are followed. Entrained air voids are introduced to a concrete mixture via chemical surfactant that also disperses the voids through out the cement paste. Since these entrained air voids are dispersed, they have little to no effect on permeability if

the total porosity of the cement mortar is less than 30% [35]. Capillary pores are the spaces between fully formed cement crystals or cement gel⁴. Capillary pores are formed by excess water used in mixing and the primary reason low water cement ratios are desired for concrete mixtures. Capillary pores have the greatest influence on the permeability of a concrete. Gel pores occur within the C-S-H gel and are too small to allow nucleation of ice crystals and therefore have little impact on the freeze-thaw resistance of concrete.

It is well known that a concrete with low permeability lasts much longer than a high permeability concrete [36]. This is because the more readily a fluid moves through a substance, the more readily dissolved ions can move through said substance. Dissolved ions can cause deterioration to any of the components of a concrete mixture (i.e., chlorides corroding rebar, alkali silicate reactions breaking down individual aggregates, sulfates breaking down the cement paste by reacting with aluminates). Since freeze-thaw cycles lead to crack development, an increase in both porosity and permeability is expected to occur in concrete subjected to cold weather conditions.

Air entrainment is typically used to increase freeze-thaw resistance of a concrete. As was mentioned in the proceeding section on air entrainment, crumb rubber concretes may perform just as well as air entrained concrete when subjected to freeze-thaw cycles as well as arrest some crack development [21]. Due to the crack prevention, it is hypothesized that crumb rubber concretes may exhibit superior performance to that of air entrained concretes.

Topcu and Demir [37] conducted freeze-thaw tests on rubberized concrete only containing crumb rubber. It was found that the freeze-thaw resistance decreases with increasing rubber content, but that at a 10 % replacement level the freeze-thaw resistance was superior to ordinary concrete. This indicates that there is a benefit to adding small amounts of crumb rubber to concrete. It was also concluded that crumb rubber concrete should not be used in high temperature settings.

Alkali aggregate reactivity (AAR) occurs when alkali hydroxides react with either siliceous or carbonate type aggregates. Alkali silicate reactivity (ASR) produces an expansive gel which swells

⁴ Cement crystals are fibrous and form a cross linking pattern, cement gel has a highly disorganized crystal structure similar to that of tobermorite [35].

when moisture is present, leading to expansion of the concrete causing cracking and pop-outs. Alkali carbonate reactivity (ACR) is much less common, it occurs due to a process known as dedolomization, which has brucite as one of its products. The crystallization of brucite can be quite expansive leading to similar symptoms as that of ASR. Since crumb rubber has neither silicate or carbonate derived minerals AAR is of little concern. In fact, as many fine aggregates contain silicate materials, replacing a portion with a non-siliceous material should hypothetically reduce the risk, and consequences of ASR.

Thakur and Singh [32] submerged rubberized concrete in sulfate solutions in accordance to ASTM C1012. It was found that the maximum length change of a specimen occurred at 12 % replacement and was a factor of 1.14 at 90 days. The lowest replacement level in this study (3 %) still had a length change factor of 1.08 after 90 days. These results indicate that rubberized concretes are not suitable for use in sulfate rich environments.

3. Research Objectives and Methodology

A study to investigate the influence of crumb rubber (produced by the ambient grinding method) on various material properties of concrete was undertaken at Lakehead University. The main objectives were to validate previous work done and complete work that has yet to be published such as RCP results of crumb rubber concrete. To isolate the crumb rubber influence as a parameter, no supplementary cementing material were used in the batches. Standard test methods were used to find the results of crumb rubber concrete along with a control mix that had no crumb rubber and a mix that met MTO criteria for concrete in pavement structures for comparison purposes. Crumb rubber was used only to replace the fine aggregate, where the replacement value was calculated as a percentage of the volume of fine aggregate. In increments of 5 % rubber replacement by fine aggregate volume, different batches were cast from 0-25 %. The following properties were investigated:

- Compressive Strength
- Flexural Strength
- Splitting Tensile Strength
- Air Entrainment
- Bulk Resistivity
- Surface Resistivity
- Chloride Ion Penetrability (Before and After Freeze-Thaw cycles)
- Freeze -Thaw Durability

As was mentioned in the literature review section, it is well known that the compressive strength will reduce in concrete with crumb rubber. To validate the SRF model developed by Khatib and Bayomy [29] this testing was carried out. Similar SRF models are expected to exist for both splitting tensile strength and flexural strength of the concrete. It should be obvious from the model that:

$$\lim_{R \rightarrow 1} a + b(1 - R)^m = a$$

Unity is the upper bound of R . For this reason, a horizontal asymptote drawn on a plot that has rubber content on the abscissa and compressive strength on the ordinate can be used to determine

the parameter a and subsequently b . m is then increased integer wise until the strongest correlation coefficient is achieved.

To find the influence on air entrainment, plastic air content tests were performed with every batch and no air entraining agent was used in any of the batches that contained crumb rubber. One batch with out crumb rubber or air entrainment was also cast to act as a baseline and to quantify the amount of entrapped air in the mixes.

To find the influence on electrical resistivity, bulk and surface resistivity tests were carried out. Resistivity should increase as rubber is a good electrical insulator. Three different devices were used for bulk resistivity, to act as referees to one another and each device had features that the other two did not. One device (modeled after a Wenner probe array) was used for surface resistivity tests, as it was the only device available capable of performing these tests.

The chloride ion penetrability is expected to decrease for two reasons. The first being the lower conductivity will result in resisting the flow of charged particles. And the second being the weak bonding of the rubber with the cement paste; the particles can act as interstitials in the capillaries blocking the flow of dissolved ions. To verify this RCP tests were performed on every batch.

Traditional freeze-thaw tests were also performed to obtain durability factors. Visually these tests also allowed the difference in scaling between the crumb rubber specimens and control specimens to be observed.

4. Materials

Nine different Portland Cement concrete mixtures were proportioned by using the absolute volume method. Each mix had a different amount of crumb rubber added to replace a portion of the fine aggregate (by volume). Two control mixes were cast, one to simulate a concrete that would meet MTO specifications for pavement structures that had a water cement ratio of 0.40, and one with a 0.45 water cement ratio as a water cement ratio of 0.40 presented workability problems. Seven of the nine mixes had a water cement ratio of 0.45 and two had a water cement ratio of 0.4. To properly identify each mix, a 15-digit alphanumeric code is used such that the first 4 digits are the water cement ratio followed by the letters WCM, the following two digits are the plastic air content as a percent if air entrainment was used, otherwise 00 is in this place. This is followed by the letters AE. The last two numbers are the percent of fine aggregate that has been replaced by crumb rubber followed by the letters CR. For example, 0.45WCM00AE15CR, is a concrete mixture with a 0.45 water cement ratio, no air entrainment and 15 % fine aggregate replacement of crumb rubber by volume.

Mineral aggregates were provided by the structures laboratory at Lakehead University. The coarse aggregate is primarily crushed dolomite with a nominal maximum size of 19 mm. The fine aggregate is a sand. Portland cement was the only cementing material used in this study. Thunder Bay Municipal tap water sourced from Lake Superior and subjected to a microfiltration process was used for mixing. BASF MasterPozzolith 210 water reducer was used to make casting easier and to keep mixes economical by lowering the overall cement content required for workability. For the air entrained mixes BASF MasterAir 200 was used as the air entraining agent. Crumb Rubber with two gradings, namely, 10-20 and 30-, were obtained from CRM Holdings in Brantford Ontario for the study. The two grading sizes were selected in order to meet CSA gradation limits. From looking at the crumb rubber under 16X magnification it was apparent that it had been milled using the ambient process as the striations present closely resembled the left-hand particle in Figure 2-4.

4.1. Coarse Aggregate

The relative density and absorption of the coarse aggregate was determined in accordance with ASTM C-127 Standard Test Method for Relative Density (Specific Gravity) and Absorption of Coarse Aggregate [38]. This test is carried out by first soaking the aggregates in water for 24 hours to fill the effective pore spaces of the particles. Samples are then towel dried with the goal of achieving a saturated surface dry (SSD) state. The SSD mass of the aggregate is measured and recorded. The aggregate is then submersed in water and its mass is recorded. The difference between the two masses of the aggregate represents the mass of water with volume equivalent to that of the aggregate. Finally, the sample is oven dried to find the mass of only the aggregate (OD mass). The relative density (RD) is calculated as:

$$RD = \frac{ODmass}{(SSDmass - Mass\ in\ Water)} \quad \text{Equation 4-1}$$

The absorption of the coarse aggregate is calculated from the following equation:

$$Absorption\ \% = \frac{SSDmass - ODmass}{ODmass} * 100 \quad \text{Equation 4-2}$$

In-situ moisture content was found by determining the mass of three samples from the stockpile and the respective oven dry masses and calculated using the following equation.

$$In - situ\ Moisture\ Content\ (\%) = \frac{In\ situ\ mass - ODmass}{ODmass} * 100 \quad \text{Equation 4-3}$$

As towel drying is subjective, three trials were conducted, and the average value for RD and Absorption is used for the mix design calculations. The results of the three trials are shown in Table 4-1.

Table 4-1 Coarse Aggregate Properties

Relative Density	Trial 1	Trial 2	Trial 3
<i>Pan (kg)=</i>	0.809	0.359	0.2483
<i>SSD Mass + pan (kg) =</i>	4.226	4.305	4.857
<i>SSD Mass (kg) =</i>	3.417	3.946	4.609
<i>Oven Dry Mass +pan (kg) =</i>	4.210	4.282	4.825
<i>Oven Dry Mass (kg) =</i>	3.401	3.923	4.577
<i>Apparent Mass in Water (kg) =</i>	2.197	2.535	2.952
<i>Relative Density Oven Dry =</i>	2.787	2.780	2.763
<i>Relative Density SSD =</i>	2.8	2.796	2.782
<i>Absorption (%) =</i>	0.47%	0.59%	0.70%
<i>In Situ Moisture Content</i>			
<i>Pan (kg) =</i>	0.25	0.358	0.255
<i>Sample +pan (kg)=</i>	3.879	5.612	4.087
<i>OD +pan (kg)=</i>	3.872	5.611	4.081
<i>Moisture content=</i>	0.19%	0.02%	0.16%

An oven dry relative density of 2.78 was used in all mix design calculations. 0.59 % was used as the absorption of coarse aggregate to adjust mixing water proportions.

Bulk density of coarse aggregate was found in accordance with ASTM C29. Dry aggregate is rodded 25 times per lift for three lifts in a seven-litre container and the mass determined. The oven dry bulk density used in the mix design was 1752.6 kg/m³. This number is high for a coarse aggregate used in concrete and is expected to affect the results of the density of the hardened concrete. Table 12-4 in Appendix A shows the data that was used to determine the oven dry bulk density.

The gradation of the coarse aggregate was determined in accordance with ASTM C136 Standard Test Method for Sieve Analysis of Fine and Coarse Aggregates [39]. A Gilson shaker with 19, 16, 12.5, 9.5 and 4.75 mm sieves was used to obtain the gradations that were then plotted along side the CSA limits for coarse aggregates used in concrete. Figure 4-1 shows the average gradation obtained from 3 samples from the stockpile. The three actual gradations may be found in Appendix

A (Table 12-1, Table 12-2, Table 12-3). Table 4-2 shows the CSA grading limits to determine the upper and lower boundaries.

The average coefficients of uniformity (C_u) and curvature (C_c) for the coarse gravel are 2.46 and 1.21, respectively (Table 4-3). Thus, according to Unified Soil Classification System (USCS) the coarse gravel is classified as poorly-graded gravel with a group symbol GP.

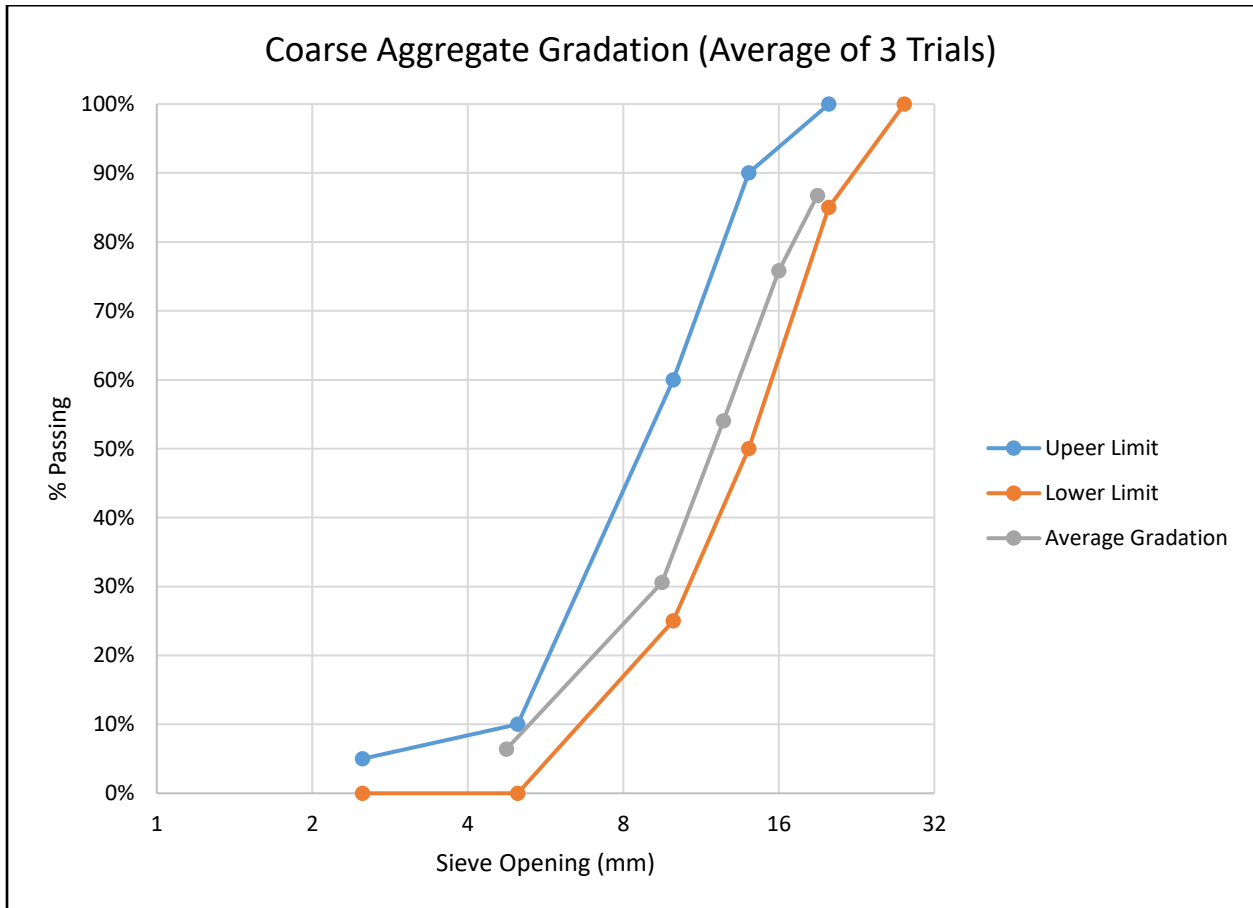


Figure 4-1 Coarse Aggregate Gradation

Table 4-2 CSA Grading Limits for Coarse Aggregates Used in OPC [36]

CSA Grading Limits for Coarse Aggregates		
Sieve Opening (mm)	Upper Limit	Lower Limit
28		100 %
20	100 %	85 %
14	90 %	50 %
10	60 %	25 %
5	10 %	0 %
2.5	5 %	0 %

Table 4-3 Average Grading and USCS Classification Criteria

Average Grading		USCS Classification Parameters	
Sieve Size (mm)	Average % Passing	D ₆₀ :	13.45
19	86.73 %	D ₃₀ :	9.43
16	75.79 %	D ₁₀ :	5.46
12.5	54.05 %	C _u :	2.46
9.5	30.59 %	C _c :	1.21
4.75	6.40 %		

4.2. Fine Aggregate

The relative density and absorption of the fine aggregate were determined in accordance with ASTM C-128 Standard Test Method for Relative Density (Specific Gravity) and Absorption of Fine Aggregate [40]. Like in the method for coarse aggregate, the test begins by soaking the sample for 24 hours. To achieve the saturated surface dry (SSD) state, a warm air current (provided by a heat gun) is blown across the sample. SSD state is verified by lightly tamping the aggregate in a mold 25 times, in which when the mold is removed, the aggregate should slump slightly. No slump occurring is an indication that surface moisture is still present, and collapse of the molded aggregate is an indication that the pores of the particles are not filled. To determine absorption of the fine aggregate, the masses of the sample in SSD and OD states are determined similarly to that of the coarse aggregate.

To determine the relative density of the fine aggregate, 500 g of the sample conditioned to SSD is added to a 500 ml pycnometer with a calibration mark. Water is then added to approximately 90 % of the capacity of the pycnometer and the mixture in the pycnometer is agitated (either by rolling the pycnometer or by other mechanical means to remove air). The pycnometer is then filled to the calibration mark and the mass is determined. The sample is then oven dried, after which the OD mass is determined. The mass of the pycnometer filled with water is determined. The following equation is then used to determine the relative density.

$$RD = \frac{OD_{mass}}{(SSD_{mass} + Filled\ Pycnometer - Pycnometer\ with\ sample\ and\ water)} \quad \text{Equation 3-4}$$

The relative density, absorption and in-situ moisture content results are shown in Table 4-4.

Table 4-4 Fine Aggregate Properties

Relative Density						
Trial 1			Trial 2		Trial 3	
SSD Mass (g)=	500.80		SSD Mass (g)=	500.00	SSD Mass (g)=	500.10
Mass of pan (g) =	258.70		Mass of pan (g) =	137.00	Mass of pan (g) =	176.30
Oven dry mass + pan (g) =	753.10		Oven dry mass + pan (g) =	633.80	Oven dry mass + pan (g) =	672.50
Oven dry mass (g) =	494.40		Oven dry mass (g) =	496.80	Oven dry mass (g) =	496.20
Mass of pycnometer (g)=	200.10		Mass of pycnometer (g)=	200.10	Mass of pycnometer (g)=	200.10
Mass of sand + pycnometer + water (g) =	1011.90		Mass of sand + pycnometer + water (g) =	995.50	Mass of sand + pycnometer + water (g) =	994.12
Mass of Pycnometer + water (g) =	698.10		Mass of Pycnometer + water (g) =	680.70	Mass of Pycnometer + water (g) =	680.40
Relative Density =	2.64		Relative Density =	2.68	Relative Density =	2.66
Absorption						
Pan (g)=	174.70		Pan (g)=	219.20	Pan (g)=	151.00
SSD Mass + pan (g) =	849.30		SSD Mass + pan (g) =	719.20	SSD Mass + pan (g) =	653.00
Oven Dry mass +pan (g)=	844.00		Oven Dry mass +pan (g)=	716.30	Oven Dry mass +pan (g)=	650.60
Absorption (%) =	0.79 %		Absorption (%) =	0.58 %	Absorption (%) =	0.48 %
In Situ Moisture Content						
Pan (g) =	175.20		Pan (g) =	218.40	Pan (g) =	175.70
Sample +pan (g)=	795.80		Sample +pan (g)=	928.10	Sample +pan (g)=	865.10
OD + pan (g)=	794.10		OD + pan (g)=	926.50	OD + pan (g)=	863.20
Moisture Content =	0.27 %		Moisture Content =	0.23 %	Moisture Content =	0.28 %

Sieve analyses were carried out on the fine aggregate in accordance with ASTM C136 to confirm that the gradation of the fine aggregate was within the acceptable zone and to calculate the fineness modulus for the concrete mix design. The fineness modulus is calculated by adding the percent retained on the 150-micron, 300-micron, 600 microns, 1.18 mm, 2.36 mm, 4.75 mm, 9.5 mm and so on, doubling in size for each larger sieve then dividing by 100. The percent retaining on the 600-micron sieve was found on the grading curve as this size of sieve was unavailable at the time of the sieve analysis. The fineness modulus used in the mix design was 2.55, the average grading of three different sieve analyses is shown in Figure 4-2, and the data for the average gradation is shown in Table 4-5. Table 4-6 shows the CSA grading limits for fine aggregates used in concrete.

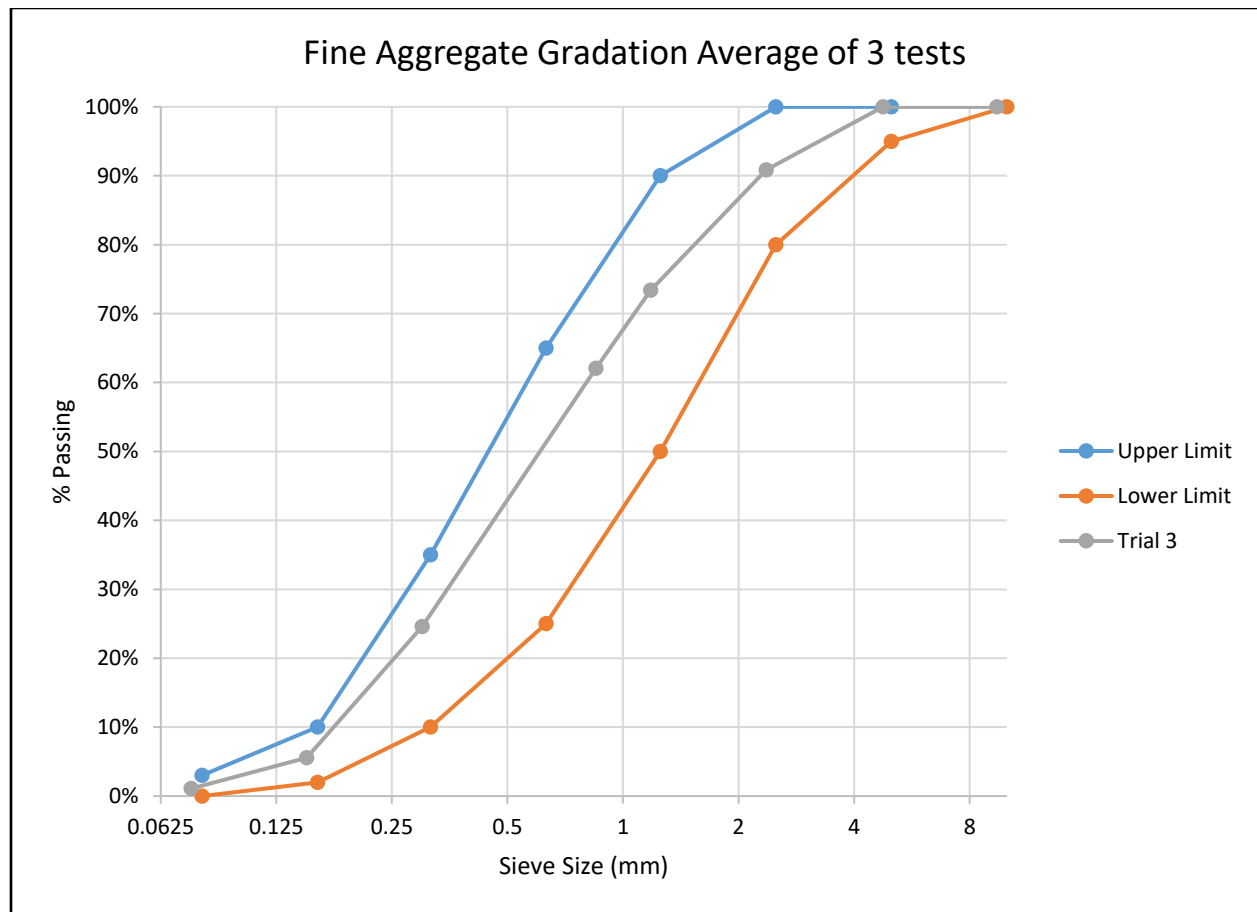


Figure 4-2 Fine Aggregate Average Grading

Table 4-5 Fine Aggregate Average Grading

Sieve Opening (mm)	Average %Passing
9.423	100.00 %
4.76	100.00 %
2.36	90.83 %
1.18	73.41 %
0.85	62.06 %
0.3	24.62 %
0.15	5.55 %
0.075	1.09 %

Table 4-6 CSA Gradation limits for Fine Aggregates

Gradation Limits for Fine Aggregate %Passing		
Sieve Size (mm)	Upper Limit	Lower Limit
10		100 %
5	100 %	95 %
2.5	100 %	80 %
1.25	90 %	50 %
0.63	65 %	25 %
0.315	35 %	10 %
0.16	10 %	2 %
0.08	3 %	0 %

The average of coefficient of uniformity is 4.45 and the average coefficient of curvature is 0.95. The sand is classified as a poorly graded sand with a group symbol SP (according to the Unified Soil Classification System).

4.3. Crumb Rubber

For concrete mixture design purposes, two properties are needed to be known about the crumb rubber, the gradation and the relative density. CRM Holdings produced crumb rubber in 4 different gradings (see Appendix A). The gradings were plotted and it was found that a combined grading of 10-20 mesh size crumb rubber and 30- mesh size fits the CSA grading curves for fine aggregates (Figure 4-3 and Figure 4-4). The amount of rubber by mass of the two sizes is 46 % of the 10-20 size and 54 % of the 30- size (Table 4-7 and Table 4-8).

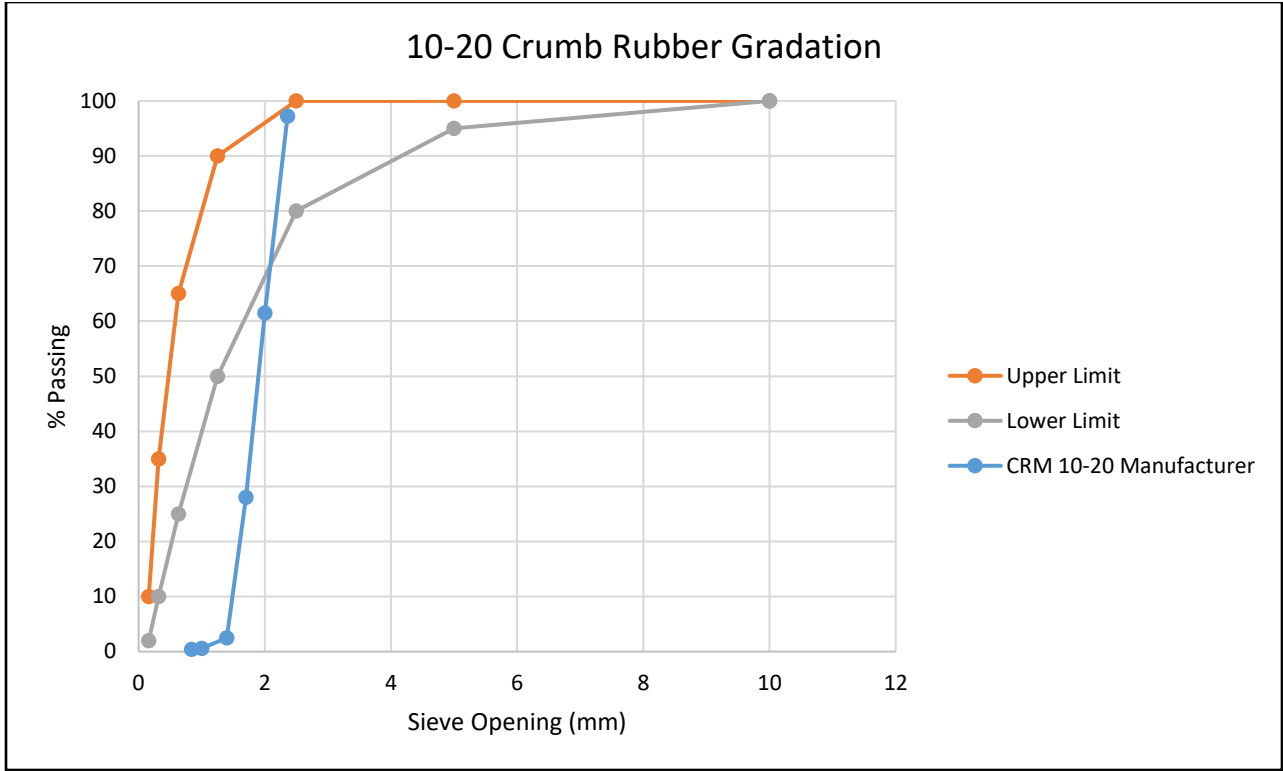


Figure 4-3 Crumb Rubber Grading Curve 10-20 size

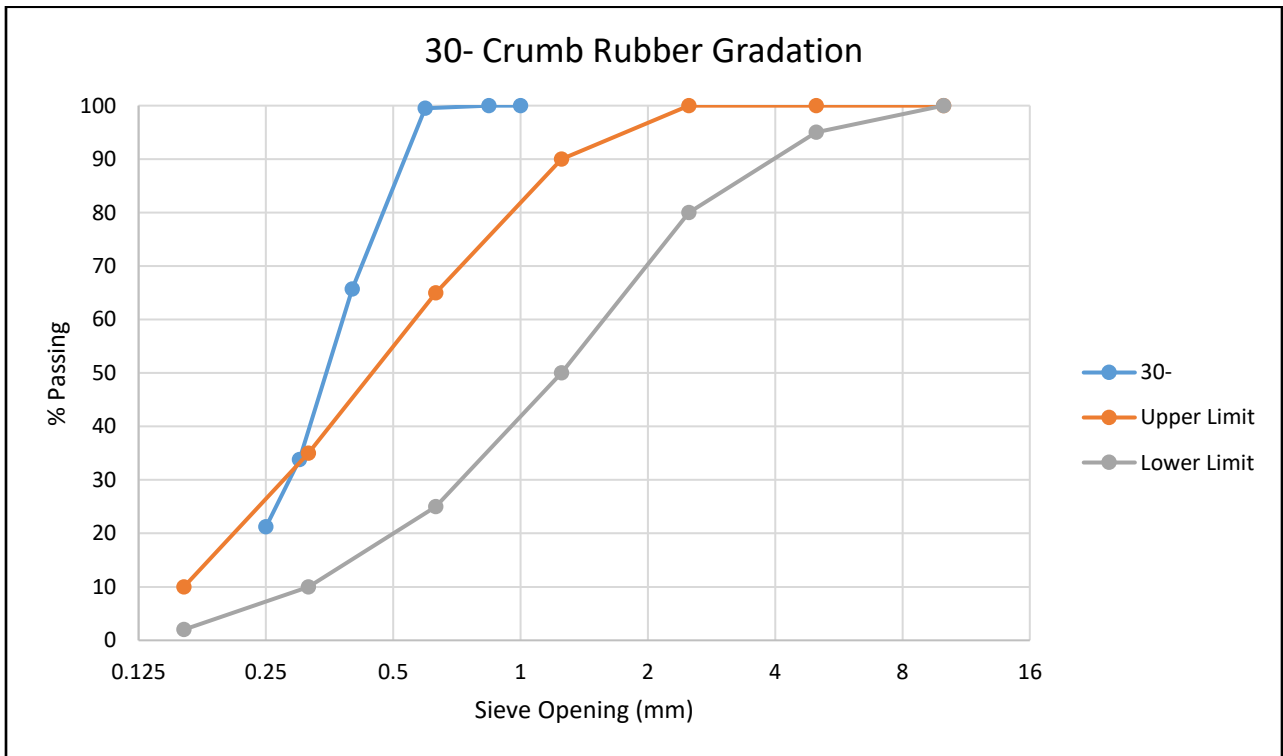


Figure 4-4 Crumb Rubber Grading Curve 30- Size

Table 4-7 Combined Grading of 10-20 and 30- Crumb Rubber from Manufacturers Data

Combined Gradation of 10-20 and 30-					
Sieve #	Sieve (mm)	% Passing 10- 20	% Retained 10- 20	% Passing 30-	% Retained 30-
8	2.36	97.2	2.8	100	0
10	2	61.5	35.7	100	0
12	1.7	28	33.5	100	0
14	1.4	2.5	25.5	100	0
16	1	0.6	1.9	100	0
20	0.841	0.4	0.2	100	0
30	0.595	0	0	99.5	0.5
40	0.4	0	0	65.7	33.8
50	0.3	0	0	33.8	31.9

Table 4-8 Combined Grading of 10-20 and 30- Crumb Rubber from Manufacturers Data Cont'd

Combined Grading			
% Passing	% Retained	10-20 multiplier	30- multiplier
98.7	1.3	0.46	0.54
82.3	16.4		
66.9	15.4		
55.2	11.7		
54.3	0.9		
54.2	0.1		
53.7	0.3		
35.5	18.3		
18.3	17.3		

Once the crumb rubber had arrived, sieve analyses were done on the crumb rubber and it was found that a 50/50 split of the two sizes would provided an adequate gradation to fit with in the CSA limits (Table 4-9 and Table 4-10) as opposed to the predicted 46/54 split. The combined grading curve is shown in Figure 4-5.

Table 4-9 Combined Crumb Rubber Grading from Laboratory Sieving

Sieve Size	% Retained 30-	% Passing 30-	% Retained 10- 20	%Passing 10- 20
9.423	0.00	100.00	0	100
4.76	0.00	100.00	0	100
2.36	0.00	100.00	11.62666375	88.37333625
1.18	0.00	100.00	87.08470821	1.288628037
0.85	0.48	99.52	0.245572747	1.043055291
0.3	74.95	24.58	0.050581689	0.992473601
0.15	21.52	3.06	0	0.992473601
0.075	2.76	0.30	0	0.992473601
pan	0.21	0.09	0	0.992473601

Table 4-10 Combined Crumb Rubber Grading from Laboratory Sieving Cont'd

Sieve Size	Combined % Passing	10-20 Multiplier	30-Multiplier
9.423	100	0.5	0.5
4.76	100		
2.36	94.18666812		
1.18	50.64431402		
0.85	50.2837549		
0.3	12.78592886		
0.15	2.026917018		
0.075	0.646698442		
pan	0.542654693		

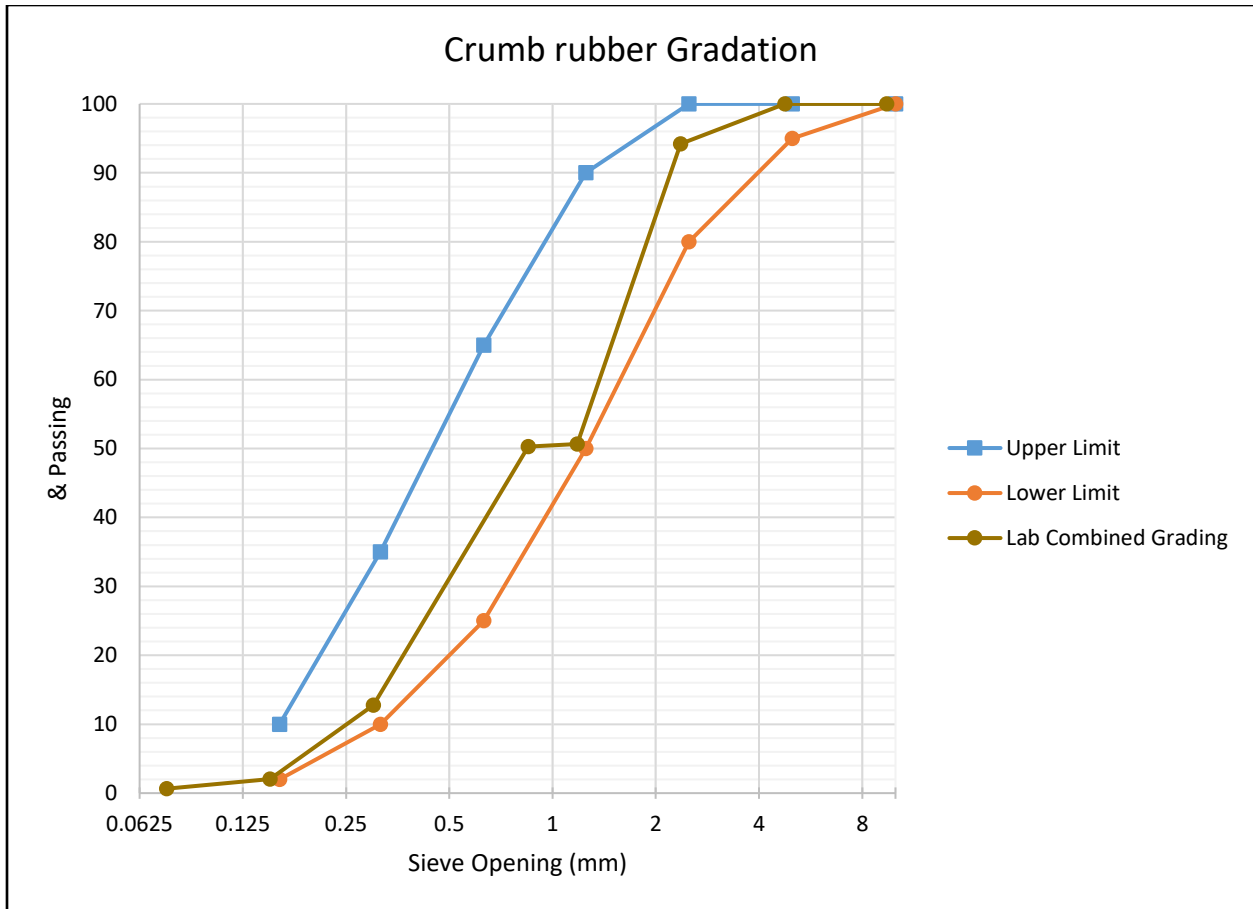


Figure 4-5 Combined Grading of Two Crumb Rubber Sizes Based on Laboratory Results

Figure 4-6 shows a plot of CSA FA gradation limits, the gradation of the crumb rubber found in the lab and the fine aggregate. Combining different amounts of crumb rubber and fine aggregate will change the fineness modulus and the true gradation of the fine aggregate slightly, however this gradation will always be between the two gradation curves shown, as the fine aggregate and crumb rubber curves represent the upper and lower boundaries of replacing an amount of fine aggregate with crumb rubber.

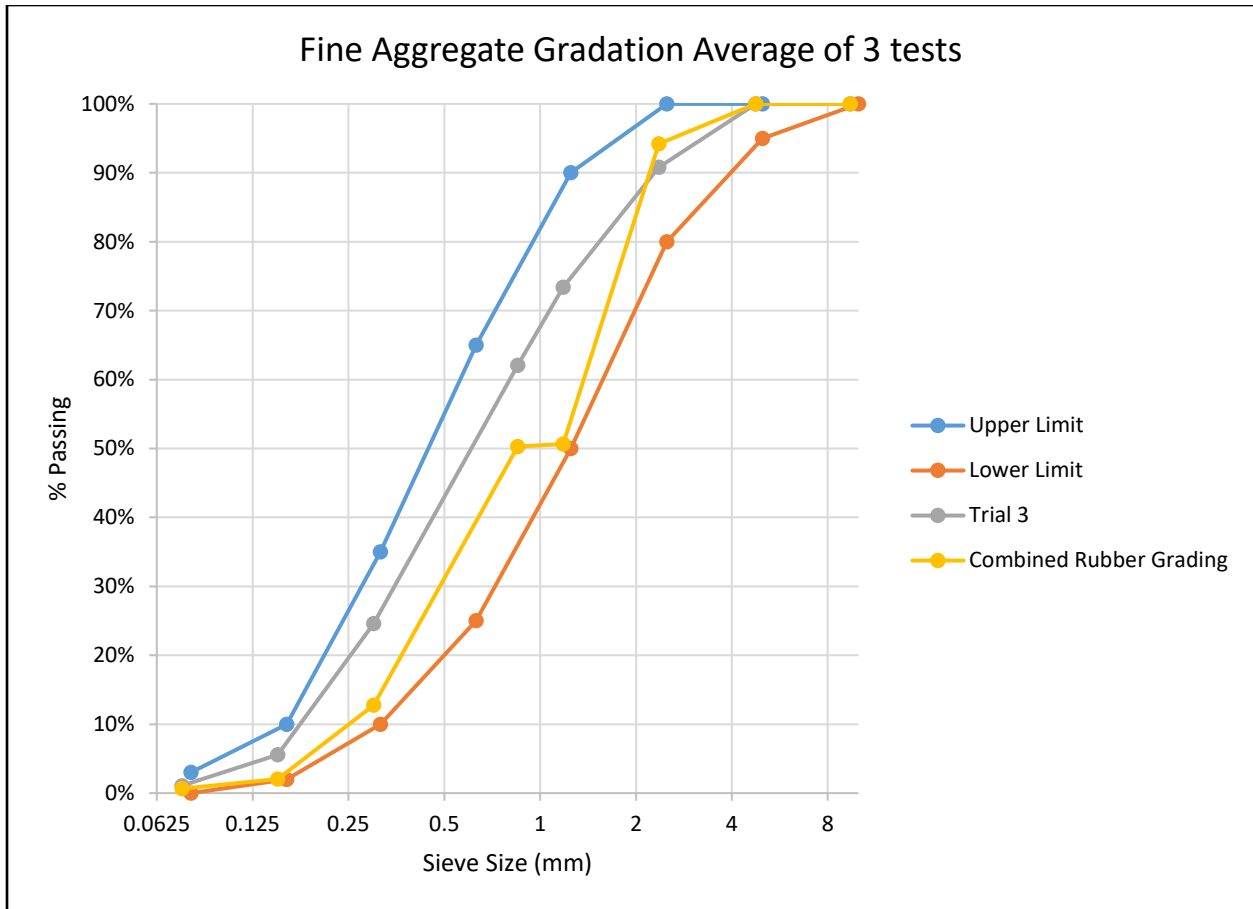


Figure 4-6 Fine Aggregate and Combined Rubber Grading Curves

Finding the relative density of the crumb rubber presented a unique challenge in that the density was very close to water, because when a pycnometer was used, roughly half of the particles floated. Since the particles were floating, they weren't displacing 100 % of their constituent volume. For such cases, the standard test method advises to use a solvent other than water for which the specific gravity is known. Out of fear that any other solvent may cause the rubber to either swell or deteriorate, this pathway was set aside. To find the relative density, a coffee press was used to push the rubber down and keep it from floating. A line was drawn on the glass of the press with a marker at the meniscus of the water before rubber was added, but the plunger was in it, then the plunger was taken out and a sample of crumb rubber with known mass was added and the pressed back down. The water level would now rise to accommodate the volume of rubber added. This extra water was poured into a graduated cylinder until the water was just above the mark made without rubber. The remaining water was syringed into a graduated cylinder until the meniscus was where

it was before. The volume of water extracted was taken to be the same as the volume of rubber added, and thus the relative density was able to be found. This was done four times, twice the relative density was greater than one and twice it was less. The average of the four was 1.0005 and was taken as unity for mix design purposes. For the detailed data see Appendix A.

4.4. Portland Cement

Due to confidentiality concerns, a detailed breakdown of the composition of Portland Cement provided by Lafarge will not be given. The percent by weight for the main components as taken from the material safety data sheet is shown in Table 4-11. The relative density of the Portland Cement is 3.15

Table 4-11 Portland Cement Composition

Component	Percent by Weight
Portland Cement	100
Calcium Sulfate	2-10
Calcium Carbonate	0-15
Calcium Oxide	0-5
Magnesium Oxide	0-4
Crystalline Silica	0-0.2

5. Mix Design

All mixes were designed in accordance with the absolute volume mix design method, a mix of 1 cubic metre was designed, and then reduced to the appropriate size depending. A 335 kg/m³ cementing materials content was chosen as this produced concrete with a desirable slump and workability when combined with a water reducer admixture. A mix was designed with a 0.4 water cement ratio, as this would be required to for the chloride exposure that concrete pavements in northern Ontario would be subjected to. As there were workability issues, mixes containing crumb rubber were designed with a 0.45 water cement ratio and a mix without crumb rubber was also cast at this water cement ratio to act as a control. As the amount of air entrained by the crumb rubber was a desired property no air entrainment was used, and its volume was taken as zero for design purposes. Totaling the volume of the cement, water, and coarse aggregate from the preceding information and subtracting this value from 1, gave the amount of fine aggregate required. The fine aggregate was then adjusted by subtracting the percent of crumb rubber to replace the fine aggregate. Once all these volumes were known, they were converted to constituent mass by using the relative density. The water content as well as the fine and coarse aggregate masses were then adjusted to account for the absorption/donation values found earlier. It was assumed that the crumb rubber would not absorb any water due to its hydrophobic nature [18]. Table 5-1 shows a sample mix design spread sheet and Table 5-2 shows the formulae used within the spreadsheet.

Two rounds of testing were performed, one in the summer of 2017 and the other in the spring of 2018. In the summer 2017 testing regime, each mix was tested for compressive strength (ASTM C39), flexural strength (ASTM C78), splitting tensile strength (ASTM C496), electrical resistivity (both bulk and surface), and rapid chloride ion penetration (ASTM C1202). The spring 2018 testing regime consisted of retesting any tests that did not meet ASTM tolerances. freeze-thaw testing (ASTM C666) and rapid chloride ion penetration after subjecting samples to freeze thaw testing. For each compressive strength, three 100 mm by 200 mm cylinders were cast, and two additional cylinders of this size were cast for RCP tests. For each splitting tensile test, three 150mm by 300 mm samples were cast and three 150 mm by 150 mm by 500 mm beams were cast for each flexural strength test. Three freeze thaw beams (75 mm by 100 mm by 400 mm) were cast for each freeze thaw test.

Table 5-1 Sample Mix Design

Mix Design Calculator				
Number of Freeze/Thaw Beams	0			
Number of Cylinders Cast	5		Volume of 4x8 Cylinder (m ³) =	0.001647
Number of Prisms Cast	3		Volume of Prism (m ³) =	0.0135
Waste Buffer	1.1		Air test (m ³) =	0.007
Number of 6x12 Cylinders	3		Slump (m ³) =	0.005
Volume of Mix Req'd (L)=	85.15874		Volume of 6x12 Cylinder (m ³) =	0.00556
			Volume of Freeze-Thaw Beams (m ³) =	0.003375
Water (kg) =	13.65017			
Portland Cement (kg) =	28.52818			
Fine Aggregate (kg) =	64.25111			
Coarse Aggregate (kg) =	97.05828			
Crumb Rubber (kg) =	4.255334			
Water Reducer (ml) =	111.2599			
Air Entraining Agent (ml) =	0			
Water Reducer dosage (130-390ml/100kg Cement)	390			
Air Entrainment Dosage (8-98 ml/100kg Cement)	0			
Water Cement Ratio =	0.45			
Fineness Modulus =	2.55			
Cement Req'd (kg/m ³) =	335			
Air Content (%) =	0			
Oven Dry Bulk Density of CA (kg/m ³) =	1752.56			
Relative Density of CA=	2.78			
Relative Density of FA=	2.66			
Absorption of FA (%) =	0.62			
Moisture Content of FA (%) =	0.17			
Absorption of CA (%) =	0.59			
Moisture Content of CA (%) =	0.05			
Bulk Volume of CA=	0.65			
Crumb Rubber Fraction of FA (%) =	15			
Relative Density of Crumb Rubber	1			
1 m ³ Batch Before Adjustments	Mass (kg)	Volume (m ³)		
Water =	150.75	0.15075		
Coarse Aggregate =	1139.164	0.409771223		
Portland Cement=	335	0.106349206		
Fine Aggregate (before rubber adjustment) =	886.1247	0.333129571		
Fine Aggregate After Rubber Adjustment=	753.206	0.283160135		

Crumb Rubber	49.96944	0.049969436		
Adjustments				
Coarse Aggregate =	1139.734			
Fine Aggregate =	754.4864			
Water=	160.2909			

Table 5-2 Mix Design Formulae

Mix Design Calculator				
Number of Freeze/Thaw Beams	0			
Number of Cylinders Cast	5		Volume of 4x8 Cylinder (m ³) =	$= \frac{(\pi) \cdot (0.1016^2)}{4} \cdot 0.2032$
Number of Prisms Cast	3		Volume of Prism (m ³) =	$= 0.15 \cdot 0.15 \cdot 0.6$
Waste Buffer	1.1		Air test (m ³) =	0.007
Number of 6x12 Cylinders	3		Slump (m ³) =	0.005
Volume of Mix Req'd (L) =	$= ((B3 \cdot E3) + (B4 \cdot E4) + (B6 \cdot E7) + (B2 \cdot E8) + E5 + E6) \cdot B5 \cdot 1000$		Volume of 6x12 Cylinder (m ³) =	$= \frac{(\pi) \cdot (0.1524^2)}{4} \cdot 0.3048$
			Volume of Freeze-Thaw Beams (m ³) =	$= 0.45 \cdot 0.1 \cdot 0.075$
Water (kg) =	$= B45 \cdot (B7/1000)$			
Portland Cement (kg) =	$= B37 \cdot (B7/1000)$			
Fine Aggregate (kg) =	$= B44 \cdot (B7/1000)$			
Coarse Aggregate (kg) =	$= B43 \cdot (B7/1000)$			
Crumb Rubber (kg) =	$= B40 \cdot (B7/1000)$			
Water Reducer (ml) =	$= B17 \cdot (B10/100)$			
Air Entraining Agent (ml) =	$= B18 \cdot (B10/100)$			
Water Reducer dosage (130-390ml/100kg Cement)	390			
Air Entrainment Dosage (8-98 ml/100kg Cement)	0			
Water Cement Ratio =	0.45			
Fineness Modulus =	2.55			
Cement Req'd (kg/m ³) =	335			
Air Content (%) =	0			

Oven Dry Bulk Density of CA (kg/m ³) =	1752.56			
Relative Density of CA=	2.78			
Relative Density of FA=	2.66			
Absorption of FA (%) =	0.62			
Moisture Content of FA (%) =	0.17			
Absorption of CA (%) =	0.59			
Moisture Content of CA (%) =	0.05			
Bulk Volume of CA=	0.65			
Crumb Rubber Fraction of FA (%) =	15			
Relative Density of Crumb Rubber	1			
1 m ³ Batch Before Adjustments	Mass (kg)	Volume (m ³)		
Water =	=B19*B21	=B35/ (1000*1)		
Coarse Aggregate =	=B30*B23	=(B36/(1000*B24))		
Portland Cement=	=B21	=B37/ (1000*3.15)		
Fine Aggregate (before rubber adjustment) =	=C38*B25*1000	=(1-(C35+C36+C37+(B22/100)))		
Fine Aggregate After Rubber Adjustment=	=C39*B25*1000	=C38-(C38*(B31/100))		
Crumb Rubber	=C40*B32*1000	=C38*(B31/100)		
Adjustments				
Coarse Aggregate =	=B36*(1+(B29/100))			
Fine Aggregate =	=B39*(1+(B27/100))			
Water=	=B35+B36*((B28-B29)/100)+B39*((B26-B27)/100)			

6. Procedures

ASTM standards were followed in preparing and testing samples, and any deviation from these standards is discussed in the following subsections. The standards and methods used to obtain the aggregate properties required to design different mixes are discussed in Chapter 4. Guidelines for mixing and sample preparation are found in ASTM C192 Standard Practice for Making and Curing Concrete Test Specimens in the Laboratory [41]. Slump tests were performed after mixing every batch in accordance with ASTM C143 Standard Test Method for Slump of Hydraulic Concrete [42]. Plastic air content of every mix was determined in accordance with ASTM C231 Standard Test Method of Freshly Mixed Concrete by the Pressure Method [43]. The density of each batch was determined in accordance with ASTM C138 Standard Test Method for Density (Unit Weight), Yield and Air Content (Gravimetric) of Concrete [44].

All specimens were cured in a lime water bath for 28 days, except the splitting tensile test specimens and freeze-thaw specimens. The splitting tensile test specimens were lime water cured for 7 days, after which the specimens were air cured for 21 days. The freeze thaw specimens were lime water cured for 14 days, after which the specimens were wrapped in burlap and kept moist until the start of the freeze thaw cycles.

6.1. Mixing

All mixes were prepared in a Crown Equipment C9 Concrete Mixer, Figure 6-1. After the mixer was rinsed out, the materials were added in the following order; coarse aggregate, fine aggregate, crumb rubber (if applicable), Portland cement, water and admixtures. The mixer would be turned on before the Portland cement was added to distribute the aggregates evenly. Once the water was added the mixer was ran for three minutes after which it was turned off for three more minutes, then turned on for another two minutes. Once the mixing was completed a slump test, an air content test and density tests were performed.

The slump test was performed using a standard cone meeting the requirements of ASTM C143, a 16 mm diameter tamping rod (16 inches in length), a metal pan, a measuring tape and a scoop.



Figure 6-1 Concrete Mixer Source: Primary

During the mixing period, the slump cone was dampened. The mold was filled in three separate lifts with 25 rod blows between each lift to achieve consolidation. After rodding, the mold is removed slowly, over a period of 5 seconds (+/- 2 seconds) and placed upside down next to the slumped concrete. The tamping rod was then placed across the top of the slump cone and the distance from the top of the slumped concrete (taken as a visual average) to the bottom of the rod was measured and taken as the slump. Concrete used for the slump test was returned to the batch and used in casting

The air content test was performed using a plastic air content bucket with a vertical air chamber (Figure 6-6-2), a 16 mm tamping rod (16 inches in length), a rubber mallet, and a squirt bottle. During the mixing period the bucket, lid and seal were all dampened. Concrete was placed in the bucket in three layers and rodded 25 times with each lift. After rodding, the outside of the bucket was struck with a mallet to close the air pockets that were left from rodding. Once the final lift was completed the tamping rod was used as a strike bar to level the concrete with the surface of the container. The lid of the bucket was then clamped on with the petcocks open. Water was then injected into one petcock until it flowed out the other one, this was repeated for the other petcock. The petcocks were then closed, and the air chamber was pumped until the pressure gauge met the calibration mark. After every 5 pumps the gauge was lightly tapped to remove any air locks that may have formed. With the pressure gauge at the calibration mark the main air valve was then



Figure 6-6-2 Air Meter, Source: Primary

opened and the reading on the pressure gauge recorded after the system came to equilibrium. Concrete used for the air content test was discarded and not used in casting.

The fresh mix density was found using a bucket with a 2.8 L volume, a 10 mm diameter tamping rod, and a mass balance. The mass of the bucket was found and recorded during the mixing time. Concrete was placed in the bucket in two separate lifts and rodded 25 times then using the tamping bar was struck level. The mass of the bucket and the concrete was then found and recorded. Concrete used for the density test was returned to the batch and used in casting.

6.2. Casting and Curing

For each batch of concrete prepared in the summer of 2017, five 100 mm diameter by 200 mm height cylinders were cast, three 150 mm by 300 mm height cylinders and three 150 mm by 150 mm by 500 mm prisms were cast. Three of the smaller cylinders were used for compressive strength testing while the remaining two were used for RCP tests, electrical resistivity both bulk and surface testing was performed on all five. The larger cylinders were used for splitting tensile tests and the prisms were used for flexural strength tests using third point loading. The cylinder molds were dampened during the mixing process and the prism molds were treated with Duoguard II water base form release agent produced by W.R Meadows. The 100 mm by 200 mm cylinders

were rodded using a 10 mm rod in 2 separate lifts, while the 150 by 300 mm cylinders were rodded using a 16 mm rod in 3 separate lifts. The prisms were rodded 54 times in two separate lifts. Once rodding was completed the samples were struck level with the top of their constituent mold. The prisms were also finished with a steel trowel after being struck to gain a feel for the workability of the different mixes.

For each batch of concrete produced in the spring of 2018 three 400 mm by 100 mm by 75 mm prisms were cast for freeze-thaw testing and at least two 100 mm by 200 mm cylinders. In addition, any tests that did not yield statistical significance in the summer were repeated and the required samples cast. The prisms were rodded 29 times in 2 separate lifts, then struck with the tamping rod, then finished with a steel trowel.

For both rounds of sample preparation, the samples were covered overnight by a piece of 6 mm poly. The following day samples were removed from their molds and marked with a unique identifier. The samples were then transferred to a lime water curing bath, that had at least 3 g/ L of high calcium hydrated lime mixed in to satisfy the requirements of ASTM C511 Standard Specification for Mixing Rooms, Moist Cabinets, Moist Rooms and Water Storage Tanks used in the Testing of Hydraulic Cements and Concretes [45]. The 100 mm by 200 mm cylinders along with the larger prisms were cured for 28 days before being tested. The 150 mm by 300 mm cylinders were cured for 7 days in lime water and 21 days in air. The smaller prisms were cured for 14 days in lime water.

To ensure good surfaces for bulk resistivity testing all the smaller cylinders had a slight amount of concrete sawn off the end for the summer 2017 testing as a cylinder grinder was not available. The cylinders that were used for compressive strength testing were sulfur capped after being tested for bulk resistivity to reduce eccentricities. A cylinder grinder was available for the spring testing and sulfur capping was not necessary.

6.3. Electrical Resistivity (Bulk and Surface)

Three different devices were used to determine the bulk electrical resistivity of the concrete samples; the RCON produced by Giatec, the Merlin produced by Germann Instruments and the Resipod produced by Proceq. Only one device was used to determine the surface resistivity, the Resipod. Since surface resistivity tests require the sample to be in a saturated surface wet (SSW) state these tests were performed first after which the samples could come to a saturated surface dry (SSD) condition and the bulk resistivity was determined. The ends of the samples were kept wet between tests by using the cylinder end caps and foam inserts that came with the Merlin system.

To determine surface resistivity, first the samples diameter and length were measured and recorded. Then a mark was made in the center of one of the cylinder faces. From this mark intersecting lines were drawn on the sample so that 90° rotations were marked out. The sample was then placed on the provided stand with one of the marks pointing directly upwards. The Resipod was turned on and the contacts dipped in water. Next, the Resipod was placed over the sample such that the contacts were in line with the upward facing mark and the center of the sample was between the two inner probes of the Resipod. The Resipod was then firmly pushed downwards and a reading was taken and recorded. The sample was then rotated 90° and another reading was obtained. This was repeated until the sample had made two complete revolutions. The average of the eight readings multiplied by 1.1 to correct for lime water curing, was taken as the surface resistivity of the sample.

To determine bulk resistivity using the Resipod, the contacts and springs were removed from the probes and the Resipod was mounted in the provided stand. Cables were then attached to where the contacts and springs were and plugged in to two separate plates. The two foam inserts were then moistened. The resistivity of one of the foam inserts was determined and recorded by placing it between the two plates, this insert would be on top of the sample for the sake of the test. The resistivity of the other foam insert was determined by placing it between the plates and placing the sample to be tested on the top plate, this insert would be placed below the sample for the test. The sample was then placed between the plates and inserts, and the resistivity recorded. The resistivity then was corrected by first subtracting the resistivity of the two inserts and applying a correction factor. The correction factor is applied by first dividing the cylinder resistivity by $2 \cdot \pi \cdot 3.8$, then

multiplying by the ratio Area/Length where the area is the cross-sectional area not the surface area. This corrected value was taken as the bulk resistivity of the sample.

To use the RCON the first step is to connect the device to a laptop with RCON DM software installed. Foam inserts were moistened and placed on both sides of the sample, all of which were placed between the conductive plates. The top plate was clamped down with the nuts on the rods. A new project file needs to be started for every sample. Once the new project was opened the 100 mm by 200mm cylinder sample size was selected. Readings were taken at 1, 10, 40, 100, 300, 1000 and 10000 Hz. The readings at 40 and 300 Hz were taken so that a comparison could be made to the other two devices. The rest of the readings were taken in a logarithmic manner, so that any effects that the crumb rubber may have had on capacitance could be observed. The reading at 300 Hz was taken as the samples resistivity after a geometric correction factor was applied. First the Length/Area that was programmed in to the software was multiplied by the reading, then the Area/Length of the actual sample was multiplied by this value.

To use the Merlin the first step was to connect the device to a laptop with the Germann Instruments Merlin conductivity/resistivity software installed. After opening the software, samples were placed on the stand provided in the same manner that was used for the Resipod stand. The two foam ends of the Merlin were sprayed with water before mounting the device on the specimen. The actual diameter and length were input in to the software and resistivity was chosen to be measured. The test was started, and a reading was taken. This reading was divided by ten to match the units of the other two devices and then recorded. No correction to this reading needed to be performed.

6.4. Rapid Chloride Penetration Test

Rapid Chloride Penetration tests were performed in accordance with ASTM C1202 Standard Test Method for Electrical Indication of Concrete's Ability to Resist Chloride Ion Penetration [46]. After the resistivity testing was performed two 50 mm samples were cut from two cylinders for a total of four 50 mm height by 100 mm diameter cylinders. One of these cylinders from each sample was conditioned and tested while the other sample remained as a referee in case of inconclusive results. This test consisted of two main components, conditioning and testing. For the conditioning a vacuum pump, chamber with a two way stop cock, and a water trap were used. For the testing,

two load cells, two power supplies and two Agilent digital multimeters with Keysight technology integration were used.

To condition the samples, they were placed in a desiccator and a vacuum of 50 mmHg was maintained for 3 hours. Once this was achieved de-aired water was added to cover the samples in the desiccator and the vacuum maintained for another hour. After this hour was up the vacuum was turned off and air could re-enter the desiccator, the samples were soaked for 18 hours (+/- 2 hours).

To test the samples, the samples were placed in load cells provided by Giatec. These load cells use rubber gaskets to seal the samples hence no need of a curing compound in the conditioning step. Once the cells were tightened, a 3 % by mass NaCl solution was added to the anode side and a 0.3 N NaOH solution (12 g/L) added to the cathode side. The cell was then checked for leaks and retightened if need be. The test was started by applying a 60 V direct current across the specimen and a current reading recorded. Current readings were recorded every 30 minutes until 6 hours had passed. This current was integrated with time using the trapezoidal rule to find the charge passed in coulombs. This charge was then checked against Table X1.1 from ASTM C1202 [46] to classify the specimens chloride ion penetrability.

To facilitate ease of data collection Keysight's command expert was used to write a sequence of SCPI commands to log the current from the two different multimeters. Keysight command expert has an Excel add-in to store the data and perform the integration, as well as produce a current vs. time plot. The SCPI commands are in Appendix F. A screen shot of the excel sheet is shown in Figure 6-3.

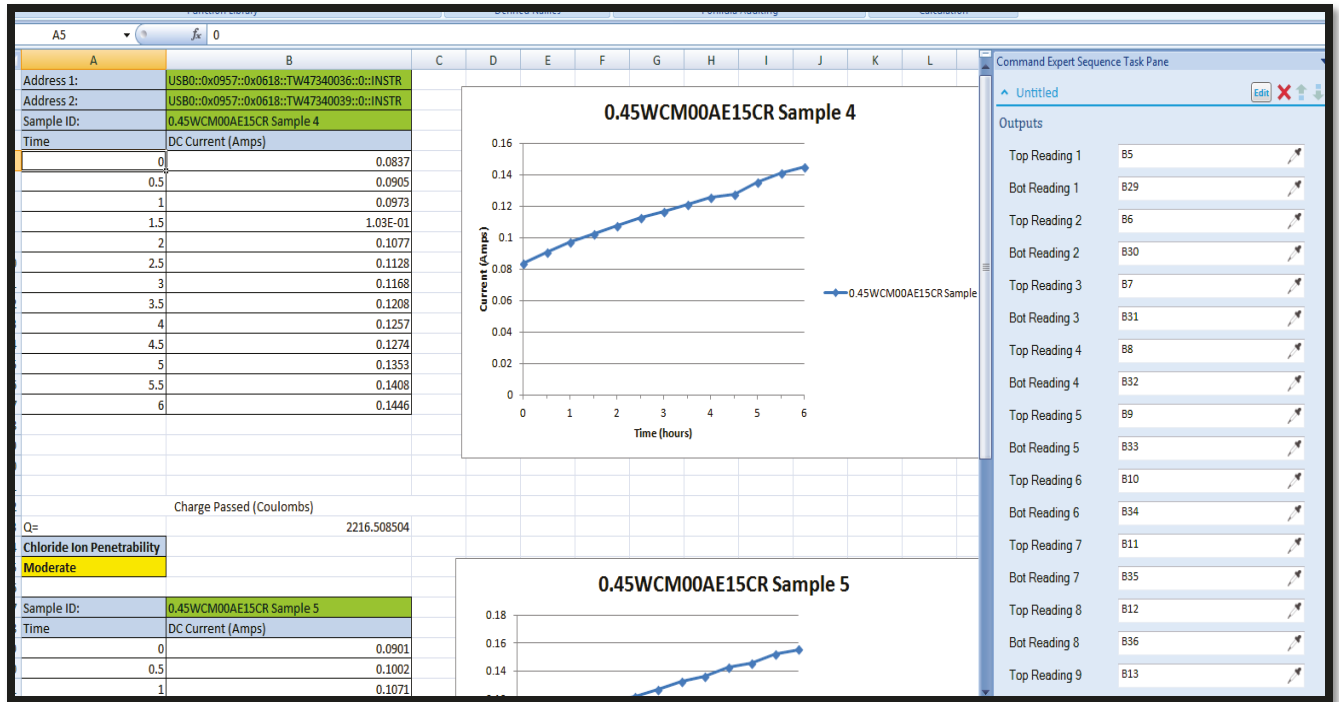


Figure 6-3 RCP Excel Sheet, Source: Primary

6.5. Compressive Strength

ASTM C39 Standard Test Method for Compressive Strength of Cylindrical Concrete Specimens [47] was followed. Samples were crushed using a SATEC hydraulic press and the maximum load recorded. After a sample was tested the fracture type was visually identified and recorded. Since the output of the hydraulic press was pounds, this number was first converted to kN using Excel's convert function. Then using the geometric data gathered during the resistivity tests along with the maximum load the compressive strength was calculated using Equation 6-1

$$f_{cm} = \frac{4000P_{max}}{\pi D^2} \quad 6-1$$

Where: f_{cm} = Compressive strength, MPa

P_{max} = Maximum Load, kN

D = Average diameter mm [47]

During the summer 2017 a cylinder grinder was not available, so specimens were sulfur capped. To sulfur cap a fume hood was turned on above the melting pot containing the sulfur compound. The melting pot was running for a few hours, while resistivity testing was being performed. Long

sleeve lab coats and laboratory oven mitts were required PPE to be worn before proceeding. A steel mold for the cap was lubricated with WD-40 then hot liquid compound poured into the mold. The sample was then gently placed in the compound and held in place momentarily while the compound set. The sample and cap were released from the mold with a few light hammer blows. This was repeated for the other side of the sample.

6.6. Flexural Strength

ASTM C78 Standard Test Method for Flexural Strength of Concrete (Using Simple Beam with Third-Point Loading) [48] was followed. The specimen's length, width and depth were all measured prior to testing. To begin the centre of the beam was found and then marked with a permanent marker using a steel tape. From this mark two more marks were made 225 mm on either side of it. This was so that the effective length of the beam was 450 mm. Using a straight edge these marks were extended so that solid lines were on at least three faces of the specimen. From these two outer marks two more marks were made 150 mm on the interior side of both marks and extended to lines on three faces. Two steel roller supports were placed on the base plate of the SATEC hydraulic press, underneath the specimen in line with the outer marks. A steel head with two roller points 150 mm apart was placed so that the two roller points rested on the inner marks. The hydraulic press was then used to cause the specimen to fail. The max load was recorded, and a value determined if the fracture occurred outside of the middle third of the specimen. The max load was converted to Newtons using Excel's convert function. Using the geometric data and the max load the modulus of rupture was determined according to Equation 6-2.

$$R = \frac{PL}{bd^2} \quad \text{Equation 6-2}$$

Where: R = Modulus of Rupture (MPa)

P = Max Applied Load (N)

L = Span (mm)

b = Width (mm)

d = Depth (mm)

6.7. Splitting Tensile Strength

ASTM C496 Standard Test Method for Splitting Tensile Strength of Cylindrical Concrete Specimens [49] was followed. Each specimen's length and diameter were determined prior to testing. A steel jig was used to hold the sample in place (Figure 6-6-4). To begin two wooden shims were placed at the bottom of the jig to keep the specimen from rolling, then the specimen was placed in the jig and visually centred. After which two bearing bars were placed across the specimen in the jig to transfer load from the hydraulic press. The hydraulic press was then used to cause the specimen to fail, and the maximum load recorded. Once the sample was removed from



Figure 6-6-4 Splitting Tensile Jig, Source: Primary

the jig, the two halves were laid with the former interior side face up. A visual percentage of how much of the failure occurred in the coarse aggregate was then recorded. After using Excel's convert function to convert the recorded load from pounds to Newtons, the splitting tensile strength was calculated according to

$$T = \frac{2P}{\pi ld} \quad \text{Equation 5-3}$$

Where: T = Splitting Tensile Strength (MPa)

P = Maximum Load Applied (N)

l = Specimen Length (mm)

d = Specimen Diameter (mm)

6.8. Freeze-Thaw Test

ASTM C666 Standard Test Method for Resistance of Concrete to Rapid Freezing and Thawing [50] was followed. A Humboldt 3186-S Freeze Thaw Cabinet was used as it meets the requirements of Procedure A Rapid Freezing and Thawing in water. Specimens were stored at the thaw temperature until the beginning of the test. To bring the cabinet to the thaw temperature the machine was programmed to go through 1 cycle of freeze-thaw and then hold the thaw temperature. Specimens were added to the machine and routinely checked to maintain a constant water level. Before beginning the test and after every 30 cycles the fundamental frequency was determined, this is repeated until 300 cycles have been achieved. This was used to obtain the relative dynamic modulus of elasticity from:

$$P_c = \left(\frac{n_1^2}{n^2} \right) \times 100 \quad \text{Equation 6-4}$$

Where: P_c = Relative Dynamic Modulus of Elasticity, after c cycles of freezing and thawing, percent

n_1 = Fundamental Transverse Frequency after c cycles of freezing and thawing

n = Fundamental Transverse Frequency at 0 cycles of freezing and thawing.

The relative dynamic modulus of elasticity is used to calculate the durability factor as follows

$$DF = PN/M \quad \text{Equation 6-5}$$

Where: DF = Durability Factor

P = Relative Dynamic Modulus at N cycles %

N = Number of cycles at which P reaches the predetermined cut-off or number of cycles of the test whichever is less

M = Number of cycles at which test is to be terminated

Before starting the test, the fundamental frequency in the transverse mode was determined in accordance with ASTM C215 Standard Test Method for Fundamental Transverse, Longitudinal, and Torsional Resonant Frequencies of Concrete Specimens [51]. The impact resonance method was used to determine the fundamental transverse frequency. Due to the hardware available time domain data was gathered at the test and post-processed in MATLAB. To begin each sample's

geometry and mass were determined and recorded. Two lines were drawn on three faces of the samples a distance of 0.224 of the length from the end to mark the nodal points where the specimens were to be supported. The specimens were supported on roller supports, the same ones used for the flexural strength tests. An adxl-337 accelerometer was affixed with UHU-tac to the end of the specimen once it was dry enough to adhere. This accelerometer was connected to a data acquisition (DAQ) system along with associated software that was provided by Bruce Misner an engineering technologist at Lakehead University. This DAQ was then connected to a laptop and the provided software opened. A sampling frequency of 20000 Hz was chosen and as soon as the sampling was triggered in the software the concrete specimen was struck with a hammer. The acquisition was halted, and the data file was then exported to MATLAB for further processing. The code is available in Appendix F.

The fundamental frequency was then chosen from the frequency plot. A typical frequency plot is shown in Figure 6-5. The largest peak is taken as the fundamental.

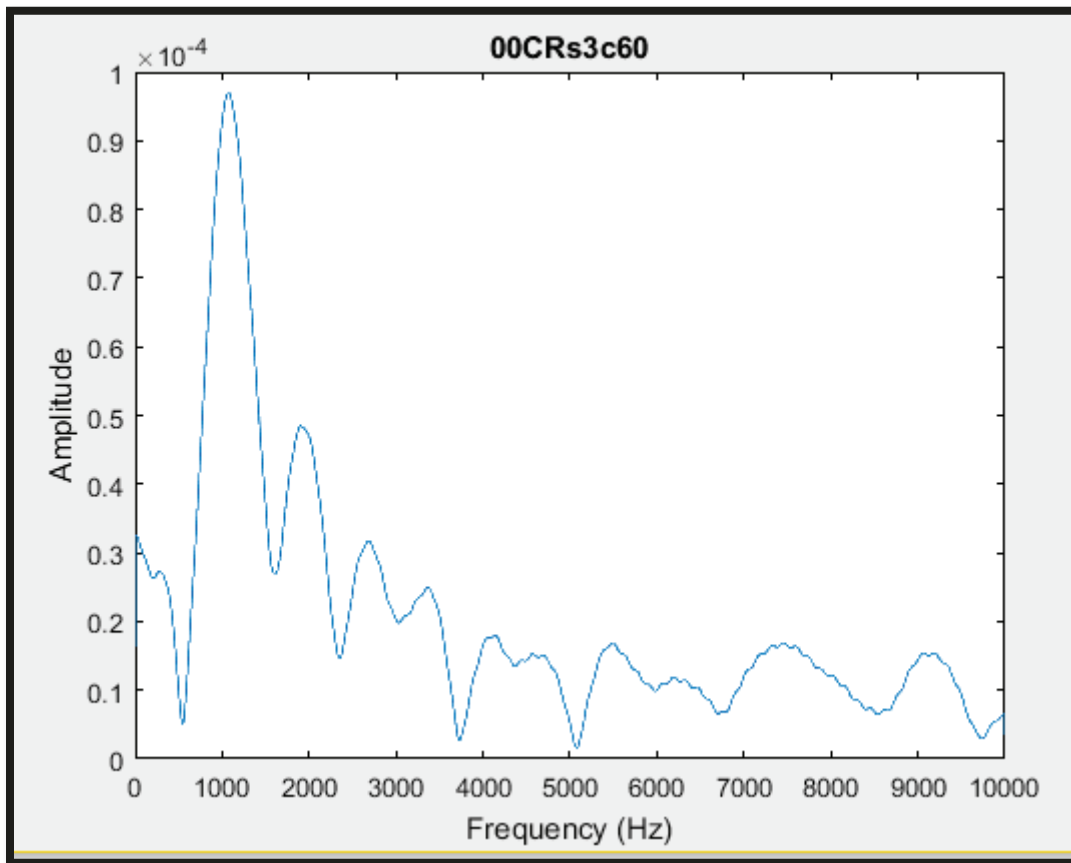


Figure 6-5 Example Frequency Plot, Source: Primary

7. Results

7.1 Compressive Strength

Taken as the average of the two closest values out of three tests, a declining compressive strength trend is observed with the addition of crumb rubber used as portion of fine aggregate (Table 7-1 and Table 7-2). The reason for the drastic increase of compressive strength for the samples tested in the spring of 2018 is most likely laboratory induced as the lime used in the curing water was a different brand than that of the lime used in the summer of 2017. This may be investigated in another research project.

The MTO mix had a water cement ratio of 0.4 and was cast to mimic MTO pavement requirements. The 0 % crumb rubber mix had a water cement ratio of 0.45 as did the mixes that contained crumb rubber. The low value of 28 day compressive strength for the control mix is believed due to the low slump of mixture interfering with the rodding procedure and not obtaining proper consolidation.

Table 7-1 Compressive Strength Result

Crumb Rubber Replacement as Percent of Mineral Aggregate (%)	Crumb Rubber Replacement as Percent of Fine Aggregate (%)	28 Day Compressive Strength (MPa)
0	MTO	19.7 (Not Used)
0	0	36.0
3.7	5	30.2
7.4	10	29.2
11.1	15	27.6
14.8	20	22.5
18.5	25	24.5

Table 7-2 Compressive Strength Results for Repeated Mixes

Crumb Rubber Replacement as Percent of Mineral Aggregate (%)	Crumb Rubber Replacement (%)	28 Day Compressive Strength (MPa)
0	MTO	46.8
0	0	N/A
3.7	5	39.7
7.4	10	39.5
11.1	15	37.6
14.8	20	27.7
18.5	25	N/A

A visual asymptote of 24 MPa was chosen to find the curve fit parameters for the SRF developed by Khatib and Bayomy [29]. The parameter m was found using multiple goal seek analyses in Microsoft Excel. A conservative parameter was chosen. These parameters are summarized in Table 7-3. It should be noted that the model suggested by Khatib and Bayomy considers crumb rubber fraction as a percent of the total mineral aggregate content where in this study the replacement fraction is of the fine aggregate volume only. A graph of the SRF model and the obtained data is shown in Figure 7-1, in which the rubber contents have been corrected to be a percentage of the total mineral aggregate for direct comparison to Khatib and Bayomy's results [29].⁵

Table 7-3 SRF Model Parameters for Compressive Strength

SRF Model Parameters		
a	b	m
0.67	0.33	18

⁵ 3.7 % of the total mineral is equal to 5% of the fine aggregate as the total aggregate content was 74% by volume

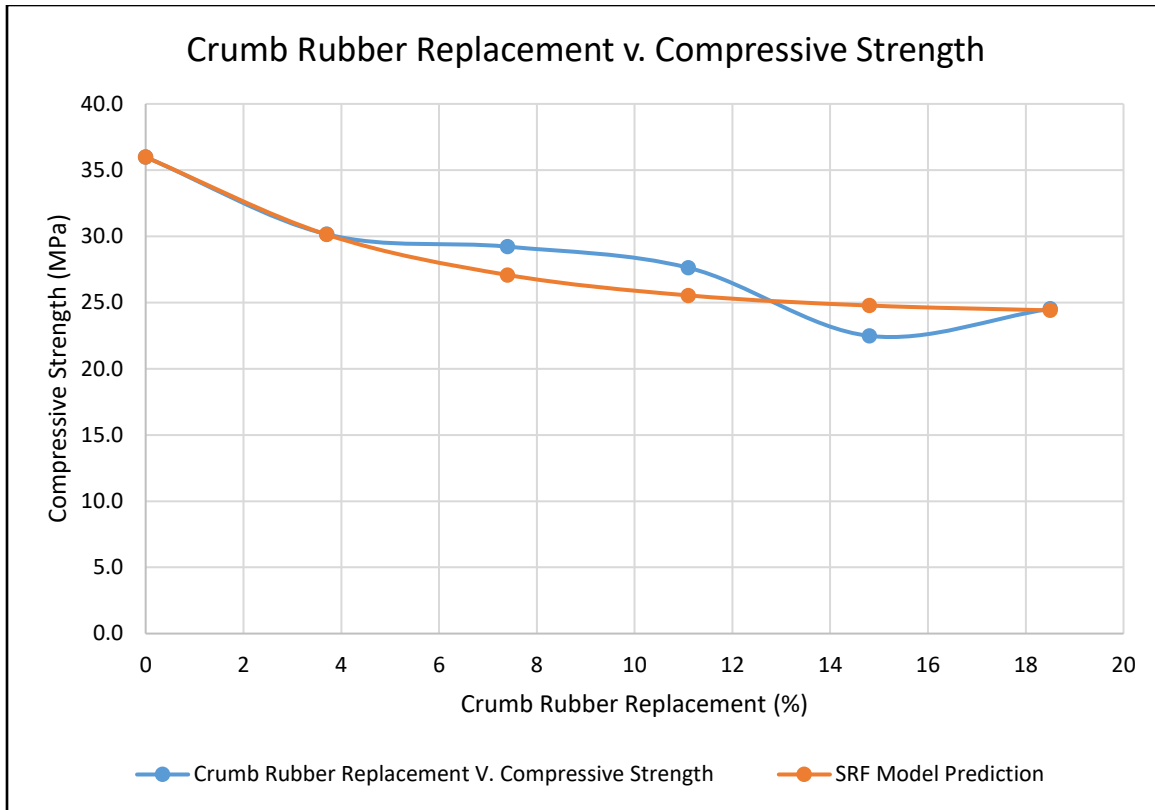


Figure 7-1 Crumb Rubber v. 28 Day Compressive Strength

7.2. Splitting Tensile Strength

Taking the average of the two closest values of three trials a declining trend is also noticed in the splitting tensile strength with the addition of a rubber fraction (Table 7-4 and Table 7-5). The increasing trend seen in the repeated mixes most likely laboratory induced for the same reason an increase in compressive strength was found.

The curve fitting parameters for the SRF model were different from that used for compressive strength. The value of a was chosen such that the lowest value obtained in the test results could still be conservatively estimated using this model. The curve fit parameters are summarized in Table 7-6. A graph of the model and the actual results is shown in Figure 7-2, in which the rubber contents have been corrected to be a percentage of the total mineral aggregate for direct comparison to Khatib and Bayomy's results [29].

Table 7-4 Splitting Tensile Strength Results

Crumb Rubber Replacement as Percent of Mineral Aggregate (%)	Crumb Rubber Replacement (%)	Splitting Tensile Strength (MPa)
0	MTO	3.49
0	0	3.11
3.7	5	3.08
7.4	10	2.66
11.1	15	2.85
14.8	20	1.97
18.5	25	2.06

Table 7-5 Splitting Tensile Strength Results for Repeated Mixes

Crumb Rubber Replacement as Percent of Mineral Aggregate (%)	Crumb Rubber Replacement (%)	Splitting Tensile Strength (MPa)
0	MTO	2.99
0	0	3.02
3.7	5	3.29
7.4	10	3.65
11.1	15	N/A
14.8	20	2.29
18.5	25	N/A

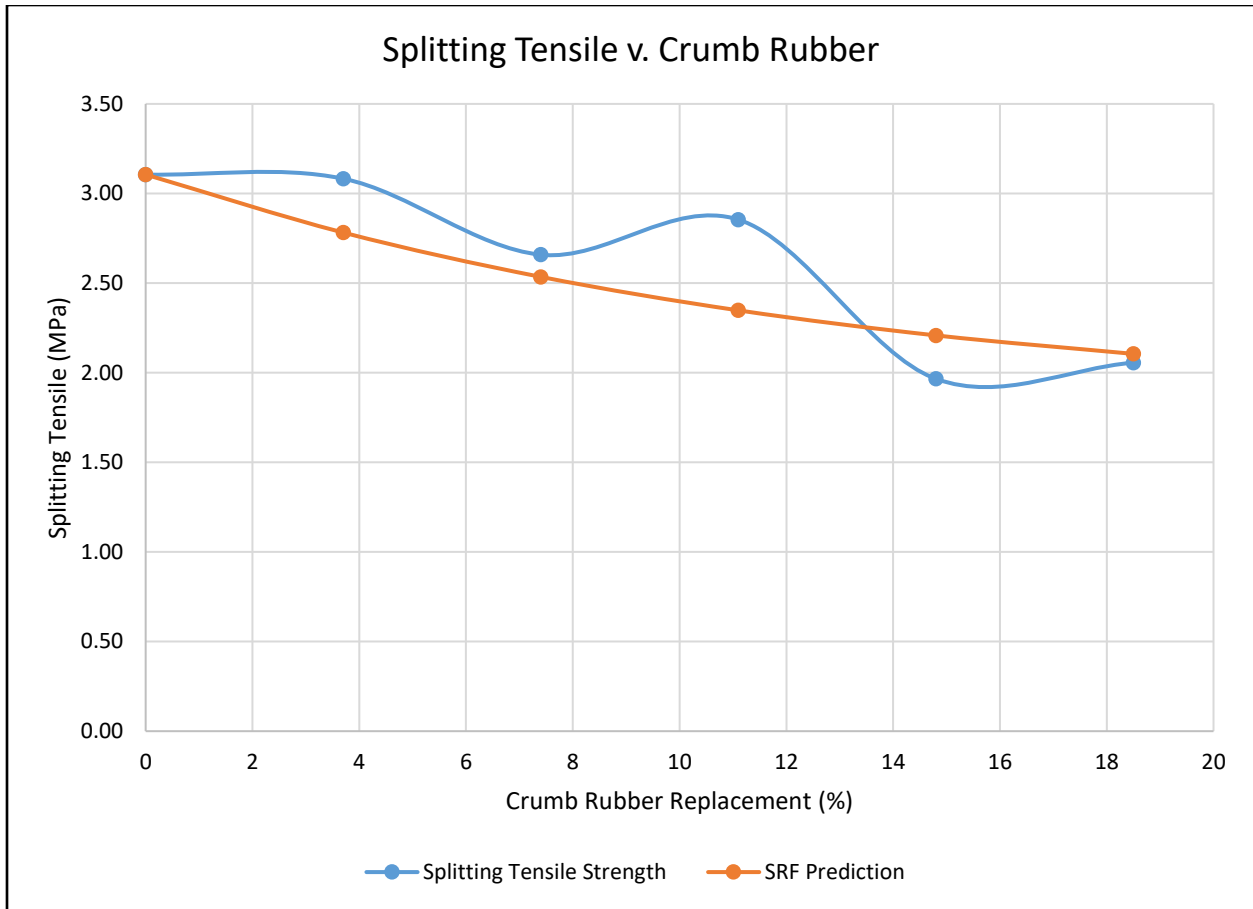


Figure 7-2 Splitting Tensile Strength v. Crumb Rubber

Table 7-6 SRF Model Parameters for Splitting Tensile Strength

SRF Model Parameters		
a	b	m
0.6	0.4	8

7.3. Flexural Strength

As predicted the flexural strength decreased with the addition of crumb rubber. Table 7-7 and Table 7-8 show the results of the flexural strength tests by taking the average of the closest two of three trials.

Table 7-7 Flexural Strength Results

Crumb Rubber Replacement as Percent of Mineral Aggregate (%)	Crumb Rubber Replacement (%)	Modulus of Rupture (MPa)
0	MTO	6.13
0	0	5.91
3.7	5	5.20
7.4	10	5.65
11.1	15	5.15
14.8	20	5.12
18.5	25	5.04

Table 7-8 Flexural Strength Results for Repeated Tests

Crumb Rubber Replacement as Percent of Mineral Aggregate (%)	Crumb Rubber Replacement (%)	Modulus of Rupture (MPa)
0	MTO	N/A
0	0	N/A
3.7	5	N/A
7.4	10	N/A
11.1	15	N/A
14.8	20	4.69
18.5	25	N/A

The SRF curve parameters were derived in the same manner as that of the compressive strength and are shown in Table 7-9. A graph of the model and results is shown in Figure 7-3, in which the rubber contents have been corrected to be a percentage of the total mineral aggregate for direct comparison to Khatib and Bayomy's results [29]

Table 7-9 SRF Model Parameters for Flexural Strength

SRF Model Parameters		
a	b	m
0.85	0.15	16

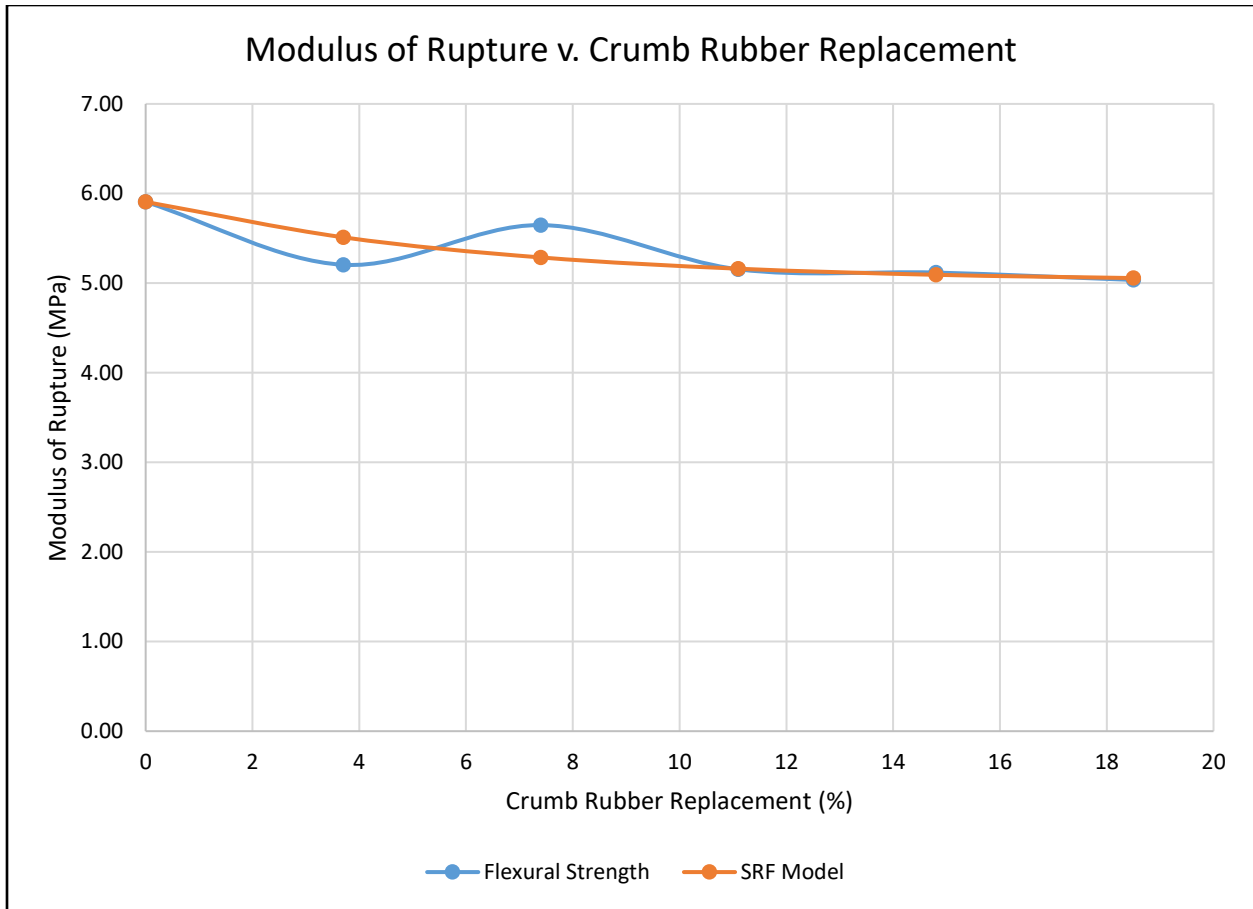


Figure 7-3 Modulus of Rupture v. Crumb Rubber

The value of alpha from the ACI equation is larger than that found by both Toutanji and Siringi et al. [15] [20] and is summarized in Table 7-10.

Table 7-10 Alpha factor in ACI Modulus of Rupture Equation

Crumb Rubber Replacement (%)	α
0	0.98
5	0.95
10	1.04
15	0.98
20	1.08
25	1.02
Average	1.01

7.4. Bulk Resistivity

The bulk resistivity increases with the addition of crumb rubber to the concrete mix. The results of the bulk resistivity obtained with the three different devices are shown in Table 7-11 and Table 7-12. It should be noted that for the repeated tests, any test in which compressive strength tests were not performed only had two cylinders to sample, the rest had five. The reason for the higher values read by the Resipod is attributed to a lack of clamping force on the electrodes, leading to less surface contact with the concrete sample. The other two devices do have some sort of clamping mechanism putting a compressive force on the cylinder and electrodes. The larger value of bulk resistivity for the five percent crumb rubber replacement should be treated as an outlier. The mix with 25 % crumb rubber replacement had the least variability across the devices and represents the maximum increase that could be expected due to crumb rubber substitution. The percent increase row is calculated by subtracting the value for 0 % replacement from the value from 25 % replacement and dividing by the value for 0 % replacement.

Table 7-11 Bulk Resistivity Results

Crumb Rubber Replacement (%)	Resipod (kΩcm)	Merlin (kΩcm)	RCON @ 300 Hz (kΩcm)
MTO	9.72	6.938	6.82
0	8.34	5.88	5.94
5	10.92	6.86	6.34
10	9.26	6.16	5.96
15	8.47	6.06	5.68
20	9.54	6.76	6.38
25	10.24	7.04	6.52
% Increase	23	20	10

Table 7-12 Bulk Resistivity Results for Repeated Mixes

Crumb Rubber Replacement (%)	Resipod (kΩcm)	Merlin (kΩcm)	RCON @ 300 Hz (kΩcm)
MTO	9.37	7.9	8.08
0	7.35	5.3	6.7
5	8.76	6.3	6.62
10	8.72	6	6.4
15	7.58	6.52	6.96
20	10.37	7.424	7.42
25	9.66	7.55	7.45
% Increase	31	42	11

A plot of the bulk resistivity against the crumb rubber replacement is shown in Figure 7-4. It can be seen in this figure that the bulk resistivity is relatively unaffected by the presence of low amounts of crumb rubber but starts to increase after the rubber replacement surpasses 10 % of the fine aggregate.

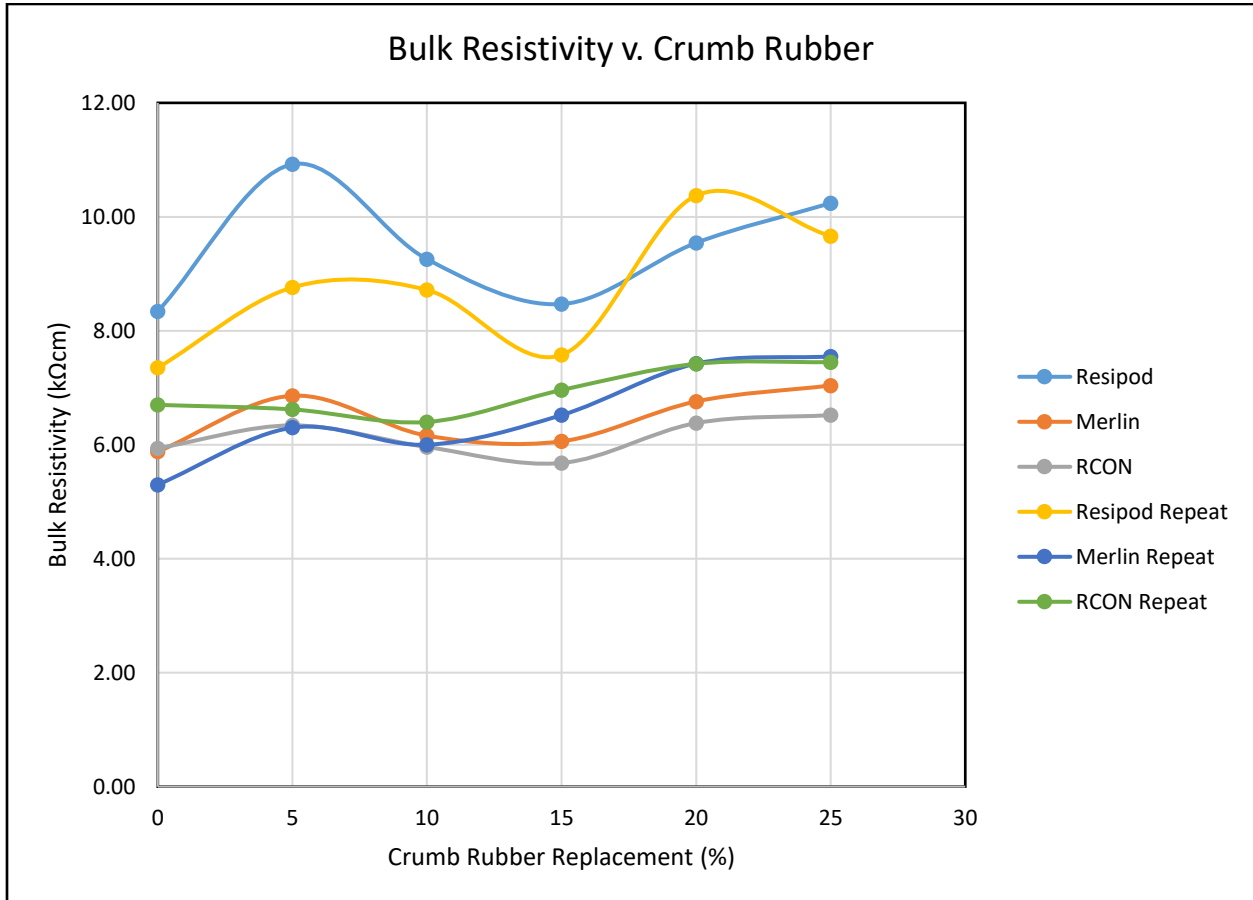


Figure 7-4 Bulk Resistivity v. Crumb Rubber

7.5. Surface Resistivity

The surface resistivity follows similar trends as that seen for the bulk resistivity. The results are summarized in Table 7-13 and Table 7-14. A plot of the results is shown in Figure 7-5.

Table 7-13 Surface Resistivity Results

Crumb Rubber Replacement (%)	Surface Resistivity (kΩcm)
MTO	19.86
0	17.14
5	17.60
10	16.79
15	17.38
20	19.96
25	19.93
% Increase	16

Table 7-14 Surface Resistivity Results for Repeated Mixes

Crumb Rubber Replacement (%)	Surface Resistivity (kΩcm)
MTO	21.63
0	14.69
5	17.58
10	17.46
15	17.75
20	19.37
25	18.51
%Increase	26%

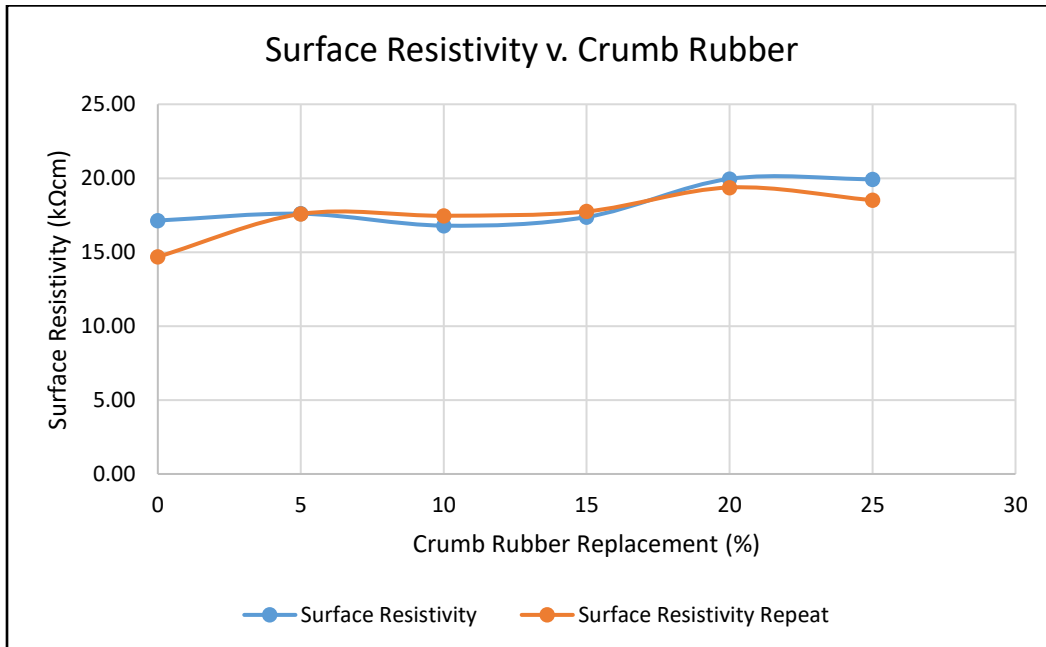


Figure 7-5 Surface Resistivity v. Crumb Rubber

7.6. Rapid Chloride Penetration

For detailed RCP test results see Appendix D. The results from the rapid chloride penetration test show that crumb rubber does decrease the susceptibility of concrete to chloride ingress a small amount but not enough to be relied upon for design. A plot of the charge passed in coulombs against the amount of crumb rubber added is shown in Figure 7-6. Each point is the average of two samples containing the same proportion of crumb rubber.

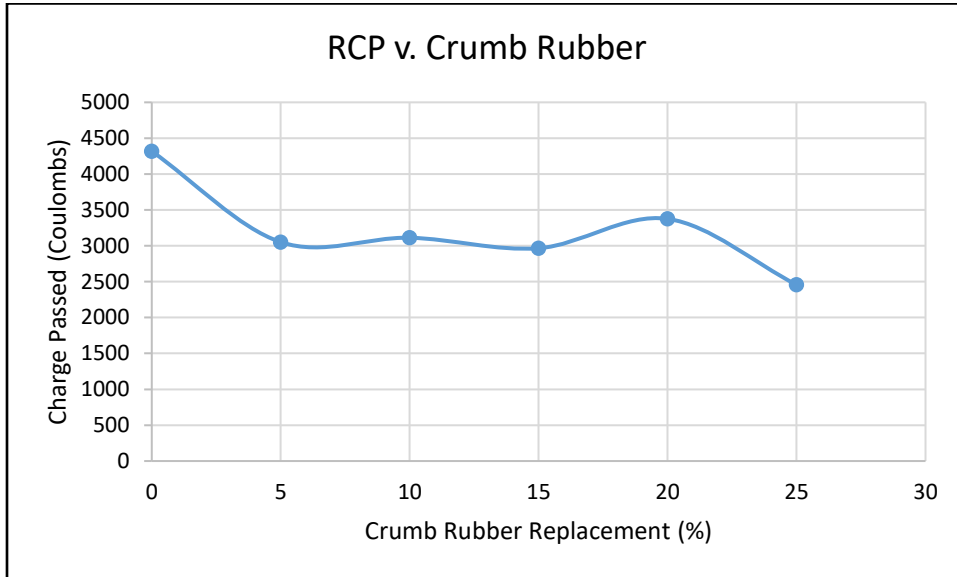


Figure 7-6 RCP Test Results v. Crumb Rubber

7.7. Air Entrainment

The results of the plastic air content tests are shown in Table 7-15 and Table 7-16. The reason for the outlier values in the repeated mixes is the air meter used may have needed to be recalibrated. Figure 7-7 shows a plot of the air content against the crumb rubber content. The air content at 0% can be taken as the mechanically entrapped air due to the mixing process.

Table 7-15 Air Content Results

Crumb Rubber Replacement (%)	Plastic Air Content (%)
0	2.2
5	2.6
10	3.2
15	3.4
20	4.2
25	4

Table 7-16 Air Content Results for Repeated Mixes

Crumb Rubber Replacement (%)	Plastic Air Content (%)
0	2.5
5	3.2
10	5
15	8
20	7.5
25	4.5

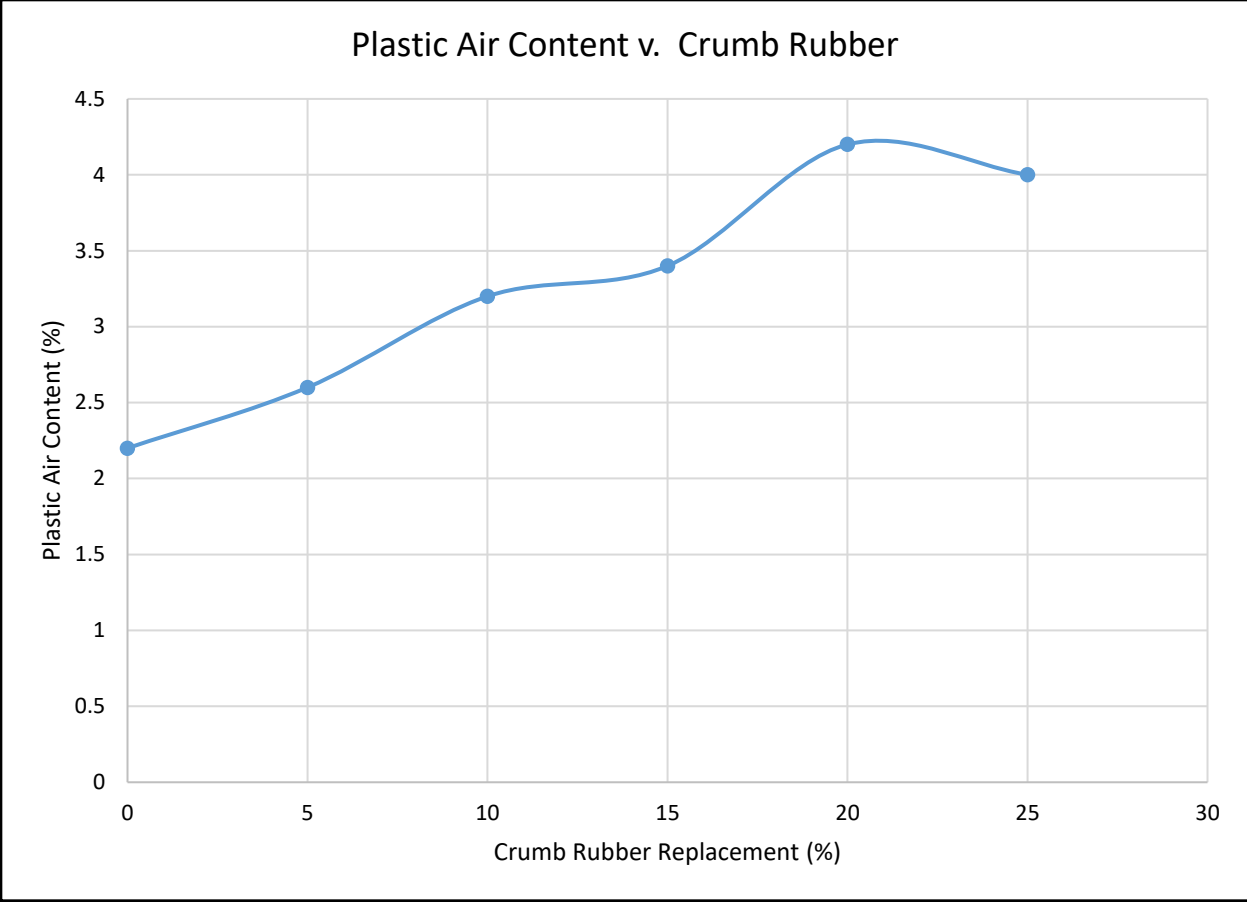


Figure 7-7 Air Content v. Crumb Rubber

7.8. Freeze Thaw

At the beginning of the freeze thaw testing there was difficulty tuning the data acquisition system and as such much lower fundamental frequencies were read at zero cycles of freezing and thawing than subsequent cycles. The effect of this was that the durability factors for most samples was 100. Appendix E has a table of these results. A plot of the relative dynamic moduli calculated throughout the course of a test does show that the dynamic moduli was increasing with increasing rubber content (Figure 7-8).

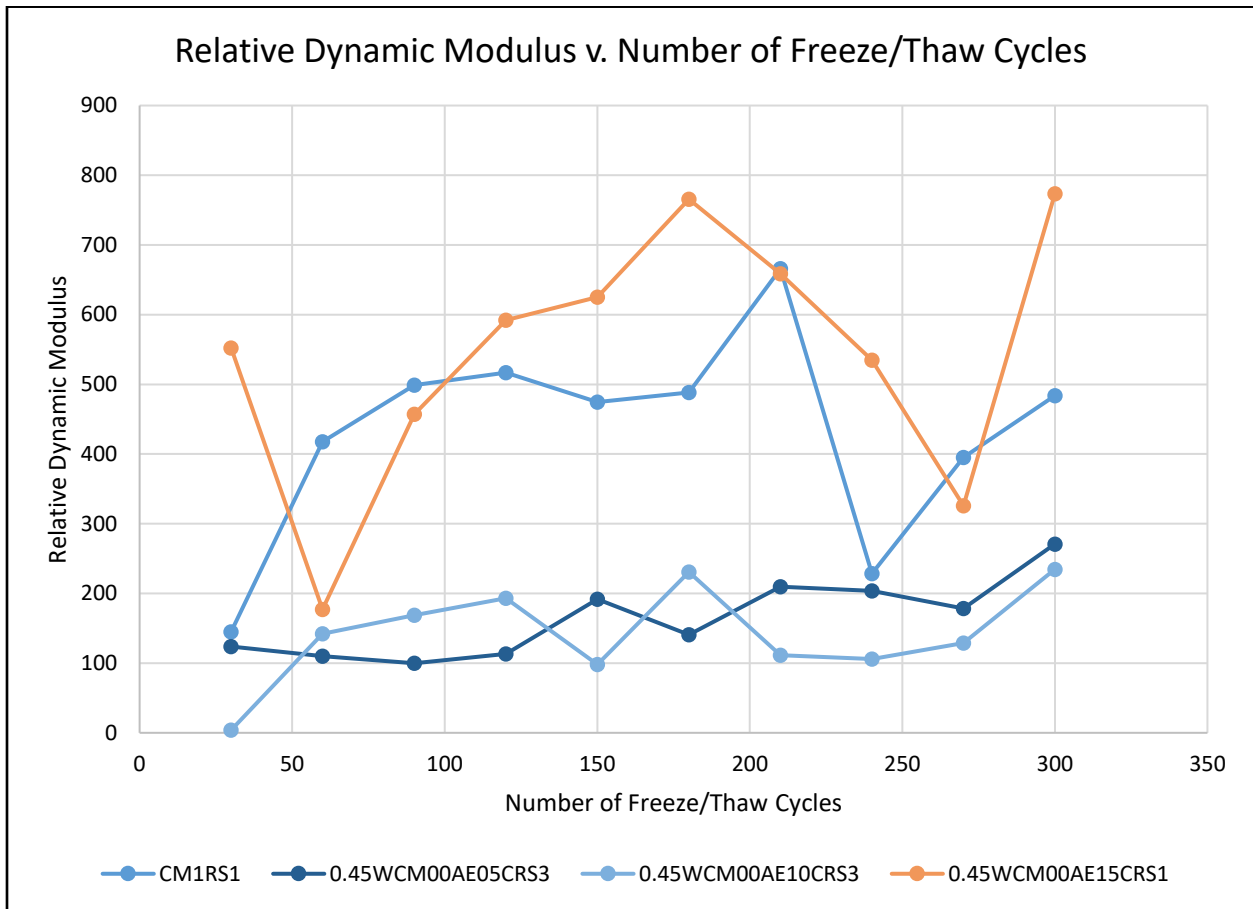


Figure 7-8 Relative Dynamic Moduli v. Freeze Thaw Cycles

8. Discussion

8.1. Compressive Strength

The results indicate that 28-day compressive strength of 25 MPa can be achieved with crumb rubber replacement levels as high as 15 %. Therefore, crumb rubber concretes containing up to 15 % crumb rubber can be used as a suitable building material for many structures. As was expected, it is observed that the finer crumb rubber particles have a lesser influence on the compressive strength than that of coarser particles such as chips or fibres. The large value of a , 0.67 as opposed to 0.1 used by Khatib and Bayomy [29] in the SRF model is indicative that the smaller particle size of crumb rubber has less of an influence on the compressive strength than coarser particles such as chips or fibres.

The increase in post fracture strength was also observed in the compressive strength samples. Instead of abrupt failure of the specimen, it was slow and controlled. This is a more desirable failure mode for concrete structures as it gives some warning to occupants that the structure is no longer safe before collapse. Figure 8-1 shows a failed compressive strength specimen that has had 15 % of the fine aggregate replaced with crumb rubber. While there is a clear crack on the surface indicating failure of the compressive strength test, this specimen is still able to sustain a substantial compressive load.



Figure 8-1 Failed Compressive Strength Specimen, Source: Primary

8.2. Splitting Tensile Strength

A decrease in splitting strength with addition of crumb rubber is observed. Values larger than 2 MPa are possible with crumb rubber concretes using up to 15 % fine aggregate replacement. The curve fit parameters for the SRF model indicate that the splitting tensile strength almost follows a linear trend and is directly dependent on the amount of rubber added. Again it is confirmed that the smaller particles have less of a detrimental influence on the mechanical properties, hence the much larger value of a .

8.3. Flexural Strength

The flexural strength decreased with the addition of crumb rubber as was to be expected. The SRF curve fit parameters indicate that the modulus of rupture is very sensitive to the presence of crumb rubber but not dependent on it. While the SRF model does not give a conservative prediction of the modulus of rupture for a 5 % crumb rubber replacement, the overestimation is only by four percent and this can be accounted for by applying a safety factor when designing flexure controlled concrete structures. The greater α value from the ACI modulus of rupture equation indicates that crumb rubber has a lesser influence on the flexural strength than it does on compressive strength. This further confirms the hypothesis put forward by Siringi et al. [20] that the weak

interfacial bonds are more pronounced in tension than compression. The larger value of α also confirms that the influence of smaller rubber particles is less detrimental than more coarse particles.

8.4. Bulk Resistivity and Surface Resistivity

The increase of the electrical resistivity is attributed to two main factors. The first being that rubber in itself acts as an electrical insulator and as such is impeding the flow of electrical currents. The second being the entrained air caused by the hydrophobic nature and weak interfacial bonding of the crumb rubber is further acting as an insulator. Since at least a 15 % replacement level is required for a substantial increase in the bulk resistivity of the concrete, any mix containing less crumb rubber should be thought of as if no crumb rubber is present regarding electrical resistivity. For mixes containing more than 15 % crumb rubber an increase of 10-30 % depending on the amount of rubber used can be expected in the bulk resistivity. In certain cases, this may be enough to reduce the chloride penetration classification in ASTM C1202 [46].

8.5. Rapid Chloride Penetration

The results of the rapid chloride penetration confirm the results found with the electrical resistivity testing. That is that the susceptibility of the concrete to chloride ingress is reduced. Larger amounts of crumb rubber do seem to cause a significant change to the rapid chloride penetration results. However these larger portions of rubber are more detrimental to the mechanical performance of the concrete mixture.

8.6. Air Entrainment

As it was expected, the crumb rubber did increase the plastic air content of the mix. It appears to be an almost linear relationship with every 5 % increment of crumb rubber added increasing the plastic air content by 0.5 %. This may be enough air entrainment to forgo the use of air entraining agents in concrete exposed to low to moderate amounts of freeze-thaw cycles.

8.7. Freeze-Thaw

Since the reference frequency was low for most of the tests, it is impossible to assign a durability factor to any given sample. Increasing relative dynamic moduli were observed with increasing

rubber contents regardless of the inconclusivity of the test. This observed increase agrees with the hypothesis that the malleability of the rubber particles decreases the internal stresses that develop due to the volume change associated with the crystallization of ice.

Aesthetically, the concrete containing crumb rubber had much less scaling after enduring 300 cycles of freezing and thawing. Figure 8-2 is a photograph of a freeze-thaw specimen containing no crumb rubber added with a contrast filter applied to make the scaling more visible whereas the specimen shown in Figure 8-3 is from the batch that had 15 % of the crumb rubber placed. Both photographs are of the face that was upright during freezing and thawing, there was mores scaling on the other faces as well. This is a desirable property for exterior concrete, such as sidewalks and patios placed in colder environments.

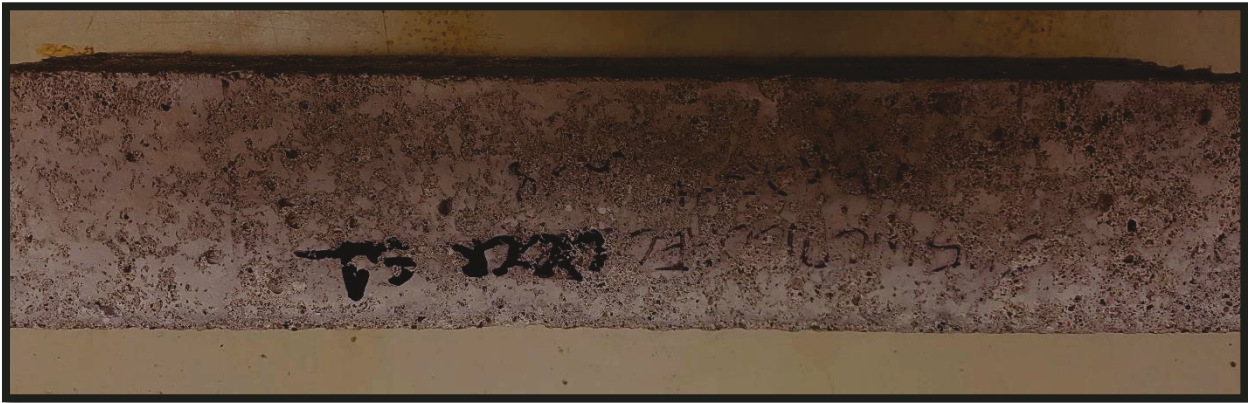


Figure 8-2 Sample Containing 0 % of the Fine Aggregate as Crumb Rubber After 300 Cycles of Freeze Thaw

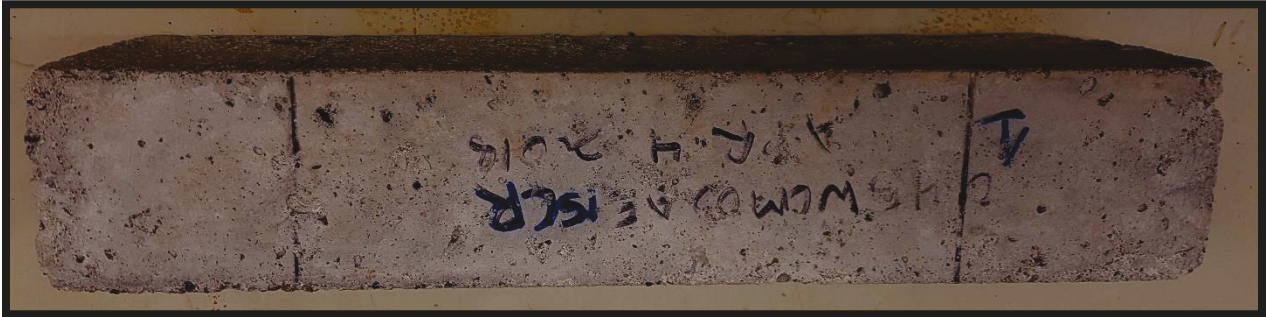


Figure 8-3 Sample Containing 15 % of the Fine Aggregate as Crumb Rubber After 300 Cycles of Freeze/Thaw

9. Conclusion

Around one cubic metre of concrete is poured per person in Canada and else where in the developed world. Utilizing crumb rubber as an alternative aggregate in this concrete will reduce the number of stockpiled tires. For instance, in Canada if only 10 % of the concrete produced replaced 15 % of the fine aggregate with crumb rubber, 180 million kg of reclaimed rubber would be required. With around 5 kg of rubber being reclaimed from every tire this would equate to the recycling of 36 million tires, the amount expected to be stockpiled every year.

Concrete mixtures that use crumb rubber to replace up to 15 % of the fine aggregate are suitable for most concretes designed with a 25 MPa 28-day compressive strength. The modulus of rupture of a similar mix reduced by 12 %, and the splitting tensile strength reduced by 9 %. This indicates that crumb rubber concrete's have less tensile strength than that of regular Portland cement concretes.

For every 5 % of fine aggregate replaced with crumb rubber the entrained air content increases by around 0.5 %. Concrete containing a crumb rubber fraction is more durable in regard to fatigue loading, chloride ion penetration and freeze-thaw. The bulk resistivity of a mix with 15 % of the fine aggregate replaced improved by 2 % over that of a similar mix with no crumb rubber added. The chloride ion penetrability did not change classification. However, these improvements are small and should not be relied upon to achieve permeability requirements.

The freeze-thaw durability of a mix containing 15 % crumb rubber increased by 37.5 % over a mix with a lower water cement ratio (0.45 opposed to 0.4), indicating that crumb rubber concretes are suitable for exterior exposure in cold weather environments.

Crumb rubber is more expensive than traditional fine aggregates but as the number of stockpiled tires increase its value as an aggregate may begin to outweigh the cost.

The following considerations should be taken in to account for design of such mixtures:

- Crumb rubber used as a concrete aggregate should be produced using an ambient temperature grinding method.

- The compressive strength, modulus of rupture and splitting tensile strength will decrease with the addition of crumb rubber. For concrete projects that include these in design considerations, the SRF model may be used to predict the associated decreases.
- The bulk resistivity and surface resistivity do increase with the addition of crumb rubber, but this increase should not be relied upon to decrease the permeability of a concrete when the amount of crumb rubber used is small.
- Depending on the air entrainment required, crumb rubber may be a suitable alternative to air entraining admixtures.
- While the presence of crumb rubber does increase the durability of a concrete mixture, it should not be relied upon to ensure the durability of a concrete structure nor should it be used as a substitute to good concreting practices.

10. Recommendations for Future Study

Full-scale field tests in colder environments and long-term studies of crumb rubber pavement structures should be carried out to validate the lab results.

Batch reactor studies should be performed with crumb rubber concrete to investigate the possibility of leaching and subsequent ground water contamination.

The interaction between rubber particles and supplementary cementing materials should be investigated further.

Effects of higher and lower water cement ratios of concrete containing crumb rubber should be examined to confirm the independency of the effect that rubber has on the compressive, flexural and tensile strengths of concrete.

The use of crumb rubber in pneumatically applied concrete (shotcrete) should be investigated as it is hypothesized that the increase in post fracture durability would make it a favourable additive.

11. Acknowledgements

The author would like to acknowledge the following people and organizations that were fundamental to the success of this research program,

Dr. Eltayeb Mohamedelhassan, thesis supervisor

Dr. Ehsan Rezazadeh Azar, thesis supervisor

Mr. Conrad Hagstrom, laboratory technologist

Mr. Rob Timoon, laboratory technologist

Ms. Suddha Reddy, undergrad research assistant

Lafarge, Thunder Bay

CRM Holdings

Thank you all so much for your help, support and guidance throughout this project.

12. References

- [1] I. B. Topcu, "The Properties of Rubberized Concretes," *Cement and Concrete Research*, vol. 25, no. 2, pp. 304-310, 1995.
- [2] C. Meyer, "The greening of the concrete industry," *Cement & Concrete Composites*, no. 31, pp. 601-605, 2009.
- [3] M. S. M. Y. O. Mukesh Limbachiya, "Use of recycled concrete aggregate in fly ash concrete," *Construction and Building Materials*, no. 27, pp. 434-449, 2012.
- [4] S. C. L.M. Frederico, "Waste glass as a supplementary cementitious material in concrete - Critical review of treatment methods," *Cement & Concrete Composites*, vol. 31, pp. 606-610, 2009.
- [5] M. R. M. T. H. B. M. Schneider, "Sustainable cement production-present and future," *Cement and Concrete Research*, vol. 41, pp. 642-650, 2011.
- [6] J. L. D. H. D. S. E. G. J.S. Damtoft, "Sustainable development and climate change initiatives," *Cement and Concrete Research*, vol. 38, pp. 115-127, 2008.
- [7] J. K. P. D. S.-R. C. D.G. Snelson, "Sustainable construction: Composite use of tyres and ash in concrete," *Waste Management*, vol. 29, pp. 360-367, 2009.
- [8] R. S. T. R. Naik, "Properties of concrete containing scrap-tire rubber - an overview," *Waste Management*, vol. 24, pp. 563-569, 2004.
- [9] J. K. I. K. Rafat Siddique, "Use of recycled plastic in concrete: A review," *Waste Management*, vol. 28, pp. 1835-1852, 2008.
- [10] I. M. I. A. Malek Batayneh, "Use of selected waste materials in concrete mixes," *Waste Management*, vol. 27, pp. 1870-1876, 2007.
- [11] F. L. G. C. A. M. M.A. Aiello, "Use of steel fibres recovered from waste tyres as reinforcement in concrete: Pull-out behaviour, compressive and flexural strength," *Waste Management*, vol. 29, pp. 1960-1970, 2009.

- [12] IllinoisEPA, "Youtube," 27 January 2011. [Online]. Available: <https://www.youtube.com/watch?v=aJmK3WDuEV4&index=7&t=195s&list=PLKqBUIF0p9X5YbJNaFUq1UOWRHcZetugo>. [Accessed 15 November 2017].
- [13] D. Nolan, "The Record," Metroland Media Group Ltd., 2018. [Online]. Available: <https://www.therecord.com/community-story/5335111--tbt-25-years-ago-today-the-hagersville-tire-fire-that-burned-17-days/>. [Accessed 2 May 2018].
- [14] G. L. S.-S. P. J. E. Baoshan Huang, "Investigation into Waste Tire Rubber-Filled Concrete," *Journal of Materials in Civil Engineering*, pp. 184-194, May 2004.
- [15] H. A. Toutanji, "The Use of Rubber Tire Particles in Concrete to Replace Mineral Aggregates," *Cement & Concrete Composites*, vol. 18, pp. 135-139, 1996.
- [16] S. W. J. Z. Xudong Chen, "Experimental Study on Dynamic Tensile Strength of Cement Mortar Using Split Hopkinson Pressure Bar Technique," *Journal of Materials in Civil Engineering*, vol. 26, no. 6, pp. 1-10, 2014.
- [17] C. C. Piti Sukontasukkul, "Properties of concrete pedestrian block mixed with crumb rubber," *Construction and Building Materials*, vol. 20, pp. 450-457, 2006.
- [18] M. D. P. R. Ali R. Khaloo, "Mechanical properties of concrete containing a high volume of tire rubber particles," *Waste Management*, vol. 28, pp. 2472-2482, 2008.
- [19] C. A. I. a. G. Salem, "Utilization of recycled crumb rubber as fine aggregates in concrete mix design," *Construction and Building Materials*, vol. 42, pp. 48-52, 2013.
- [20] A. A. a. P. B. A. Gideon M. Siringi, "Properties of Concrete with Crumb Rubber Replacing Fine Aggregates (Sand)," *Advances in Civil Engineering Materials*, vol. 2, no. 1, pp. 218-232, 2013.
- [21] P. R. R. Shubhada Gadkar, "The Effect of Crumb Rubber on Freeze-Thaw," *Advances in Civil Engineering Materials*, vol. 2, no. 1, pp. 566-585, 2013.
- [22] Recycling Research Institute, "Scraptire New," Recycling Research Institute, 2017. [Online]. Available: <http://www.scraptirenews.com/crumb.php>. [Accessed 15 November 2017].
- [23] ASTM International, *Standard Practice for Use of Scrap Tires in Civil Engineering Applications*, West Conshohocken, PA: ASTM International, 2012.

- [24] G. G. J. E. C. A. M. A. S. S.-S. P. Guoqiang Li, "Waste tire fiber modified concrete," *Composites, Part B:engineering*, no. 35, pp. 305-312, 2004.
- [25] F. L. M.A. Aiello, "Waste tyre rubberized concrete: Properties at fresh and hardened state," *Waste Management*, no. 30, pp. 1696-1704, 2010.
- [26] A. B. S. Neil N. Eldin, "Observations on Rubberized Concrete Behaviour," *Cement, Concrete, and Aggregates*, vol. 15, no. 1, pp. 74-84, 1993.
- [27] N. Z. T. A. L. A. M. B. Fernando Pelisser, "Concrete mad with recycled tire rubber: Effect of alkaline activation and silica fume addition," *Journal of Cleaner Production*, vol. 19, pp. 757-763, 2011.
- [28] M. A. S. G. G. J. E. C. A. B. H. Guoqiang Li, "Development of waste tire modified concrete," *Cement and Concrete Research*, vol. 34, pp. 2283-2289, 2004.
- [29] Z. K. K. a. F. M. Bayomy, "Rubberized Portland Cement Concrete," *Journal of Materials in Civil Engineering*, vol. 11, no. 3, pp. 206-213, 1999.
- [30] N. N. E. a. A. B. Senouci, "Rubber-Tire Particles As Concrete Aggregate," *Journal of Materials in Civil Engineering*, vol. 5, no. 4, pp. 478-496, 1993.
- [31] N. J. A. S. M. J. Schmizze RR, "Use of waste rubber in light-duty concrete pavements.," in *Proceedings of the third material engineering conference, infrastructure: new materials and methods of repair*, San Diego, CA, 1994.
- [32] B. S. Munish Thakur, "Innovative Application of Waste Tyre in Concrete Mixes," *International Journal of Recent Research Aspects*, vol. 3, no. 2, pp. 79-91, 2016.
- [33] X. S. H. Y. Y. L. Zheng, "Experimental investigation on dynamic properties of rubberized concrete," *Construction and Building Materials* , vol. 22, pp. 939-947, 2008.
- [34] G. B. M. B. B. W. F. Hernandez-Olivares, "Static and dynamic behaviour of recycled tyre rubber-filled concrete," *Cement and Concrete Research*, vol. 32, pp. 1587-1596, 2002.
- [35] T. Powers, "Structure and Physical Properties of Hardened Portland Cement Paste," *Journal of the American Ceramic Society*, vol. 41, no. 1, pp. 1-6, 1958.
- [36] B. K. R. D. H. a. R. J. M. Steven H. Kosmatka, *Design and Control of Concrete Mixtures*, Eighth Canadian Edition ed., Ottawa, Ontario : Cement Association of Canada, 2011.

- [37] I. B. T. a. A. Demir, "Durability of Rubberized Mortar and Concrete," *Journal of Materials in Civil Engineering*, vol. 19, no. 2, pp. 173-179, 2007.
- [38] ASTM International, *Standard Test Method for Relative Density (Specific Gravity) and Absorption of Coarse Aggregate*, West Conshohocken, Pennsylvania: ASTM International, 2015.
- [39] ASTM International, *Standard Test Method for Sieve Analysis of Fine and Coarse Aggregates*, West Conshohocken, Pennsylvania: ASTM International, 2014.
- [40] ASTM International, *Standard Test Method For Relative Density (Specific Gravity and Absorption of Fine Aggregates*, West Conshohocken, Pennsylvania, 2015.
- [41] ASTM International, *Standard Practice for Making and Curing Concrete Test Specimens in the Laboratory*, West Conshohocken, Pennsylvania: ASTM International, 2016.
- [42] ASTM International, *Standard Test Method for Slump of Hydraulic-Cement Concrete*, West Conshohocken, Pennsylvania: ASTM International, 2015.
- [43] ASTM International, *Standard Test Method for Air Content of Freshly Mixed Concrete by the Pressure Method*, West Conshohocken , Pennsylvania: ASTM International, 2017.
- [44] ASTM International, *Standard Test Method for Density (Unit Weight), Yield, and Air Content (Gravimetric) of Concrete*, West Conshohocken, Pennsylvania: ASTM International, 2017.
- [45] ASTM International, *Standard Specification for Mixing Rooms, Moist Cabinets, Moist Rooms, and Water Storage Tanks Used in the Testing of Hydraulic Cements and Concretes*, West Conshohocken, Pennsylvania: ASTM International, 2013.
- [46] ASTM International, *Standard Test Method for Electrical Indication of Concrete's Ability to Resist Chloride Ion Penetration*, West Conshohocken: ASTM International, 2012.
- [47] ASTM International, *Standard Test Method for Compressive Strength of Cylindrical Concrete Specimens*, West Conshohocken, Pennsylvania: ASTM International, 2017.
- [48] ASTM International, *Standard Test Method for Flexural Strength of Concrete (Using Simple Beam with Third-Point Loading)*, West Conshohocken, Pennsylvania: ASTM International, 2016.
- [49] ASTM International, *Standard Test Method for Splitting Tensile Strength of Cylindrical Concrete Specimens*, West Conshohocken, Pennsylvania: ASTM International, 2011.

- [50] ASTM International, *Standard Test Method for Resistance of Concrete to Rapid Freezing and Thawing*, West Conshohocken, Pennsylvania: ASTM International, 2015.
- [51] ASTM International, *Standard Test Method for Fundamental Transverse, Longitudinal, and Torsional Resonant Frequencies of Concrete Specimens*, West Conshohocken, Pennsylvania: ASTM International, 2014.
- [52] R. Walker, "SI metric.co.uk," 2016. [Online]. Available: https://www.simetric.co.uk/si_water.htm. [Accessed June 2017].
- [53] F. S. M.C Bignozzi, "Tyre rubber waste recycling in self compacting concrete," *Cement and Concrete Research*, vol. 36, pp. 735-739, 2006.
- [54] K. N. J. S. M. Akash Rao, "Use of aggregates from recycled construction and demolition waste in concrete," *Resources, Conservation & Recycling*, vol. 50, pp. 71-81, 2007.
- [55] S. M. S. Shtayeh, *Utilization of Waste Tires in the Production of Non-Structural Portland Cement Concrete*, Nablus: An-Najah University, 2007.
- [56] R. C. S. S. C. P. O. A. P. J. O. E. R. P. V. Raimundo K. Vieira, "Completely random experimental design with mixture and process variables for optimization of rubberized concrete," *Construction and Building Materials*, vol. 24, pp. 1754-1760, 2010.
- [57] B. K. R. D. H. R. J. M. Steven H. Kosmatka, *Design and Control of Concrete Mixtures*, 8th ed., Ottawa, Ontario: Cement Association of Canada, 2011.
- [58] J. M. a. R. P. Michael Pigeon, "Frost Resistant Concrete," *Construction and Building Materials*, vol. 10, no. 5, pp. 339-348, 28 July 1995.

Appendix A. Data Relating to Aggregate Properties

12.3. Coarse Aggregate Sieve Analyses and Bulk Density Calculation

Table 12-1 Coarse Aggregate Gradation Trial 1

Trial 1				
pan (kg) =		0.782		
Sample +pan		6.411		
(kg)=				
Sample (kg) =		5.629		
Sieve Size (mm)	Mass Retained (kg)	% Retained	%Passing	
19	0.67	11.90 %	88.10 %	
16	0.533	9.47 %	78.63 %	
12.5	1.172	20.82 %	57.81 %	
9.5	1.379	24.50 %	33.31 %	
4.75	1.541	27.38 %	5.93 %	
pan	0.313	5.56 %		
Total=	5.608			
%error=	0.37 %			

USCS Classification Parameters

D60:	12.86851536
D30:	8.925746269
D10:	5.455564568
Cu:	2.358787106
Cc:	1.134804185

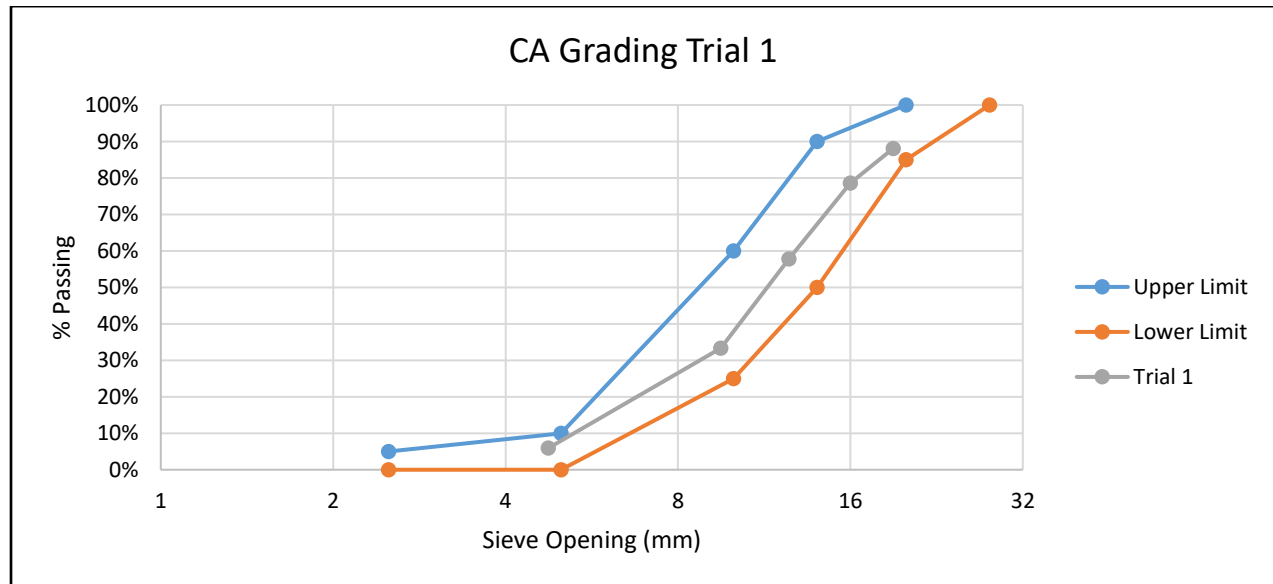


Figure 12-1 Coarse Aggregate Gradation Trial 1

Table 12-2 Coarse Aggregate Gradation Trial 2

Trial 2			
pan (kg) =		1.072	
Sample +pan (kg)=		6.729	
Sample (kg) =		5.657	
Sieve Size (mm)	Mass Retained (kg)	% Retained	% Passing
19	0.904	15.98 %	84.02 %
16	0.688	12.16 %	71.86 %
12.5	1.249	22.08 %	49.78 %
9.5	1.234	21.81 %	27.97 %
4.75	1.198	21.18 %	6.79 %
pan	0.345	6.10 %	
Total=	5.618		
% error=	0.69 %		

USCS Classification Parameters

D60:	14.1202562
D30:	9.956364775
D10:	5.470429883
Cu:	2.581196818
Cc:	1.283327694

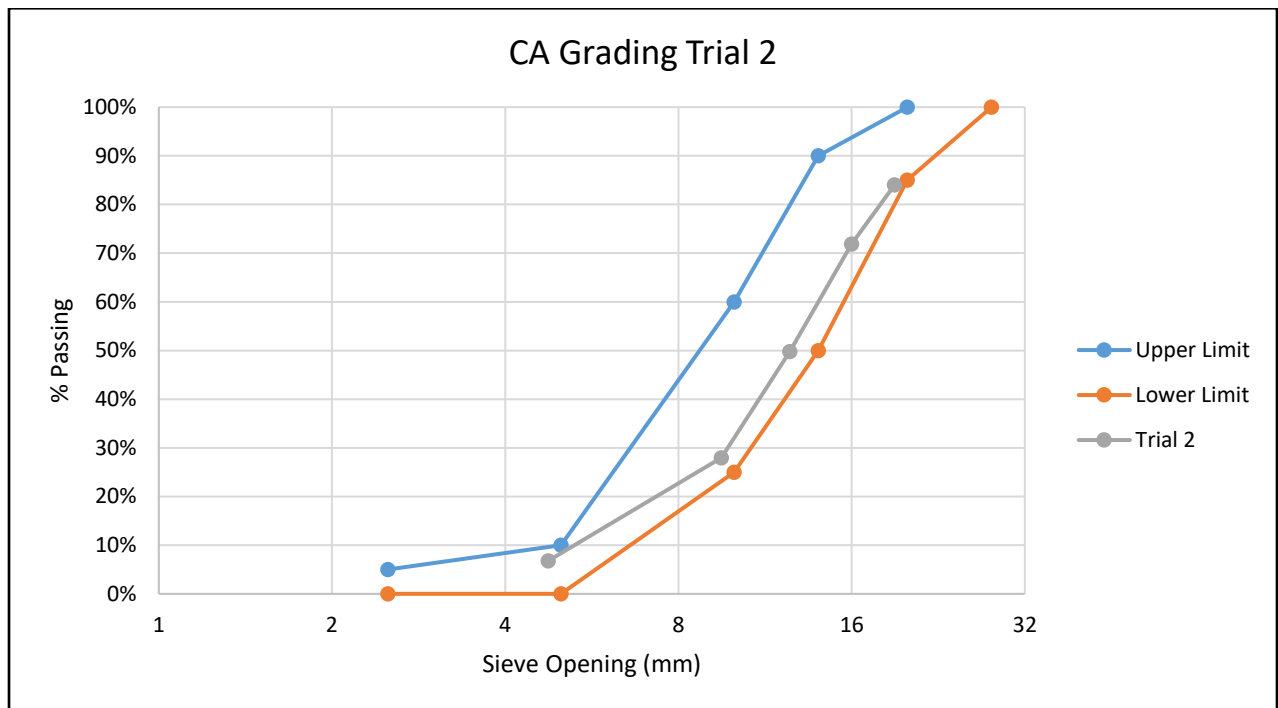


Figure 12-2 Coarse Aggregate Gradation Trial 2

Table 12-3 Coarse Aggregate Gradation Trial 3

Trial 3				
pan (kg) =		1.034		
Sample (kg) =	+pan	7.107		
Sample (kg) =		6.073		
Sieve Size (mm)	Mass Retained (kg)	% Retained	%Passing	
19	0.724	11.92 %	88.08 %	
16	0.68	11.20 %	76.88 %	
12.5	1.355	22.31 %	54.57 %	
9.5	1.462	24.07 %	30.50 %	
4.75	1.459	24.02 %	6.47 %	
pan	0.372	6.13 %		
Total=	6.052			
%error=	0.35 %			

USCS Classification Parameters

D60:	13.35188192
D30:	9.402004798
D10:	5.447686772
Cu:	2.450926876
Cc:	1.215307912

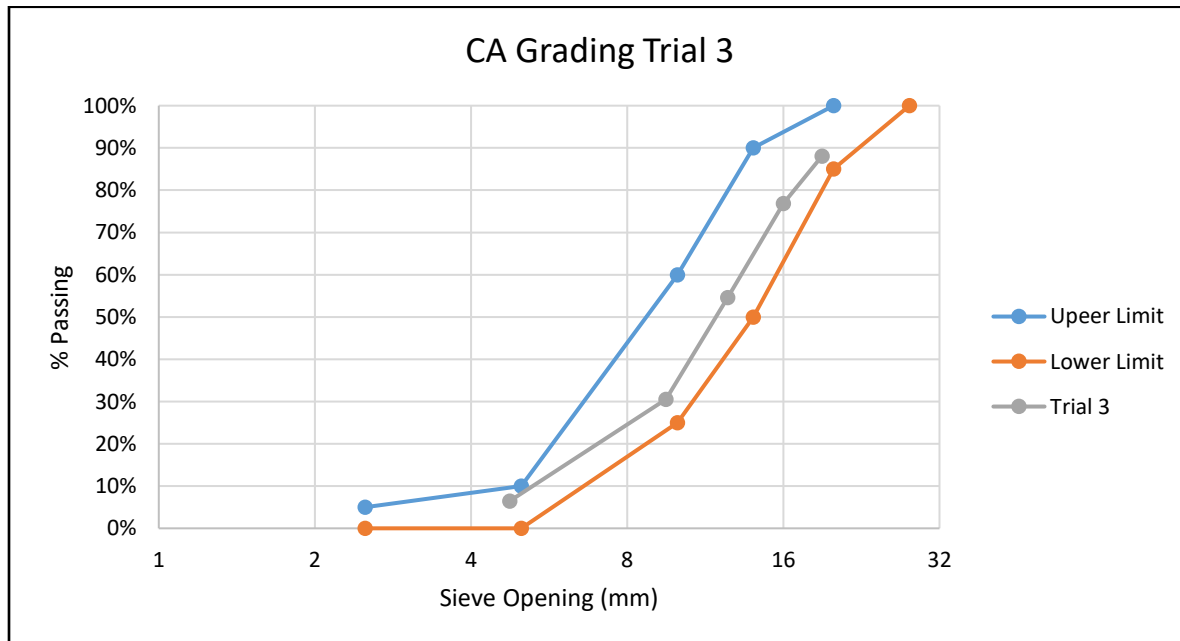


Figure 12-3 Coarse Aggregate Gradation Trial 3

Table 12-4 Bulk Density of Coarse Aggregate Calculation

Bulk Density of Coarse Aggregate	
Mass Bucket (kg) =	3.548
Mass Aggregate + Bucket (kg) =	15.831
Mass Aggregate (kg)=	12.283
Volume Bucket (m ³) =	0.007
Dry Rodded Density in Situ =	1754.714
Water Present (kg) =	0.015113
Oven Dry Mass Aggregate (kg) =	12.26789
Oven Dry Bulk Density (kg/m ³) =	1752.555

12.4. Fine Aggregate Gradations and Fineness Modulus Calculations

Table 12-5 Fine Aggregate Gradation Trial 1 Data

Trial 1

Mass of pan (g)= 218.2
 Sample + pan (g)= 683
 Sample (g)= 464.8

Sieve Opening (mm)	Mass Retained (g)	% Retained	% Passing	Fineness Modulus Calc Cumulative %Retained
9.423	0	0.00 %	100.00 %	0.00 %
4.76	0	0.00 %	100.00 %	0.00 %
2.36	44.3	9.53 %	90.47 %	9.53 %
1.18	76.8	16.52 %	73.95 %	26.05 %
0.85	53.1	11.42 %	62.52 %	50.00 %
0.3	177.7	38.23 %	24.29 %	75.71 %
0.15	89	19.15 %	5.14 %	94.86 %
0.075	19.9	4.28 %	0.86 %	99.14 %
pan	3.2	99.14 %		
Total=	464		FM=	2.56
% error=	0.17 %			
0.6 from graph=			50 %	

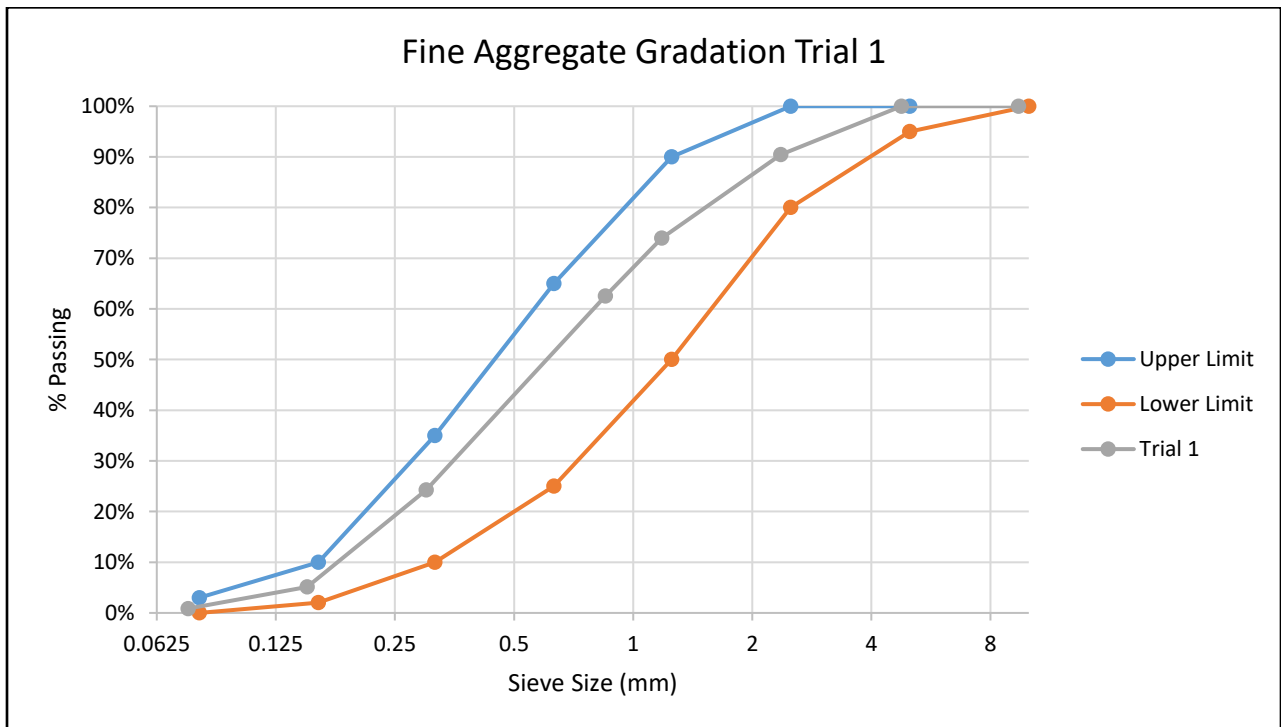


Figure 12-4 Fine Aggregate Grading Trial 1

Table 12-6 Fine Aggregate Gradation Trial 2 Data

Trial 2

Mass of pan (g)= 218.1

Sample + pan (g)= 567.5

Sample (g)= 349.4

Sieve Opening (mm)	Mass Retained (g)	% Retained	% Passing	Fineness Modulus Calc Cumulative %Retained
9.423	0	0.00%	100.00 %	0.00 %
4.76	0	0.00%	100.00 %	0.00 %
2.36	34.9	9.99 %	90.01 %	9.99 %
1.18	65.7	18.80 %	71.21 %	28.79 %
0.85	40.8	11.68 %	59.53 %	52.67 %
0.3	125.1	35.80 %	23.73 %	76.27 %
0.15	62.6	17.92 %	5.81 %	94.19 %
0.075	15.5	4.44 %	1.37 %	98.63 %
pan	3.1	0.89 %		
Total=	347.7		FM=	2.57
% error=	0.49 %			
0.6 from graph=			47 %	

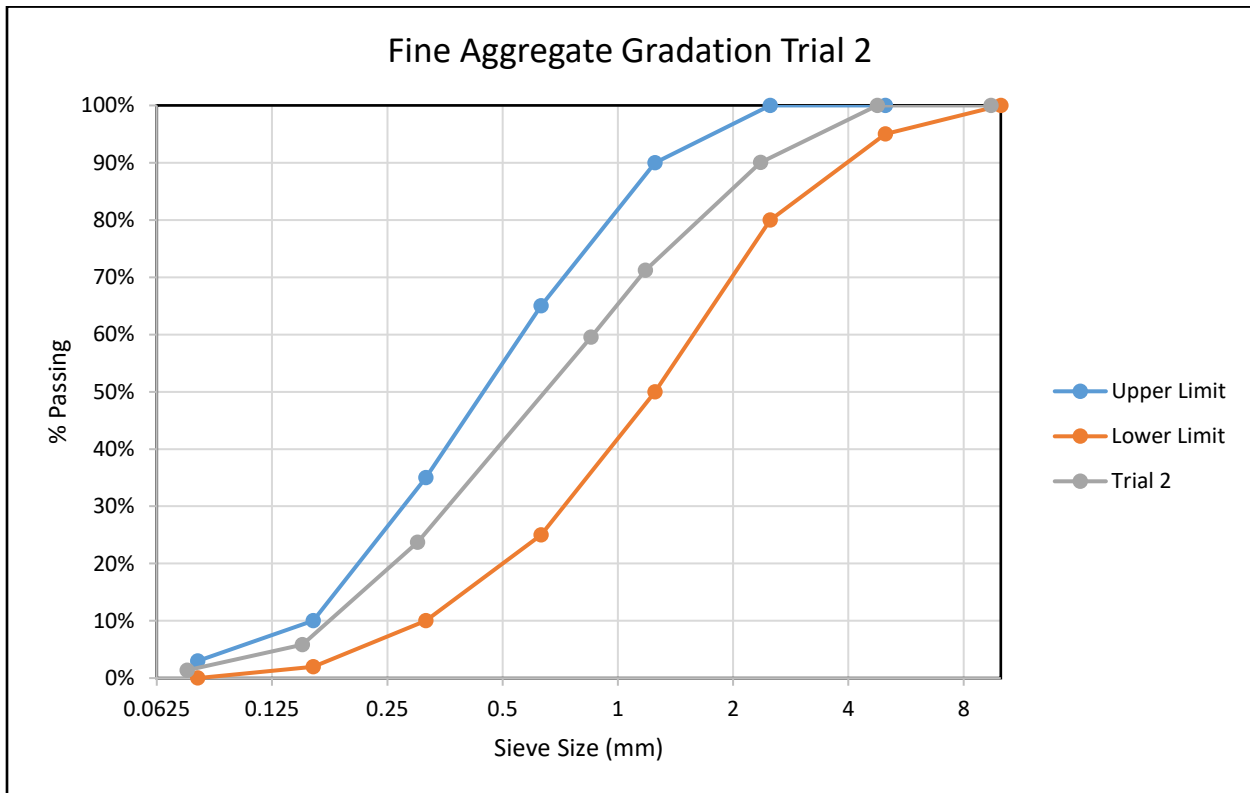


Figure 12-5 Fine Aggregate Grading Trial 2

Table 12-7 Fine Aggregate Gradation Trial 3 Data

Trial 3

Mass of pan (g)= 218.2

Sample + pan (g)= 570.8

Sample (g)= 352.6

Sieve Opening (mm)	Mass Retained (g)	% Retained	% Passing	Fineness Modulus Calc Cumulative %Retained
9.423	0	0.00 %	100.00 %	0.00 %
4.76	0	0.00 %	100.00 %	0.00 %
2.36	28.2	8.00 %	92.00 %	8.00 %
1.18	59.7	16.93 %	75.07 %	24.93 %
0.85	38.6	10.95 %	64.12 %	46.67 %
0.3	135	38.29 %	25.84 %	74.16 %
0.15	71	20.14 %	5.70 %	94.30 %
0.075	16.5	4.68 %	1.02 %	98.98 %
pan	0.2	0.06 %		
Total=	349.2		FM=	2.55
% error=	0.96 %			
0.6 from graph=			53 %	

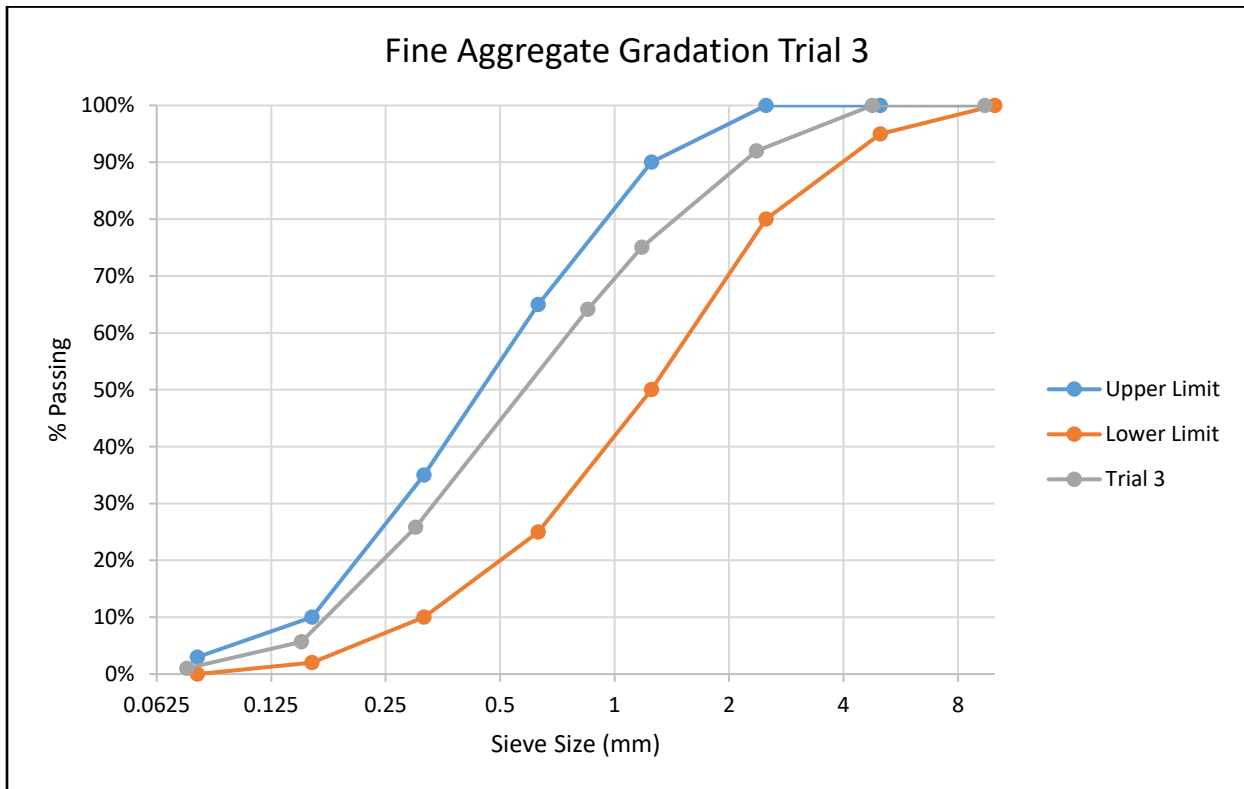


Figure 12-6 Fine Aggregate Gradation Trial 3

12.5. Crumb Rubber Gradings and Relative Density Data

CRM Gradings for various sizes of crumb rubber

Table 12-8 Manufacturer Grading of Crumb Rubber #6-#10 Mesh

CRM 6-10				
Sieve #	Sieve (mm)	% Passing	% Retained	
4	4.75	100	0	
6	3.35	88.8	11.2	
8	2.36	66.9	21.9	
10	2	15.6	51.3	
12	1.7	1.7	13.9	
14	1.4	0.5	1.2	
pan		0	0.5	

Table 12-9 Manufacturer Grading of Crumb Rubber #10-#20 Mesh

CRM 10-20				
Sieve #	Sieve (mm)	% Passing	% Retained	
8	2.36	97.2	2.8	
10	2	61.5	35.7	
12	1.7	28	33.5	
14	1.4	2.5	25.5	
16	1	0.6	1.9	
20	0.841	0.4	0.2	
pan		0	0.4	

Table 12-10 Manufacturer Grading of Crumb Rubber Nor 20 size

CRM Nor 20				
Sieve #	Sieve (mm)	% Passing	% Retained	
12	1.7	99.9	0.1	
14	1.4	85.8	14.1	
16	1	62.1	23.7	
20	0.841	23.7	38.4	
30	0.595	4.1	19.6	
40	0.4	0.1	4	
pan		0	0.1	

Table 12-11 Manufacturer Grading of Crumb Rubber #30- Mesh

CRM 30- Sieve #	Sieve (mm)	% Passing	% Retained
16	1	100	0
20	0.841	100	0
30	0.595	99.5	0.5
40	0.4	65.7	33.8
50	0.3	33.8	31.9
60	0.25	21.2	12.6
pan		0	21.2

Relative Density of Crumb Rubber Data

The alpha value was taken from https://www.simetric.co.uk/si_water.htm [52]

Table 12-12 Relative Density of Crumb Rubber Trial 1

Trial 1	
Temperature of water (°C) =	24
Mass of flask, water and rubber (g) =	967.7
Mass of flask and water (g) =	963.5
Mass of rubber (g)=	250
Mass of water (g)=	245.8
Alpha =	0.999091
Relative Density of Crumb Rubber=	1.016163

Table 12-13 Relative Density of Crumb Rubber Trial 2

Trial 2	
Temperature of water (°C) =	24
Mass of flask, water and rubber (g) =	951.8
Mass of flask and water (g) =	961
Mass of rubber (g)=	250
Mass of water (g)=	259.2
Alpha =	0.999091
Relative Density of Crumb Rubber=	0.96363

Table 12-14 Relative Density of Crumb Rubber Trial 3

Trial 3	
Temperature of water (°C) =	24
Mass of flask, water and rubber (g) =	965.4
Mass of flask and water (g) =	963.3
Mass of rubber (g)=	250
Mass of water (g)=	247.9
Alpha =	0.999091367
Relative Density of Crumb Rubber=	1.007554828

Table 12-15 Relative Density of Crumb Rubber Trial 4

Trial 4	
Temperature of water (°C) =	24
Mass of flask, water and rubber (g) =	965.9
Mass of flask and water (g) =	962.1
Mass of rubber (g)=	250
Mass of water (g)=	246.2
Alpha =	0.999091367
Relative Density of Crumb Rubber=	1.014511949

Appendix B. Mix Designs

Table 12-16 Control Mix 1 0.4WCM3.5AE00CR 85 L mix design

Water (kg) =	12.1
Portland Cement (kg) =	28.5
Fine Aggregate (kg) =	64.7
Coarse Aggregate (kg) =	97.1
Crumb Rubber (kg) =	0.0
Water Reducer (ml) =	111.3
Air Entraining Agent (ml) =	8.6

Cast on: June 29, 2017

Slump: 50 mm

Air: 3.5 %

Density: Not determined for this mix

Table 12-17 0.45WCM00AE00CR 85 L mix design

Water (kg) =	13.6
Portland Cement (kg) =	28.5
Fine Aggregate (kg) =	75.6
Coarse Aggregate (kg) =	97.1
Crumb Rubber (kg) =	0.0
Water Reducer (ml) =	111.3
Air Entraining Agent (ml) =	0

Cast on: July 6, 2017

Slump: 55 mm

Air: 2.2 %

Density: 2516.7 (kg/m³)

Table 12-18 0.45WCM00AE20CR 85 L mix design

Water (kg) =	13.6
Portland Cement (kg) =	28.5
Fine Aggregate (kg) =	60.5
Coarse Aggregate (kg) =	97.1
Crumb Rubber (kg) =	5.7
Water Reducer (ml) =	111.3
Air Entraining Agent (ml) =	0

Cast on: July 7, 2017

Slump: 60 mm

Air: 4.2 %

Density: 2378.4 (kg/m³)

Table 12-19 0.40WCM00AR15CR 85 L mix design

Water (kg) =	12.1
Portland Cement (kg) =	28.5
Fine Aggregate (kg) =	55.0
Coarse Aggregate (kg) =	97.1
Crumb Rubber (kg) =	3.6
Water Reducer (ml) =	111.3
Air Entraining Agent (ml) =	0

Cast on: July 11, 2017

Slump: 30 mm

Air: 2.6 %

Density: 2454.4 (kg/m³)

Table 12-20 0.45WCM00AE15CR 85 L mix design

Water (kg) =	13.6
Portland Cement (kg) =	28.5
Fine Aggregate (kg) =	64.3
Coarse Aggregate (kg) =	97.1
Crumb Rubber (kg) =	4.3
Water Reducer (ml) =	111.3
Air Entraining Agent (ml) =	0.000

Cast on: July 12, 2017

Slump: 65 mm

Air: 3.4 %

Density: 2399.6 (kg/m³)

Table 12-21 0.45WCM00AE10CR 85L mix design

Water (kg) =	13.6
Portland Cement (kg) =	28.5
Fine Aggregate (kg) =	68.0
Coarse Aggregate (kg) =	97.1
Crumb Rubber (kg) =	2.8
Water Reducer (ml) =	111.3
Air Entraining Agent (ml) =	0.000

Cast on: July 13, 2017

Slump: 60 mm

Air: 3.2 %

Density: 2432.8 (kg/m³)

Table 12-22 0.45WCM00AE25CR

Water (kg) =	13.5
Portland Cement (kg) =	28.5
Fine Aggregate (kg) =	56.7
Coarse Aggregate (kg) =	97.1
Crumb Rubber (kg) =	7.1
Water Reducer (ml) =	111.3
Air Entraining Agent (ml) =	0.0

Cast on: July 14, 2017

Slump: 40 mm

Air: 4 %

Density: 2365.7 (kg/m³)

Table 12-23 0.45WCM00AE05CR 85 L mix design

Water (kg) =	13.6
Portland Cement (kg) =	28.5
Fine Aggregate (kg) =	71.8
Coarse Aggregate (kg) =	97.1
Crumb Rubber (kg) =	1.4
Water Reducer (ml) =	111.3
Air Entraining Agent (ml) =	0.0

Cast on: July 19, 2017
 Slump: 65 mm
 Air: 2.6 %
 Density: 2502.0 (kg/m³)

The following mixes were prepared in the spring of 2018, the moisture contents of the fine and coarse aggregates are 0.17% and 0.05%, respectively.

Table 12-24 CM1R 0.40WCM00AE00CR 55 L mix design⁶

Water (kg) =	8.0
Portland Cement (kg) =	18.6
Fine Aggregate (kg) =	51.7
Coarse Aggregate (kg) =	63.2
Crumb Rubber (kg) =	0.0
Water Reducer (ml) =	72.5
Air Entraining Agent (ml) =	5.6

Cast on: Mar. 26, 2018
 Slump: 40 mm
 Air: 4 %
 Density: 2423.3 (kg/m³)

Table 12-25 R-0.45WCM00AE00CR 46 L mix

Water (kg) =	7.5
Portland Cement (kg) =	15.5
Fine Aggregate (kg) =	41.1
Coarse Aggregate (kg) =	52.8
Crumb Rubber (kg) =	0.0
Water Reducer (ml) =	60.5
Air Entraining Agent (ml) =	0.0

Cast on: Mar.27 2018
 Slump: 55 mm
 Air: 2.5 %
 Density: 2495.0 (kg/m³)

⁶ The R represents that this is a repeat mix

Table 12-26 R-0.45WCM00AE05CR 51 L mix design

Water (kg) =	8.3
Portland Cement (kg) =	17.3
Fine Aggregate (kg) =	43.6
Coarse Aggregate (kg) =	59.0
Crumb Rubber (kg) =	0.9
Water Reducer (ml) =	67.6
Air Entraining Agent (ml) =	0.0

Cast on: Mar. 28, 2018
 Slump: 45 mm
 Air: 3.2 %
 Density: 2441.7 (kg/m³)

Table 12-27 R-45WCM00AE10CR 51 L mix design

Water (kg) =	8.3
Portland Cement (kg) =	17.3
Fine Aggregate (kg) =	41.3
Coarse Aggregate (kg) =	59.9
Crumb Rubber (kg) =	1.7
Water Reducer (ml) =	67.6
Air Entraining Agent (ml) =	0.0

Cast on: Apr. 3, 2018
 Slump: 65 mm
 Air: 5 % (Air meter needed recalibration)
 Density: 2449.4 (kg/m³)

Table 12-28 R-0.45WCM00AE15CR 33 L mix design

Water (kg) =	5.4
Portland Cement (kg) =	11.2
Fine Aggregate (kg) =	25.2
Coarse Aggregate (kg) =	38.1
Crumb Rubber (kg) =	1.7
Water Reducer (ml) =	43.6
Air Entraining Agent (ml) =	0.0

Cast on: Apr.4 2018
 Slump: 80 mm
 Air: 8 %
 Density: Not enough material to test

Table 12-29 R- 0.45WCM00AE20CR 96 L mix design

Water (kg) =	15.4
Portland Cement (kg) =	32.3
Fine Aggregate (kg) =	68.4
Coarse Aggregate (kg) =	109.8
Crumb Rubber (kg) =	6.4
Water Reducer (ml) =	125.8
Air Entraining Agent (ml) =	0.0

Cast on: May 31, 2018
 Slump: 30 mm
 Air: 7.5 %
 Density: 2373.5 (kg/m³)

Table 12-30 R-0.45WCM00AE25CR 46 L mix design

Water (kg) =	7.4
Portland Cement (kg) =	15.5
Fine Aggregate (kg) =	30.8
Coarse Aggregate (kg) =	52.8
Crumb Rubber (kg) =	3.9
Water Reducer (ml) =	60.5
Air Entraining Agent (ml) =	0.0

Cast on: June 5, 2018

Slump: 50 mm

Air: 4.5 %

Density: 2360.4 (kg/m³)

Appendix C. Lab Result Data Sheets

12.6. MTO Comparison Mix

Test Results											
--------------	--	--	--	--	--	--	--	--	--	--	--

Batch ID: CM 1
 Test Date: July 26 2017 Air Entrained : Yes Cast Date: June 28 2017
 Water Cement Ratio: 0.4 Crumb Rubber Replacement: 0%

4" x 8" Cylinders		Resipod Surface Resistivity (kΩcm)									
Sample Number	Diameter (mm)	Length (mm)	Current (μA)	0°	90°	180°	270°	0°	90°	180°	270°
1	102	196.25	200	19.7	17.1	19.3	19.6	20	17.3	18.7	20.2
2	102	189.25	200	18.3	17.6	18.2	17	17.9	17.5	17.7	17
3	101	198.75	200	17	16.9	17.6	15.8	16.8	17.3	17.7	16.4
4	100	192	200	17.1	17.9	18.3	18.7	17.5	17.6	18.7	18.4
5	100.5	191.75	200	20.5	19.8	17.4	17.4	15.2	19.4	17.6	21.9

4" x 8" Cylinders	Resipod Bulk Resistivity			Merlin Resistivity	RCON Resistivity				Compressive Strength		
	Upper Insert (kΩcm)	Lower Insert (kΩcm)	Cylinder (kΩcm)	kΩcm	@ 300 Hz (kΩcm)	Phase Angle (°)	@ 40Hz (kΩcm)	Phase Angle (°)	Max Load (lbs)	Fracture Type	Defects
1	1.4	0	62.6	7.44	7.3	0	7.4	1	36700	Columnar	Poorly sawn ends
2	1	0	51.9	6.77	6.4	0	6.5	1	61600	Columnar	Pop out
3	1.1	0	59.2	6.53	6.6	1	6.7	1	34900	Columnar	
4	1.9	1	56.6	6.8	6.8	0	6.9	1	RCPT		
5	1.7	1	58.7	7.15	7	0	7.1	1	RCPT		

6" x 12" Cylinders		Splitting Tensile Test						
Sample Number	Diameter (mm)	Length (mm)	Max Load (lbs)	% of Coarse Fractured	Fracture Type	Defects	Notes	
1	150	300	55100	90	Typical	None	All fractures occurred straight down the middle of the sample	
2	152.5	303.75	69100	85	Typical	None		
3	152	302.25	57100	100	Typical	See Note	Honey comb at midsection	

Beams		3rd point Flexural Test				
Sample Number	Length (mm)	Width (mm)	Height (mm)	Max Load (lbs)	a value (mm)	Notes
1	456	155	150	10700	N/A	Typical Fracture
2	455	153	154	11100	N/A	Typical Fracture
3	455	160	150	10100	N/A	Typical Fracture

12.7. 0.45WCM00AE00CR

Test Results

Batch Id: 0 Air 0 CR
 Test Date: Aug.3 2017 Air Entrained : No Cast Date: July 6 2017
 Water Cement Ratio: 0.45 Crumb Rubber Replacement: 0

4" x 8" Cylinders	Sample Number	Diameter (mm)	Length (mm)	Current (μA)	Resipod Surface Resistivity (k Ω cm)							
					0°	90°	180°	270°	0°	90°	180°	270°
	1	102	185.5	200	17.4	17.4	16	15.2	17.5	17.7	16.1	15.3
	2	102	189	200	15	16.5	17.1	15.5	15.1	16.7	16.7	15.9
	3	102	189	200	14.4	16.8	14.7	13.8	14.3	17	14.9	13.7
	4	102	188.5	200	14.8	15.2	15.5	15.2	15.4	16	15.4	15.7
	5	102	185.75	200	14	14.8	15.8	15.1	13.9	15.1	15.8	14.8

4" x 8" Cylinders	Resipod Bulk Resistivity			Merlin Resistivity	RCON Impedence				Compressive Strength			
	Upper Insert (k Ω cm)	Lower Insert (k Ω cm)	Cylinder (k Ω cm)	k Ω cm	@ 300 Hz (k Ω cm)	Phase Angle (°)	@ 40Hz (k Ω cm)	Phase Angle (°)	Max Load (lbs)	Fracture Type	Defects	
	1	1.4	0	47.6	6.1	6	1	6.3	1	66600	Shear	None
	2	1.3	0	48.7	6.2	5.8	1	5.9	1	65600	Cone Shear	None
	3	1.2	0	49.3	5.5	6.8	1	5.5	1	69500	Cone Shear	None
	4	2.5	1.2	48.1	5.9	5.6	1	5.7	1	RCPT		
	5	2.5	1.2	46.2	5.7	5.5	1	5.5	1	RCPT		

6" x 12" Cylinders	Sample Number	Diameter (mm)	Length (mm)	Max Load (lbs)	% of Coarse Fractured	Fracture Type	Defects	Notes	
	1	150	305.25	61200	95	Typical	None		
	2	152.5	305.5	49000	95	Typical	None	Elastic Rebound Before Failure	
	3	152.5	305	53100	95	Typical	None		

Beams	Sample Number	Length (mm)	Width (mm)	Height (mm)	Max Load (lbs)	a value (mm)	Notes	Fracture width (mm)	Fracture Depth (mm)	Notes
	1	455	157	152	11000	N/A		157	152	Typical Fracture
	2	455	153	150	11100	N/A		154	148	Typical Fracture
	3	455	158	152	10400	N/A		159	151	Typical Fracture

12.8. 0.45WCM00AE05CR

Test Results

Test Date: Aug. 16 2017 Air Entrained : 0 Cast Date: July 19 2017
 Water Cement Ratio: 0.45 Crumb Rubber Replacement: 5%

4" x 8" Cylinders	Sample Number	Diameter (mm)	Length (mm)	Current (μA)	Resipod Surface Resistivity (kΩcm)							
					0°	90°	180°	270°	0°	90°	180°	270°
	1	102	198	200	16	15.6	16.9	16.3	15.7	15.2	16.6	16
	2	102	189	200	17.2	16.6	15	15.9	17.9	16.4	15.6	15.8
	3	102	189.75	200	16.4	15.6	15.4	16.4	16	16	15.6	16.8
	4	102.5	191.25	200	16.3	16	16.7	16.6	16.3	16.1	16.7	16.7
	5	103	193	200	15.1	15	15	15.6	15.3	14.9	15.4	15.4

4" x 8" Cylinders	Resipod Bulk Resistivity			Merlin Resistivity kΩcm	RCON Impedence			Compressive Strength				
	Upper Insert (kΩcm)	Lower Insert (kΩcm)	Cylinder (kΩcm)		@ 300 Hz (kΩcm)	Phase Angle (°)	@ 40Hz (kΩcm)	Phase Angle (°)	Max Load (lbs)	Fracture Type	Defects	
	1	1.4	0	64	6.8	6.6	1	6.9	2	54300	Cone	None
	2	1.3	0	64.3	7.1	6.3	2	6.6	2	48700	Cone Shear	Pinhole the size of a quarter
	3	1.2	0	63.6	7.5	6.8	2	7.2	2	56500	Cone Shear	
	4	2	0	59.2	6.5	6.1	1	6.3	1	RCPT		
	5	1.9	0	61.6	6.4	5.9	2	6.2	2	RCPT		

6" x 12" Cylinders	Sample Number	Diameter (mm)	Length (mm)	Splitting Tensile Test				Notes
				Max Load (lbs)	% of Coarse Fractured	Fracture Type	Defects	
	1	151.5	304.25	52400	95	Typical	None	
	2	150	305	47600	95	Typical	None	
	3	152	304.5	43100	95	Typical	None	

Beams	Sample Number	3rd point Flexural Test							Notes
		Length (mm)	Width (mm)	Height (mm)	Max Load (lbs)	a value (mm)	Fracture width (mm)	Fracture Depth (mm)	
	1	450	160	154	9700	N/A	159	152	
	2	450	155	152	9100	N/A	158	150	
	3	450	154	153	10000	N/A	154	148	

12.9. 0.45WCM00AE10CR

Test Results

Test Date: Aug. 10th 2017 Air Entrained : 0 Cast Date: July 13th 2017
 Water Cement Ratio: 0.45 Crumb Rubber Replacement: 10

4" x 8" Cylinders	Sample Number	Diameter (mm)	Length (mm)	Current (μ A)	Resipod Surface Resistivity (k Ω cm)							
					0°	90°	180°	270°	0°	90°	180°	270°
	1	102	189.5	200	15.6	15.7	15.1	16.1	14.9	15.9	15	16.1
	2	102	187.25	200	14.7	15.4	14.8	14.2	14.8	15.4	15.5	14
	3	102.5	193.5	200	15.6	15.7	14.3	15.1	15.6	15.7	14.2	15.3
	4	103	191.75	200	16.5	16.5	15.8	16.7	16.3	16.7	15.9	16.4
	5	103	188.25	200	14.2	14.5	14.3	14.3	14.4	14.5	14.5	14.5

4" x 8" Cylinders	Resipod Bulk Resistivity			Merlin Resistivity	RCON Impedence				Compressive Strength			
	Upper Insert (k Ω cm)	Lower Insert (k Ω cm)	Cylinder (k Ω cm)	k Ω cm	@ 300 Hz (k Ω cm)	Phase Angle (°)	@ 40Hz (k Ω cm)	Phase Angle (°)	Max Load (lbs)	Fracture Type	Defects	
	1	1.7	0	51.8	5.9	5.8	1	5.8	1	62300	Shear	
	2	1.4	0	48.4	6.1	6.5	1	5.7	1	52100	Cone Shear	
	3	1.3	0	58.3	6.5	6.1	1	6.3	1	55800	Shear	
	4	1.3	0	55.2	6.4	6	1	6.1	1	RCPT		
	5	1.4	0	48.1	5.9	5.4	1	5.5	1	RCPT		

6" x 12" Cylinders	Sample Number	Diameter (mm)	Length (mm)	Max Load (lbs)	% of Coarse Fractured	Fracture Type	Defects	Notes	
	1	150	300.5	44700	95	Typical	None		
	2	151.5	301.75	40500	95	Typical	None		
	3	151.5	305	54100	95	Typical	None		

Beams	Sample Number	Length (mm)	Width (mm)	Height (mm)	Max Load (lbs)	a value (mm)	Notes	Fracture width (mm)	Fracture Depth (mm)	3rd point Flexural Test	
	1	450	150	160	10200	N/A		159	151		
	2	450	154	152	9100	N/A		157	150		
	3	450	153	152	9800	N/A		156	149		

12.10. 0.45WCM00AE15CR

Test Results

Test Date: Aug. 9th 2017 Air Entrained : No Cast Date: July 12 2017
 Water Cement Ratio: 0.45 Crumb Rubber Replacement: 15%

4" x 8" Cylinders	Sample Number	Diameter (mm)	Length (mm)	Current (μ A)	Resipod Surface Resistivity (k Ω cm)							
					0°	90°	180°	270°	0°	90°	180°	270°
	1	102	184.75	200	16.1	16.1	16.7	16.3	16.1	16.1	17	16.1
	2	102	185.5	200	16.5	15.8	15.3	15.8	16.5	15.9	15.2	15.2
	3	102	187.75	200	17.1	16.1	16.9	14.5	16.9	16.2	16.3	14.4
	4	102	186	200	14.4	15.2	15.4	14.8	14.5	15.1	15	14.4
	5	102	186.75	200	15.3	14.9	16	16.7	16.7	15.1	16.5	16.8

4" x 8" Cylinders	Resipod Bulk Resistivity			Merlin Resistivity	RCON Impedence				Compressive Strength			
	Upper Insert (k Ω cm)	Lower Insert (k Ω cm)	Cylinder (k Ω cm)	k Ω cm	@ 300 Hz (k Ω cm)	Phase Angle (°)	@ 40Hz (k Ω cm)	Phase Angle (°)	Max Load (lbs)	Fracture Type	Defects	
	1	1.6	0	50	6.2	5.8	1	5.8	1	56500	Shear	None
	2	1.4	0	47.5	6	5.7	1	5.7	1	48900	Cone Shear	None
	3	1.4	0	48.2	6.1	5.7	1	5.7	1	52600	Shear	None
	4	3.2	1.3	47.6	5.9	5.5	1	5.5	1	RCPT		
	5	2	1.1	49	6.1	5.7	1	5.7	1	RCPT		

6" x 12" Cylinders	Sample Number	Diameter (mm)	Length (mm)	Max Load (lbs)	% of Coarse Fractured	Fracture Type	Defects	Notes	
	1	150	304	47100	95	Typical	None		
	2	152	304	41700	95	Typical	None	Sustained High Plastic Deformation	
	3	151.5	305.5	45500	95	Typical	None		

Beams	Sample Number	3rd point Flexural Test								
		Length (mm)	Width (mm)	Height (mm)	Max Load (lbs)	a value (mm)	Notes	Fracture width (mm)	Fracture Depth (mm)	Notes
	1	450	152	154	9100	N/A		157	151	
	2	450	154	152	8800	N/A		152	149	
	3	450	153	155	8600	N/A		153	152	

12.11. 0.45WCM00AE20CR

Test Results

Test Date: Aug. 4 2017 Air Entrained : 0 Cast Date: July 7 2017
 Water Cement Ratio: 0.45 Crumb Rubber Replacement: 20

4" x 8" Cylinders	Sample Number	Diameter (mm)	Length (mm)	Current (μA)	Resipod Surface Resistivity (kΩcm)							
					0°	90°	180°	270°	0°	90°	180°	270°
	1	102	188.25	200	18.8	19	17.8	19.8	18.5	19	17.9	19.8
	2	102	186.75	200	19.3	18.4	18.7	16.8	19.4	19.2	18.7	17.5
	3	102	184.5	200	18.6	17.9	18.2	19	18.5	17.8	17.7	19
	4	102	189.75	200	17.3	18.5	18	18.6	16.8	17.1	18.6	18.9
	5	102	190.25	200	17.5	16.6	16.4	17.7	17.6	16.3	17.1	17.4

4" x 8" Cylinders	Resipod Bulk Resistivity			Merlin Resistivity	RCON Impedence				Compressive Strength		
	Upper Insert (kΩcm)	Lower Insert (kΩcm)	Cylinder (kΩcm)	kΩcm	@ 300 Hz (kΩcm)	Phase Angle (°)	@ 40Hz (kΩcm)	Phase Angle (°)	Max Load (lbs)	Fracture Type	Defects
	1	0	52.4	6.8	6.4	1	6.5	1	41300	Shear	Rubber was holding pieces together
	2	0	55.8	6.9	6.5	1	6.6	1	51100	Shear	
	3	0	54	6.8	6.3	1	6.3	1	41300	Cone Shear	
	4	0	53.6	6.8	6.5	1	6.5	1	RCPT	RCPT	
	5	0	52	6.5	6.2	1	6.3	1	RCPT	RCPT	

6" x 12" Cylinders	Sample Number	Diameter (mm)	Length (mm)	Max Load (lbs)	% of Coarse Fractured	Fracture Type	Defects	Notes	
	1	151	305.25	33300	95	Typical	None	Rubber Stayed Intact (pullout failure for rubber grains)	
	2	152	304.75	37700	95	Typical	None	Rubber Stayed Intact (pullout failure for rubber grains)	
	3	150	304.25	30400	95	Typical	None	Rubber Stayed Intact (pullout failure for rubber grains)	

Beams	Sample Number	Length (mm)	Width (mm)	Height (mm)	Max Load (lbs)	a value (mm)	Notes	Fracture width (mm)	Fracture Depth (mm)	Notes
	1	450	155	153	9000	N/A		159	152	Beam Failed on middle 3rd line
	2	455	150	155	7700	N/A		160	148	Middle of mid-3rd
	3	455	150	152	8800	N/A		155	146	Middle of mid-3rd

12.12. 0.45WCM00AE25CR

Test Results

Test Date: Aug. 11 2017 Air Entrained : 0 Cast Date: July 14 2017
 Water Cement Ratio: 0.45 Crumb Rubber Replacement: 25

4" x 8" Cylinders	Sample Number	Diameter (mm)	Length (mm)	Current (μ A)	Resipod Surface Resistivity (k Ω cm)							
					0°	90°	180°	270°	0°	90°	180°	270°
	1	102.5	190.5	200	17.5	17.9	19.2	18.3	17.8	17.8	19	18.5
	2	101.5	190	200	17.4	18.3	19.1	20.9	17.6	18.4	19.1	20.2
	3	102	186.5	200	19	17.1	18.5	17.8	19.3	17.8	18.1	18.5
	4	101.5	186.5	200	17.6	17.1	18	17.5	18.1	17.3	18	17.8
	5	102	188.25	200	18.2	17.6	17.4	16.9	17.9	17.5	17.7	17

4" x 8" Cylinders	Resipod Bulk Resistivity			Merlin Resistivity	RCON Impedence				Compressive Strength			
	Upper Insert (k Ω cm)	Lower Insert (k Ω cm)	Cylinder (k Ω cm)	k Ω cm	@ 300 Hz (k Ω cm)	Phase Angle (°)	@ 40Hz (k Ω cm)	Phase Angle (°)	Max Load (lbs)	Fracture Type	Defects	
	1	2.1	1	65.1	7.1	6.6	1	6.7	1	44900	Shear	
	2	2.1	1.1	61.3	7.2	6.8	1	6.9	1	45200	Cone	
	3	1.9	0	54.5	7	6.4	1	6.5	1	42100	Shear	
	4	1.8	0	57.1	7	6.4	1	6.5	1	RCPT		
	5	1.6	0	56	6.9	6.4	1	6.5	1	RCPT		

6" x 12" Cylinders	Sample Number	Diameter (mm)	Length (mm)	Max Load (lbs)	% of Coarse Fractured	Fracture Type	Defects	Splitting Tensile Test	
								Notes	
	1	150	306	33700	95	Typical	None		
	2	152.5	305	33400	95	Typical	None		
	3	150	305.75	39400	95	Typical	None		

Beams	Sample Number	Length (mm)	Width (mm)	Height (mm)	Max Load (lbs)	a value (mm)	Notes	Fracture width (mm)	Fracture Depth (mm)	3rd point Flexural Test
										Notes
	1	450	158	157	7600	N/A		156	149	Roller Moved Prior to failure
	2	450	158	158	8700	N/A		154	151	
	3	450	155	152	9200	N/A		158	151	Beam support Burped

12.13. CM1 Repeat

Test Results

Batch Id: 0 Air 0 CR
 Test Date: Apr.23 2018 Air Entrained : Yes Cast Date: Mar. 26 2018
 Water Cement Ratio: 0.4 Crumb Rubber Replacement: 0%

4" x 8" Cylinders		Resipod Surface Resistivity (kΩcm)									
Sample Number	Diameter (mm)	Length (mm)	Current (μA)	0°	90°	180°	270°	0°	90°	180°	270°
1	100.5	198.3	200	22.4	17.6	20.7	20.5	21.7	18.3	20.7	20.2
2	100.5	199.5	200	20.5	17.8	18.8	17.9	20.5	18.2	17.7	18.6
3	101	198	200	20.8	20.1	18.8	19.6	20.7	20.1	24.8	20
4	100.5	199.25	200	17.5	18.2	19.6	18.5	17.9	16.8	18.6	18.4
5	100	197.25	200	21.3	20.2	20.4	21.3	20.5	19.5	20.4	20.3

4" x 8" Cylinders	Resipod Bulk Resistivity			Merlin Resistivity	RCON Impedence				Compressive Strength		
	Upper Insert (kΩcm)	Lower Insert (kΩcm)	Cylinder (kΩcm)	kΩcm	@ 300 Hz (kΩcm)	Phase Angle (°)	@ 40Hz (kΩcm)	Phase Angle (°)	Max Load (lbs)	Fracture Type	Defects
1	4.9	1.4	66.8	8.3	8	0	8.1	1	83900	Cone	Honeycomb
2	4.9	1	66.9	7.6	7.8	0	7.9	0	94400	Shear	None
3	3.4	0	69.5	8.3	8.4	0	8.5	0	83900	Cone/Somewh	None
4	3.7	0	65.3	7.6	8	0	8.2	1	RCPT		
5	3.5	0	66.4	7.7	8.2	0	8.3	1	RCPT		

6" x 12" Cylinders		Splitting Tensile Test					
Sample Number	Diameter (mm)	Length (mm)	Max Load (lbs)	% of Coarse Fractured	Fracture Type	Defects	Notes
1	150.5	306	74800	95	Typical	Pockets on Surface	
2	151.5	301.5	46800	95	Typical	None	
3	151	303.3	49800	95	Typical	None	

Beams		3rd point Flexural Test							
Sample Number	Length (mm)	Width (mm)	Height (mm)	Max Load (lbs)	a value (mm)	Notes	Fracture width (mm)	Fracture Depth (mm)	Notes
1	0	0	0	0	0	N/A	0	0	Typical Fracture
2	0	0	0	0	0	N/A	0	0	Typical Fracture
3	0	0	0	0	0	N/A	0	0	Typical Fracture

12.14. 0.45WCM00AE00CR Repeat

Test Results

Batch Id: 0 Air 0 CR
 Test Date: Apr.24th 2018 Air Entrained : No Cast Date: Mar.27th 2018
 Water Cement Ratio: 0.45 Crumb Rubber Replacement: 0%

4" x 8" Cylinders	Sample Number	Diameter (mm)	Length (mm)	Current (μA)	Resipod Surface Resistivity (kΩcm)							
					0°	90°	180°	270°	0°	90°	180°	270°
	1	101.5	200	200	13.5	13.5	13.7	13.1	13.5	13.1	13.6	12.9
	2	101	200	200	14.1	13.6	13.2	13	13	13.7	13	13.1
	3	0	0	200	0	0	0	0	0	0	0	0
	4	0	0	200	0	0	0	0	0	0	0	0
	5	0	0	200	0	0	0	0	0	0	0	0

4" x 8" Cylinders	Resipod Bulk Resistivity			Merlin Resistivity	RCON Impedence				Compressive Strength		
	Upper Insert (kΩcm)	Lower Insert (kΩcm)	Cylinder (kΩcm)	kΩcm	@ 300 Hz (kΩcm)	Phase Angle (°)	@ 40Hz (kΩcm)	Phase Angle (°)	Max Load (lbs)	Fracture Type	Defects
	1	3.5	3.1	49.4	5.3	7.2	0	6.6	1	0	0
	2	2.9	1	48.3	5.3	6.2	0	5.8	1	0	0
	3	0	0	0	0	0	0	0	0	0	0
	4	0	0	0	0	0	0	0	0	RCPT	
	5	0	0	0	0	0	0	0	0	RCPT	

6" x 12" Cylinders	Sample Number	Diameter (mm)	Length (mm)	Max Load (lbs)	% of Coarse Fractured	Fracture Type	Defects	Splitting Tensile Test		
								Notes		
	1	150	300	48900	95	Typical	None			
	2	150	300	72500	95	Typical	None			
	3	150	300	47100	95	Typical	None			

Beams	Sample Number	Length (mm)	Width (mm)	Height (mm)	Max Load (lbs)	a value (mm)	Notes	Fracture width (mm)	Fracture Depth (mm)	3rd point Flexural Test
										Notes
	1	0	0	0	0	N/A		0	0	Typical Fracture
	2	0	0	0	0	N/A		0	0	Typical Fracture
	3	0	0	0	0	N/A		0	0	Typical Fracture

12.15. 0.45WCM00AE05CR Repeat

Test Results

Batch Id: 0 Air 5 CR
 Test Date: Apr. 25 2018 Air Entrained : No Cast Date: Mar. 28 2018
 Water Cement Ratio: 0.45 Crumb Rubber Replacement: 5%

4" x 8" Cylinders	Sample Number	Diameter (mm)	Length (mm)	Current (μ A)	Resipod Surface Resistivity (k Ω cm)							
					0°	90°	180°	270°	0°	90°	180°	270°
	1	101.5	200.5	200	15	14.8	16.7	16.3	14.9	16.1	16.1	16.4
	2	101	199.75	200	16	16.2	16.3	15.9	16	15.7	16.6	15.9
	3	101	196.5	200	15.4	16	15.1	14.5	15.2	15.8	15.6	14.5
	4	101.5	201.5	200	16.9	16.7	16.3	14.6	16.8	16.9	16.4	14.3
	5	100	202	200	16.5	16.7	17	16.6	16.8	16.8	16.6	16.4

4" x 8" Cylinders	Resipod Bulk Resistivity			Merlin Resistivity	RCON Impedence				Compressive Strength			
	Upper Insert (k Ω cm)	Lower Insert (k Ω cm)	Cylinder (k Ω cm)	k Ω cm	@ 300 Hz (k Ω cm)	Phase Angle (°)	@ 40Hz (k Ω cm)	Phase Angle (°)	Max Load (lbs)	Fracture Type	Defects	
	1	2.7	1.1	56.2	6.4	6.7	0	6.7	1	71000	Cone Shear	None
	2	2.9	1.2	55.6	6.3	6.6	0	6.7	1	72600	Cone Shear	None
	3	2.1	1.4	53.5	6	6.2	0	6.3	1	79100	shear	None
	4	2.5	1.2	56.6	6.4	6.6	0	6.7	1	RCPT		
	5	2.6	0	57	6.4	7	0	7.1	1	RCPT		

6" x 12" Cylinders	Sample Number	Diameter (mm)	Length (mm)	Max Load (lbs)	% of Coarse Fractured	Fracture Type	Defects	Splitting Tensile Test	
								Notes	
	1	150	306	54800	95	Typical	None		
	2	151	305	61300	95	Typical	None		
	3	151	305	52000	95	Typical	None		

Beams	Sample Number	Length (mm)	Width (mm)	Height (mm)	Max Load (lbs)	a value (mm)	Notes	Fracture width (mm)	Fracture Depth (mm)	3rd point Flexural Test
										Notes
	1	0	0	0	0	N/A		0	0	Typical Fracture
	2	0	0	0	0	N/A		0	0	Typical Fracture
	3	0	0	0	0	N/A		0	0	Typical Fracture

12.16. 0.45WCM00AE10CR Repeat

Test Results

Batch Id: 0 Air 10 CR
 Test Date: May 1 2018 Air Entrained : No Cast Date: Apr. 3 2018
 Water Cement Ratio: 0.45 Crumb Rubber Replacement: 10%

4" x 8" Cylinders	Sample Number	Diameter (mm)	Length (mm)	Current (μ A)	Resipod Surface Resistivity (k Ω cm)							
					0°	90°	180°	270°	0°	90°	180°	270°
	1	100	200	200	13.9	13.4	14.8	13.7	14	14	14.2	13.5
	2	100	200	200	17.3	17.4	16.9	16.7	17.1	17.6	16.9	16.6
	3	100	200	200	16	17.3	15	16.8	16.2	17.1	14.6	16
	4	100	200	200	15.3	15.6	16.7	16.5	15.7	15.6	16.3	16.2
	5	100	200	200	17.8	16.1	15.6	16	17.4	16.4	15	15.8

4" x 8" Cylinders	Resipod Bulk Resistivity			Merlin Resistivity	RCON Impedence				Compressive Strength		
	Upper Insert (k Ω cm)	Lower Insert (k Ω cm)	Cylinder (k Ω cm)	k Ω cm	@ 300 Hz (k Ω cm)	Phase Angle (°)	@ 40Hz (k Ω cm)	Phase Angle (°)	Max Load (lbs)	Fracture Type	Defects
1	9.1	3.8	63.4	5.8	6	0	6.1	1	72200	Shear	None
2	9.5	2.2	66.3	6.3	6.7	0	6.8	1	67200	Cone/Shear	None
3	4.4	3.4	62	6	6.5	0	6.6	1	61300	Columnar	None
4	4.8	2.7	61.5	6	6.4	0	6.5	1	RCPT		
5	4.4	2.8	58.9	5.9	6.4	0	6.5	1	RCPT		

6" x 12" Cylinders	Sample Number	Diameter (mm)	Length (mm)	Max Load (lbs)	% of Coarse Fractured	Fracture Type	Defects	Splitting Tensile Test		
								Notes		
	1	150	300	43900	100	Typical	None			
	2	150	300	58800	95	Typical	None			
	3	150	300	57200	95	Typical	None			

Beams	Sample Number	Length (mm)	Width (mm)	Height (mm)	Max Load (lbs)	a value (mm)	Notes	Fracture width (mm)	Fracture Depth (mm)	3rd point Flexural Test
										Notes
	1	0	0	0	0	N/A		0	0	Typical Fracture
	2	0	0	0	0	N/A		0	0	Typical Fracture
	3	0	0	0	0	N/A		0	0	Typical Fracture

12.17. 0.45WCM00AE15CR Repeat

Test Results

Batch Id: 0 Air 15 CR
 Test Date: May 2 2018 Air Entrained : No Cast Date: Apr. 4 2018
 Water Cement Ratio: 0.45 Crumb Rubber Replacement: 15%

4" x 8" Cylinders	Sample Number	Diameter (mm)	Length (mm)	Current (μA)	Resipod Surface Resistivity (kΩcm)							
					0°	90°	180°	270°	0°	90°	180°	270°
	1	100	200	200	15.2	15.4	15.9	15.3	14.5	15.6	15.9	15.4
	2	100	200	200	15.8	15.4	16.2	15.7	15.6	15.6	14.2	15.6
	3	100	200	200	16.8	16.2	16.2	16.4	17	15.9	16.2	16.3
	4	100	200	200	17.1	16.2	17.1	17.8	17.2	16.2	17	17.6
	5	100	200	200	16.2	17.4	15.7	15.9	16.6	17.8	16.1	15.4

4" x 8" Cylinders	Resipod Bulk Resistivity			Merlin Resistivity	RCON Impedence				Compressive Strength		
	Upper Insert (kΩcm)	Lower Insert (kΩcm)	Cylinder (kΩcm)	kΩcm	@ 300 Hz (kΩcm)	Phase Angle (°)	@ 40Hz (kΩcm)	Phase Angle (°)	Max Load (lbs)	Fracture Type	Defects
1	2.5	1.6	57.6	6.5	6.8	0	6.8	1	67600	Columnar	None
2	2.7	1.6	59.2	6.6	7	0	7	1	58700	Columnar	None
3	2.8	1.6	58.3	6.5	6.9	0	7	1	65100	Columnar	None
4	2.1	1.6	59.9	6.7	7.2	0	7.2	1	RCPT		
5	2.5	1.6	57	6.3	6.9	0	6.9	1	RCPT		

6" x 12" Cylinders	Sample Number	Diameter (mm)	Length (mm)	Max Load (lbs)	% of Coarse Fractured	Fracture Type	Defects	Splitting Tensile Test	
								Notes	
	1	0	0	0	0	Typical	None		
	2	0	0	0	0	Typical	None		
	3	0	0	0	0	Typical	None		

Beams	Sample Number	Length (mm)	Width (mm)	Height (mm)	Max Load (lbs)	a value (mm)	Notes	Fracture width (mm)	Fracture Depth (mm)	3rd point Flexural Test
										Notes
	1	0	0	0	0	N/A		0	0	Typical Fracture
	2	0	0	0	0	N/A		0	0	Typical Fracture
	3	0	0	0	0	N/A		0	0	Typical Fracture

12.18. 0.45WCM00AE20CR Repeat

Test Results			
Batch Id:	0 Air 20 CR		
Test Date:	June 28 2018	Air Entrained :	No
Water Cement Ratio:	0.45	Crumb Rubber Replacement:	25%
		Cast Date:	May 31 2018

4" x 8" Cylinders	Sample Number	Diameter (mm)	Length (mm)	Current (μ A)	Resipod Surface Resistivity (k Ω cm)							
					0°	90°	180°	270°	0°	90°	180°	270°
	1	101	192	200	16	17.5	18	17.8	16	17.1	17.8	16.8
	2	102	201	200	17	17	19.2	19.4	16.9	17.2	18.2	19
	3	101	198	200	18.7	17.1	18.5	16.6	19.3	18.2	19.1	18.9
	4	102	201	200	19.4	17.9	16.8	18	18.2	18.1	17.7	17.4
	5	100	200	200	15.9	17.6	15.7	17.1	15.7	17.4	17.2	17.1

4" x 8" Cylinders	Resipod Bulk Resistivity			Merlin Resistivity	RCON Impedence				Compressive Strength		
	Upper Insert (k Ω cm)	Lower Insert (k Ω cm)	Cylinder (k Ω cm)	k Ω cm	@ 300 Hz (k Ω cm)	Phase Angle (°)	@ 40Hz (k Ω cm)	Phase Angle (°)	Max Load (lbs)	Fracture Type	Defects
1	3.8	0	57.8	7.27	6.8	0	6.9	1	51000	Shear	None
2	2.3	0	61.2	7.85	7.5	0	7.6	1	45700	Cone	None
3	1.7	0	62.1	7.43	7.8	0	7.8	1	48900	Shear/Column	None
4	1.4	0	59.8	7.34	7.3	0	7.3	1	RCPT		
5	1.3	0	58.7	7.23	7.7	0	7.8	1	RCPT		

6" x 12" Cylinders	Sample Number	Diameter (mm)	Length (mm)	Max Load (lbs)	% of Coarse Fractured	Fracture Type	Defects	Notes
	1	152	305	36900	100	Typical	None	
	2	151	305	37700	100	Typical	None	
	3	149	305	48900	100	Typical	None	

Beams	Sample Number	Length (mm)	Width (mm)	Height (mm)	Max Load (lbs)	a value (mm)	Notes	Fracture width (mm)	Fracture Depth (mm)	Notes
	1	450	158	155	7700	N/A		161	156	Typical Fracture
	2	450	154	150	8800	N/A		160	151	Typical Fracture
	3	450	155	155	8100	N/A		158	150	Typical Fracture

12.19. 0.45WCM00AE25CR Repeat

Test Results

Batch Id: 0 Air 25 CR
 Test Date: July 2nd 2018 Air Entrained : No Cast Date: June 4th 2018
 Water Cement Ratio: 0.45 Crumb Rubber Replacement: 15%

4" x 8" Cylinders	Sample Number	Diameter (mm)	Length (mm)	Current (μA)	Resipod Surface Resistivity (kΩcm)							
					0°	90°	180°	270°	0°	90°	180°	270°
	1	101	196	200	17.4	17.9	18.2	16.6	17.5	17.5	17.4	16.9
	2	101	198	200	17.1	15.6	16	15.9	16.5	16.5	16.4	15.9
	3											
	4											
	5											

4" x 8" Cylinders	Resipod Bulk Resistivity			Merlin Resistivity	RCON Impedence				Compressive Strength		
	Upper Insert (kΩcm)	Lower Insert (kΩcm)	Cylinder (kΩcm)	kΩcm	@ 300 Hz (kΩcm)	Phase Angle (°)	@ 40Hz (kΩcm)	Phase Angle (°)	Max Load (lbs)	Fracture Type	Defects
	1	6.2	1.9	67.3	7.4	7.7	0	7.7	1	RCPT	
	2	3	2.9	60.1	7.7	7.2	0	6.9	1	RCPT	
	3										
	4										
	5										

6" x 12" Cylinders	Sample Number	Diameter (mm)	Length (mm)	Max Load (lbs)	% of Coarse Fractured	Fracture Type	Defects	Splitting Tensile Test			
								Notes			
	1	152	305	36900	100	Typical	None				
	2	151	305	37700	100	Typical	None				
	3	149	305	48900	100	Typical	None				

Beams	Sample Number	Length (mm)	Width (mm)	Height (mm)	Max Load (lbs)	a value (mm)	Notes	Fracture width (mm)	Fracture Depth (mm)	3rd point Flexural Test	
										Notes	
	1										
	2										
	3										

Appendix D. Rapid Chloride Penetration Results

Table 12-31 0.40WCM5.7AE00CR Sample 4 RCP Table

Time (hrs)	DC Current (Amps)
0	0.1423
0.5	0.1506
1	0.1592
1.5	1.66E-01
2	0.1719
2.5	0.1773
3	0.1886
3.5	0.191
4	0.1978
4.5	0.1983
5	0.2044
5.5	0.2077
6	0.2125

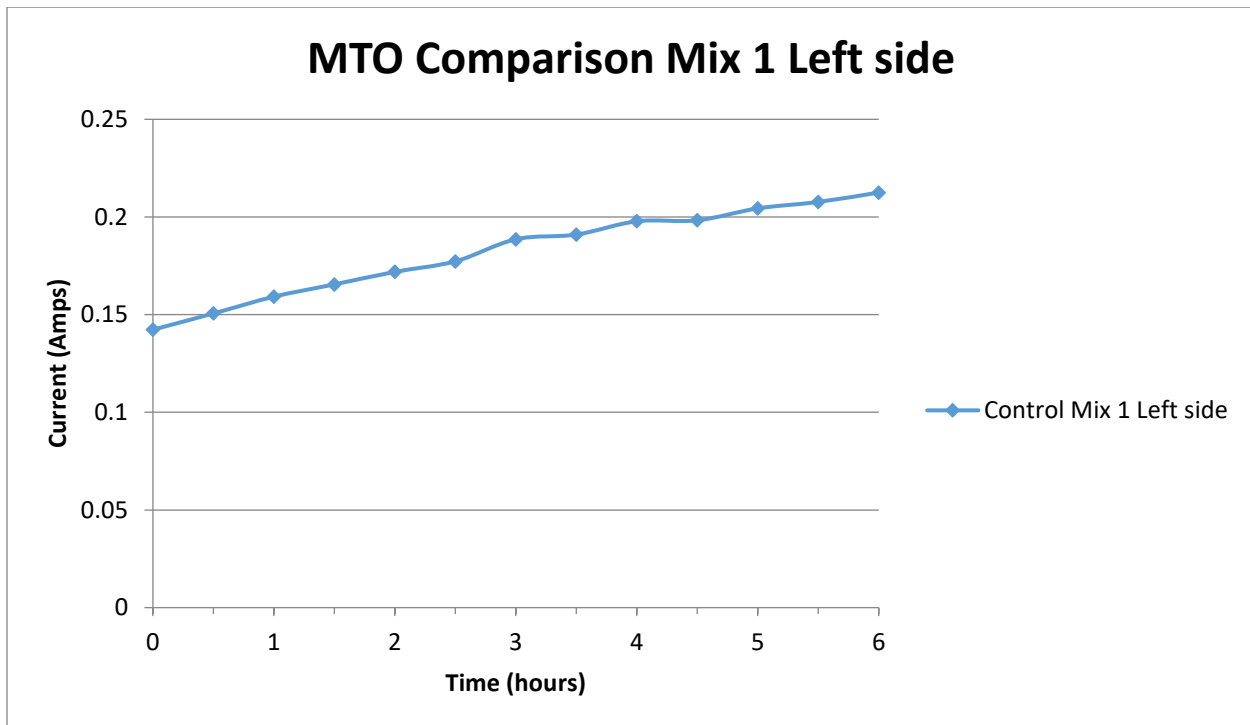


Figure 12-7 0.40WCM5.7AE00CR Sample 4 RCP Result

Charge Passed: 3487 Coulombs, Moderate Penetrability

Table 12-32 0.40WCM5.7AE00CR Sample 5 RCP Table

Time (hrs)	DC Current (Amps)
0	0.1248
0.5	0.1278
1	0.1332
1.5	0.1398
2	0.1446
2.5	0.1519
3	0.1561
3.5	0.1578
4	0.1599
4.5	0.1604
5	0.1613
5.5	0.1627
6	0.1629

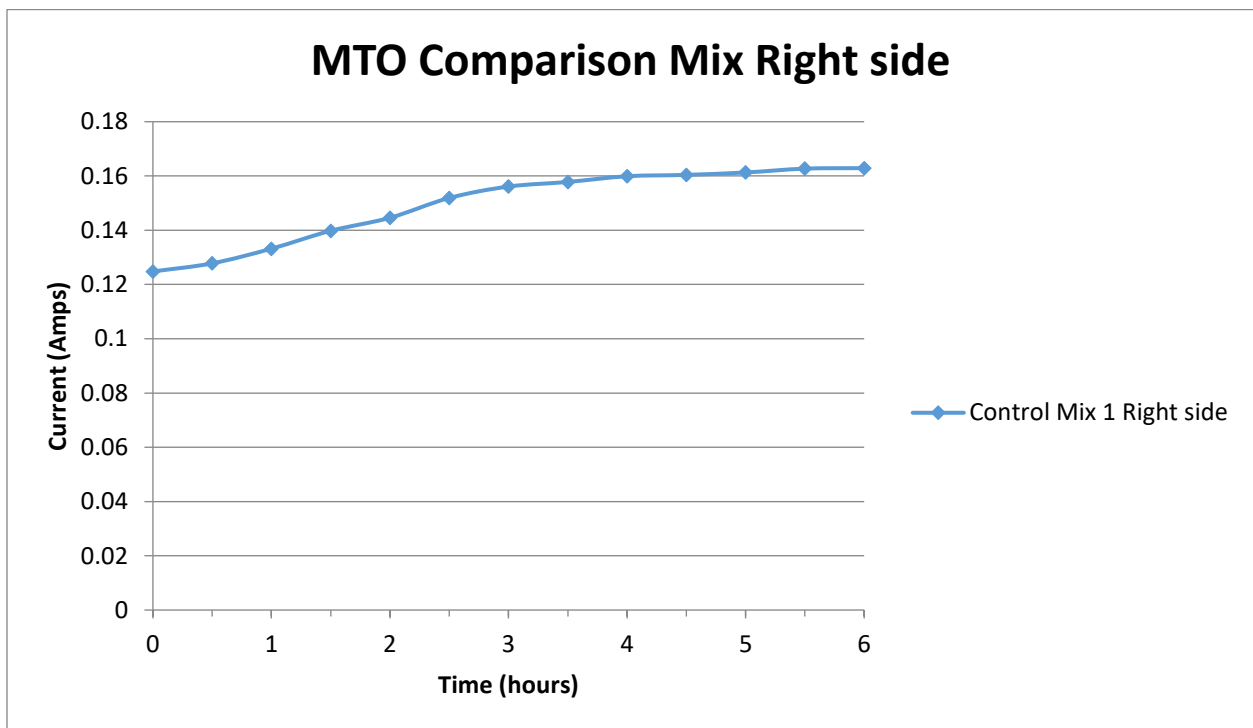


Figure 12-8 0.40WCM5.7AE00CR Sample 5 RCP Result

Charge Passed: 2865 Coulombs, Moderate Penetrability

Table 12-33 0.45WCM00AE00CR Sample 4 RCP Table

Time (hrs)	DC Current (Amps)
0	0.169
0.5	0.1872
1	0.2005
1.5	2.12E-01
2	0.2202
2.5	0.2304
3	0.2345
3.5	0.2343
4	0.2339
4.5	0.2385
5	0.2442
5.5	0.2472
6	0.2501

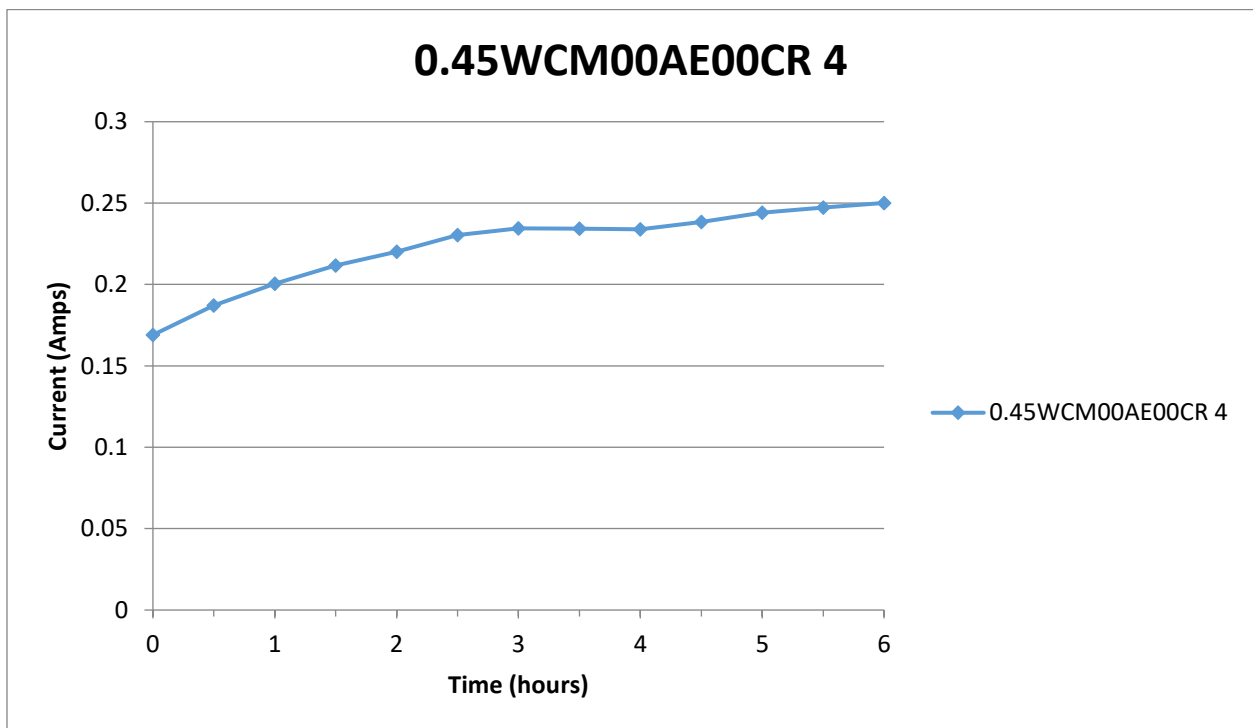


Figure 12-9 0.45WCM00AE00CR Sample 4 RCP Result

Charge Passed: 4287 Coulombs, High Penetrability

Table 12-34 0.45WCM00AE00CR Sample 5 RCP Table

Time (hrs)	DC Current (Amps)
0	0.1236
0.5	0.1917
1	0.2056
1.5	0.2203
2	0.2242
2.5	0.2208
3	0.2288
3.5	0.2409
4	0.2421
4.5	0.2494
5	0.2533
5.5	0.2604
6	0.2646

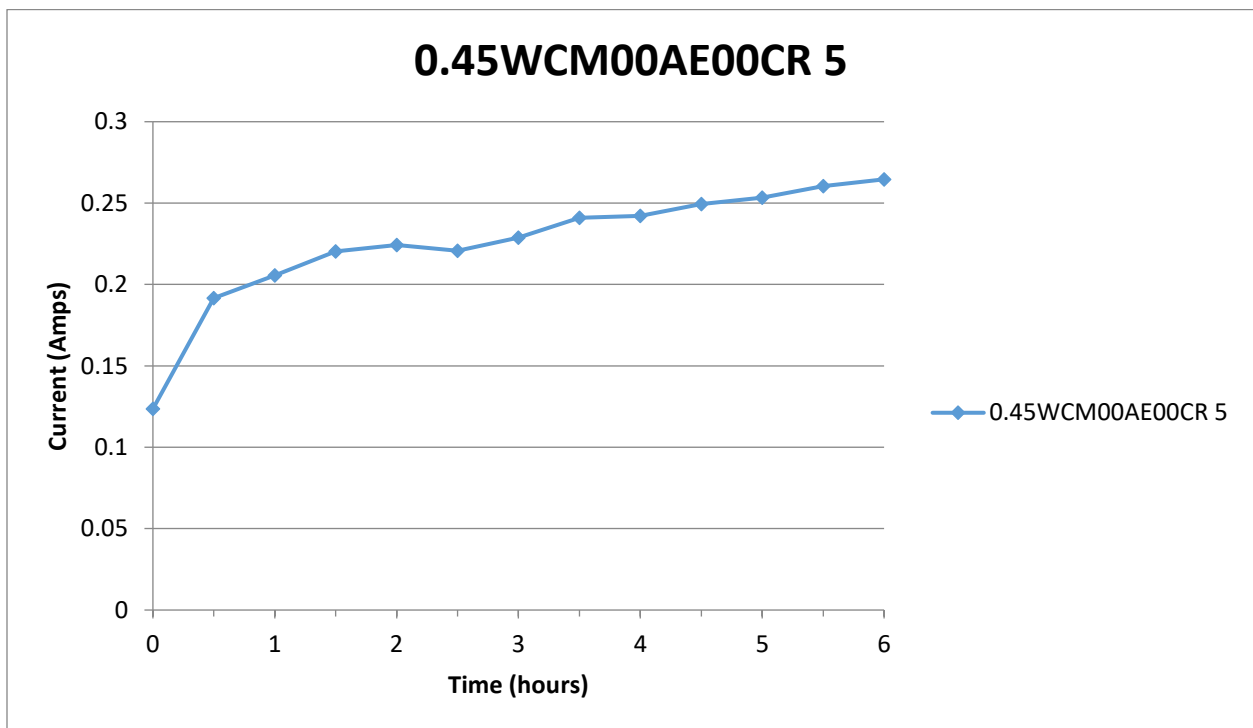


Figure 12-10 0.45WCM00AE00CR Sample 5 RCP Result

Charge Passed: 4350 Coulombs, High Penetrability

Table 12-35 0.45WCM00AE05CR Sample 4 RCP Table

Time (hrs)	DC Current (Amps)
0	0.1104
0.5	0.1172
1	0.1236
1.5	1.30E-01
2	0.1357
2.5	0.1431
3	0.1452
3.5	0.1502
4	0.1527
4.5	0.1558
5	0.1585
5.5	0.1601
6	0.1627

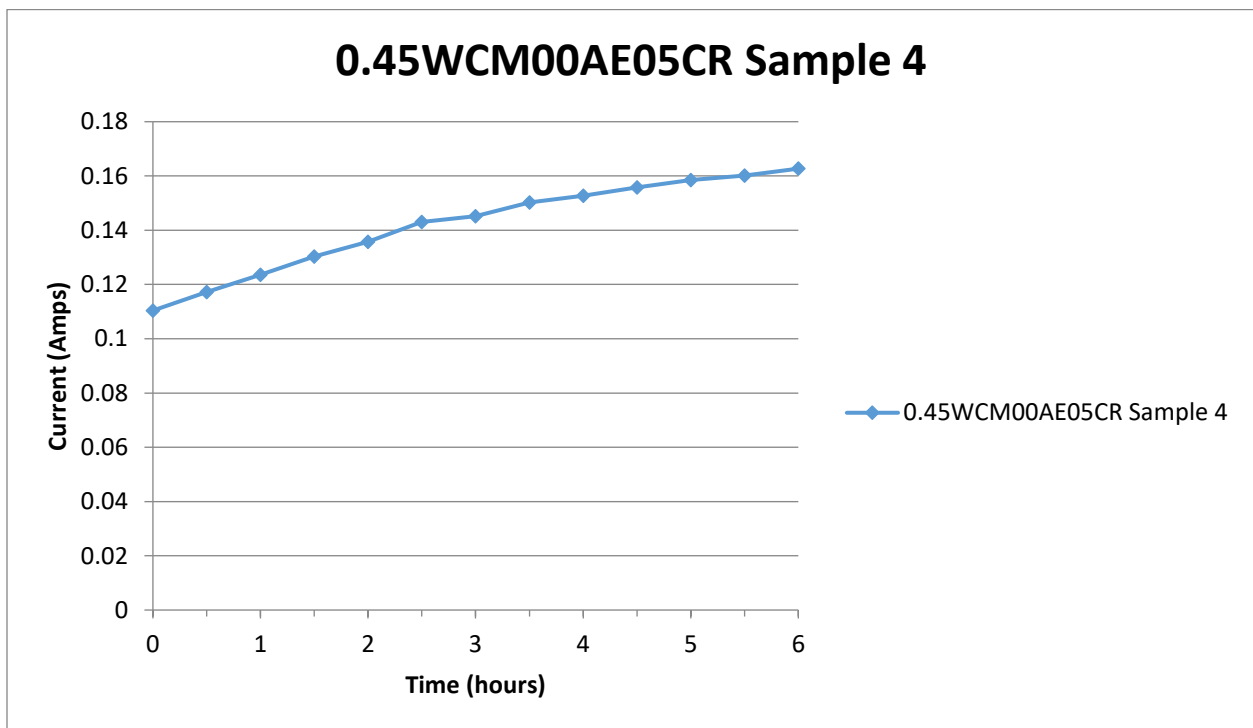


Figure 12-11 0.45WCM00AE05CR Sample 4 RCP Result

Charge Passed: 2721 Coulombs, Moderate Penetrability

Table 12-36 0.45WCM00AE05CR Sample 5 RCP Table

Time (hrs)	DC Current (Amps)
0	0.126
0.5	0.1387
1	0.149
1.5	0.158
2	0.166
2.5	0.1758
3	0.1827
3.5	0.1862
4	0.1934
4.5	0.1977
5	0.2013
5.5	0.207
6	0.2105

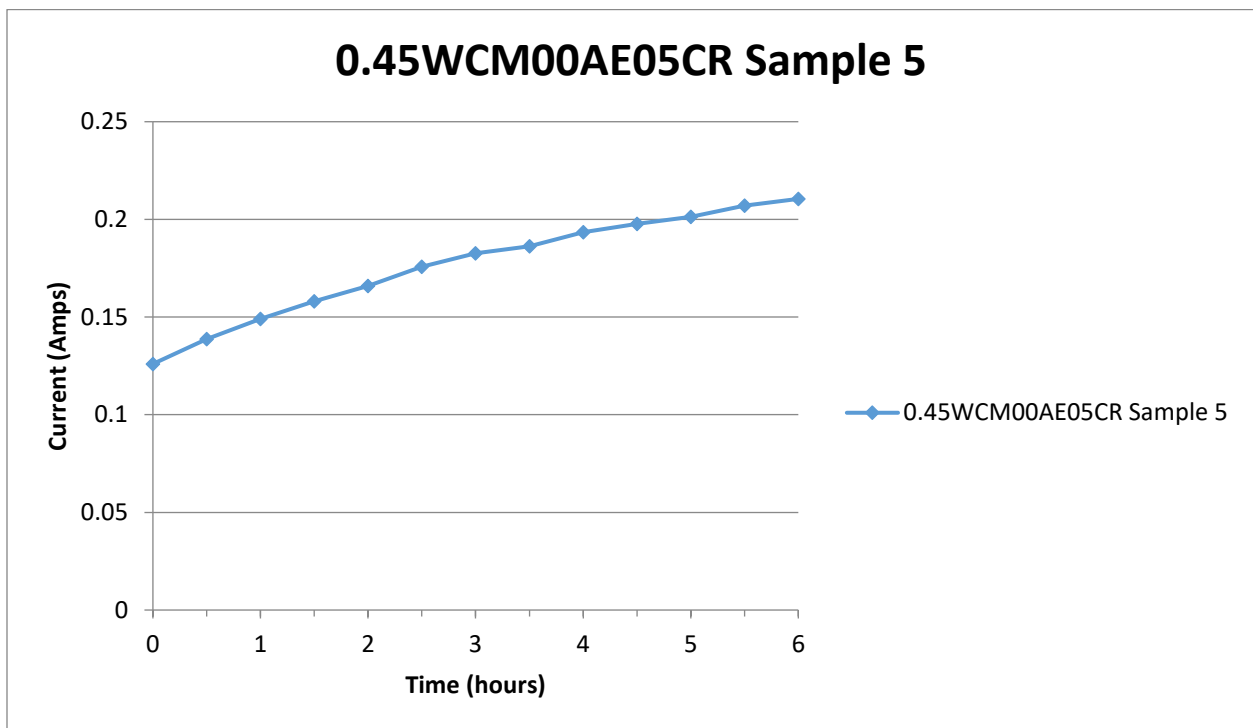


Figure 12-12 0.45WCM00AE05CR Sample 5 RCP Result

Charge Passed: 3383 Coulombs, Moderate Penetrability

Table 12-37 0.45WCM00AE10CR Sample 4 RCP Table

Time (hrs)	DC Current (Amps)
0	0.1041
0.5	0.1157
1	0.1251
1.5	1.33E-01
2	0.1404
2.5	0.1511
3	0.1579
3.5	0.1623
4	0.1702
4.5	0.1754
5	0.1787
5.5	0.1805
6	0.1824

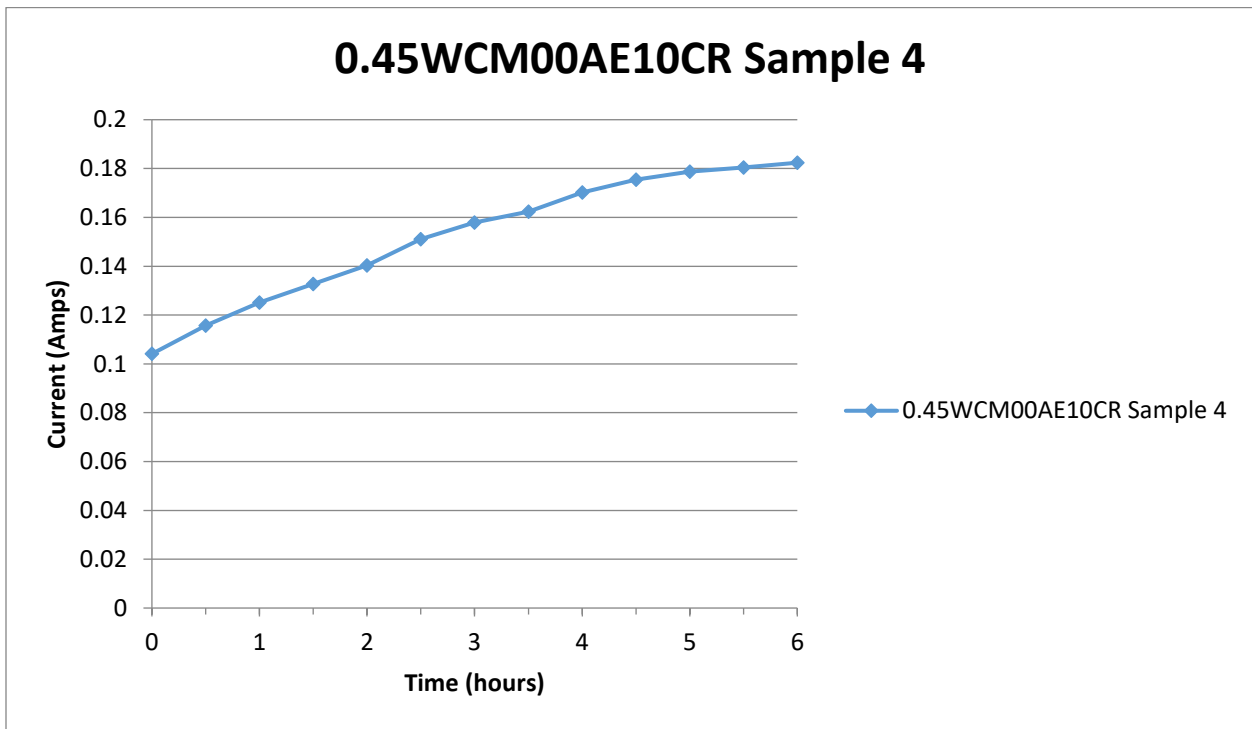


Figure 12-13 0.45WCM00AE10CR Sample 4 RCP Result

Charge Passed: 2919 Coulombs, Moderate Penetrability

Table 12-38 0.45WCM00AE10CR Sample 5 RCP Table

Time (hrs)	DC Current (Amps)
0	0.1186
0.5	0.1324
1	0.1433
1.5	0.1536
2	0.163
2.5	0.1712
3	0.1782
3.5	0.1838
4	0.1883
4.5	0.1946
5	0.2001
5.5	0.2051
6	0.2072

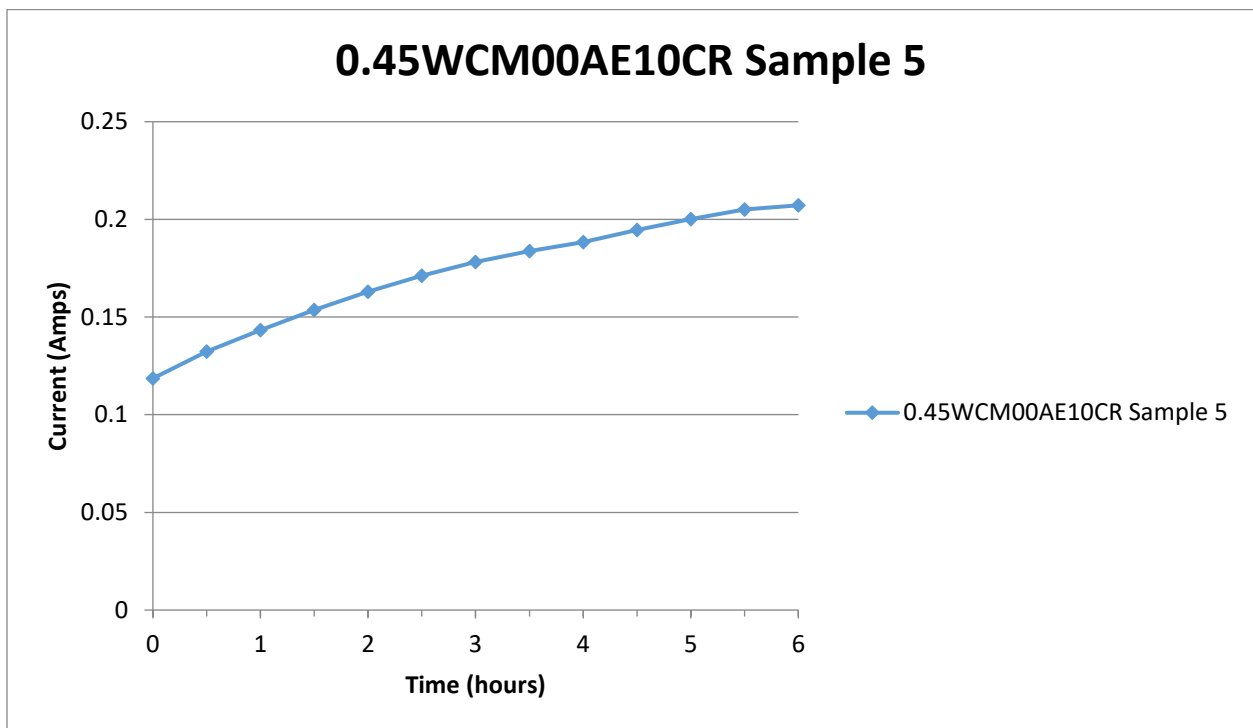


Figure 12-14 0.45WCM00AE10CR Sample 5 RCP Result

Charge Passed: 3306 Coulombs, Moderate Penetrability

Table 12-39 0.45WCM00AE15CR Sample 4 RCP Result

Time (hrs)	DC Current (Amps)
0	0.108
0.5	0.1216
1	0.1303
1.5	1.36E-01
2	0.1436
2.5	0.1497
3	0.1596
3.5	0.1656
4	0.1702
4.5	0.1763
5	0.1818
5.5	0.1882
6	0.1941

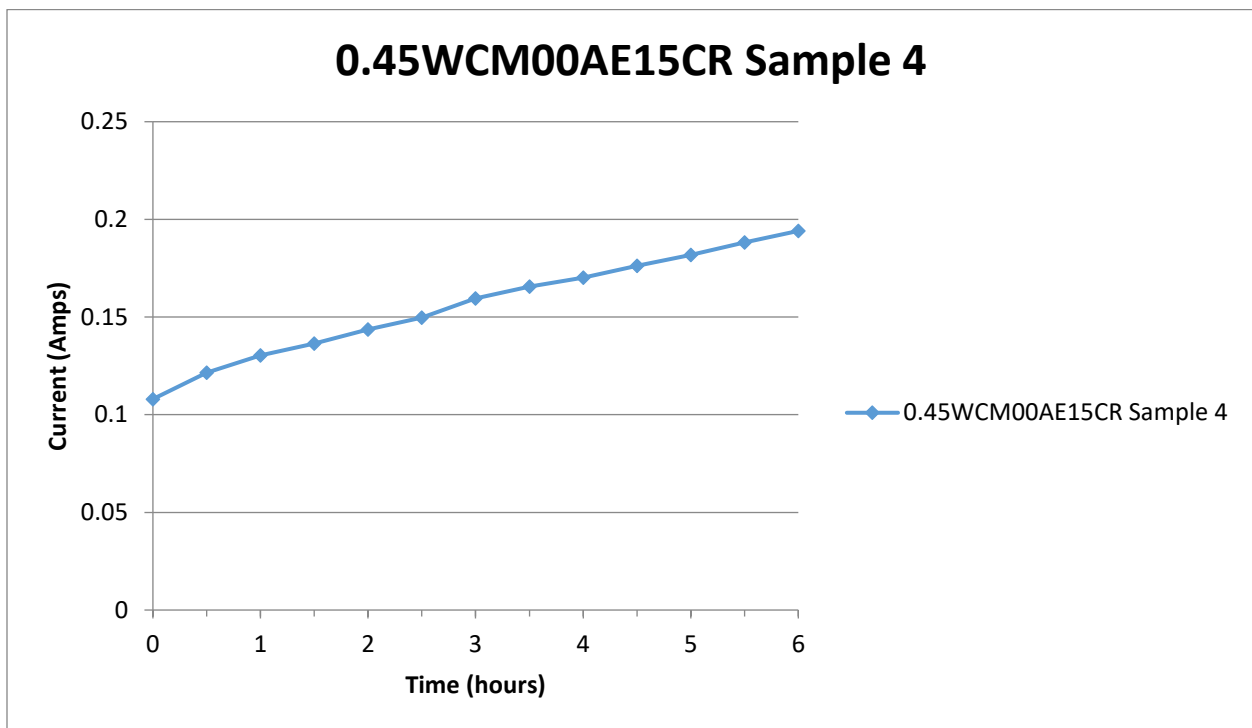


Figure 12-15 0.45WCM00AE15CR Sample 4 RCP Result

Charge Passed: 2985 Coulombs, Moderate Penetrability

Table 12-40 0.45WCM00AE15CR Sample 5 RCP Result

Time (hrs)	DC Current (Amps)
0	0.1051
0.5	0.119
1	0.1278
1.5	0.1354
2	0.1429
2.5	0.151
3	0.1574
3.5	0.1639
4	0.169
4.5	0.1753
5	0.181
5.5	0.1854
6	0.1846

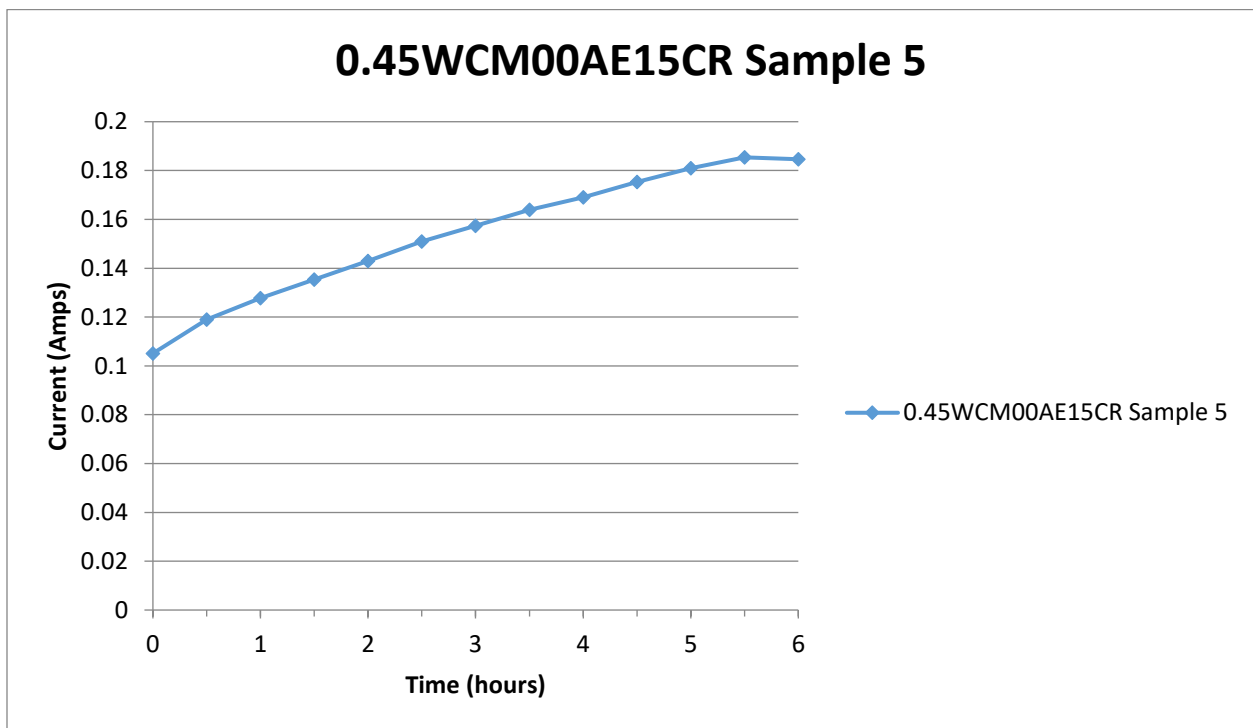


Figure 12-16 0.45WCM00AE15CR Sample 5 RCP Result

Charge Passed: 2950 Coulombs, Moderate Penetrability

Table 12-41 0.45WCM00AE20CR Sample 4 RCP Table

Time (hrs)	DC Current (Amps)
0	0.1274
0.5	0.1437
1	0.1559
1.5	1.67E-01
2	0.1762
2.5	0.1844
3	0.1903
3.5	0.1937 (Value was corrected using central different)
4	0.1971
4.5	0.2005
5	0.2042
5.5	0.2096
6	0.2133

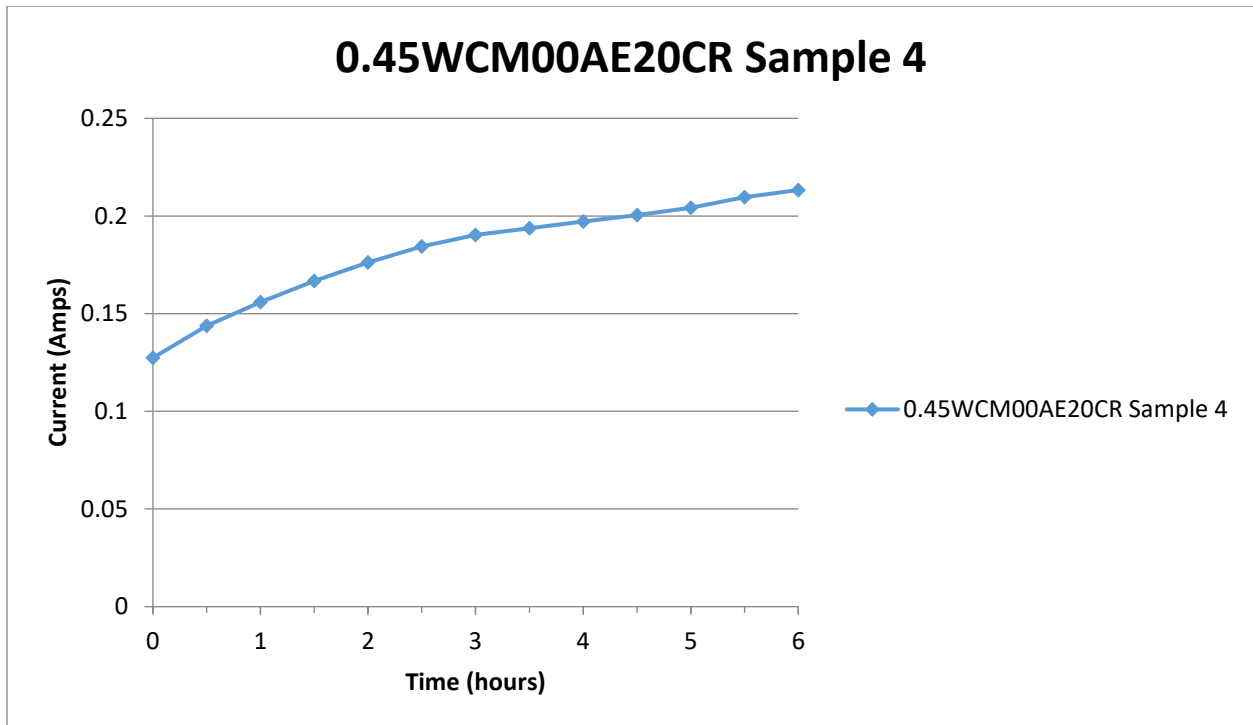


Figure 12-17 0.45WCM00AE20CR Sample 4 RCP Result

Charge Passed: 3491 Coulombs, Moderate Penetrability

Table 12-42 0.45WCM00AE20CR RCP Table

Time (hrs)	DC Current (Amps)
0	0.1148
0.5	0.129
1	0.14
1.5	0.1489
2	0.1592
2.5	0.1683
3	0.1726
3.5	0.1803
4	0.1876
4.5	0.1942
5	0.2007
5.5	0.2045
6	0.2103

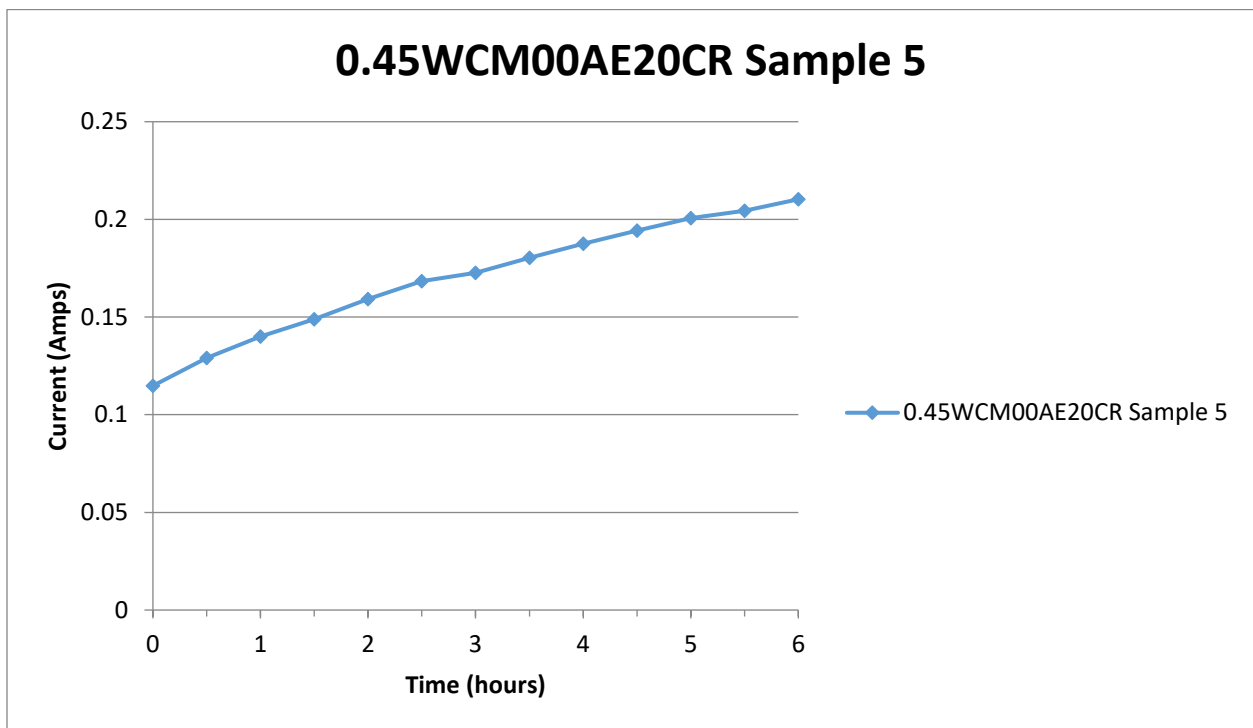


Figure 12-18 0.45WCM00AE20CR RCP Result

Charge Passed: 3261 Coulombs, Moderate Penetrability

Table 12-43 0.45WCM00AE25CR RCP Table

Time (hrs)	DC Current (Amps)
0	0.0884
0.5	0.0959
1	0.1028
1.5	1.09E-01
2	0.1141
2.5	0.1183
3	0.1221
3.5	0.1286
4	0.1343
4.5	0.1408
5	0.1472
5.5	0.1541
6	0.1581

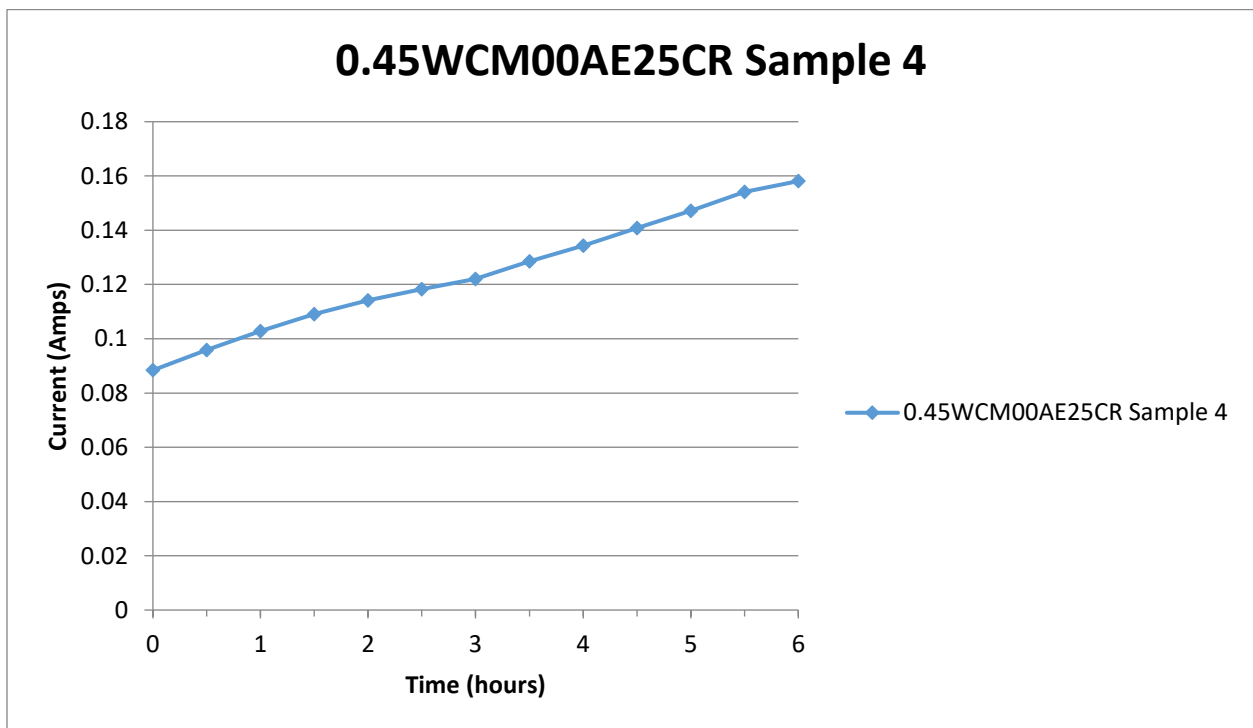


Figure 12-19 0.45WCM00AE25CR RCP Result

Charge Passed: 2374 Coulombs, Moderate Penetrability

Table 12-44 0.45WCM00AE25CR Sample 5 RCP Table

Time (hrs)	DC Current (Amps)
0	0.093
0.5	0.1042
1	0.1102
1.5	0.1183
2	0.1244
2.5	0.1306
3	0.1356
3.5	0.1409
4	0.1423
4.5	0.1471
5	0.1545
5.5	0.1606
6	0.161

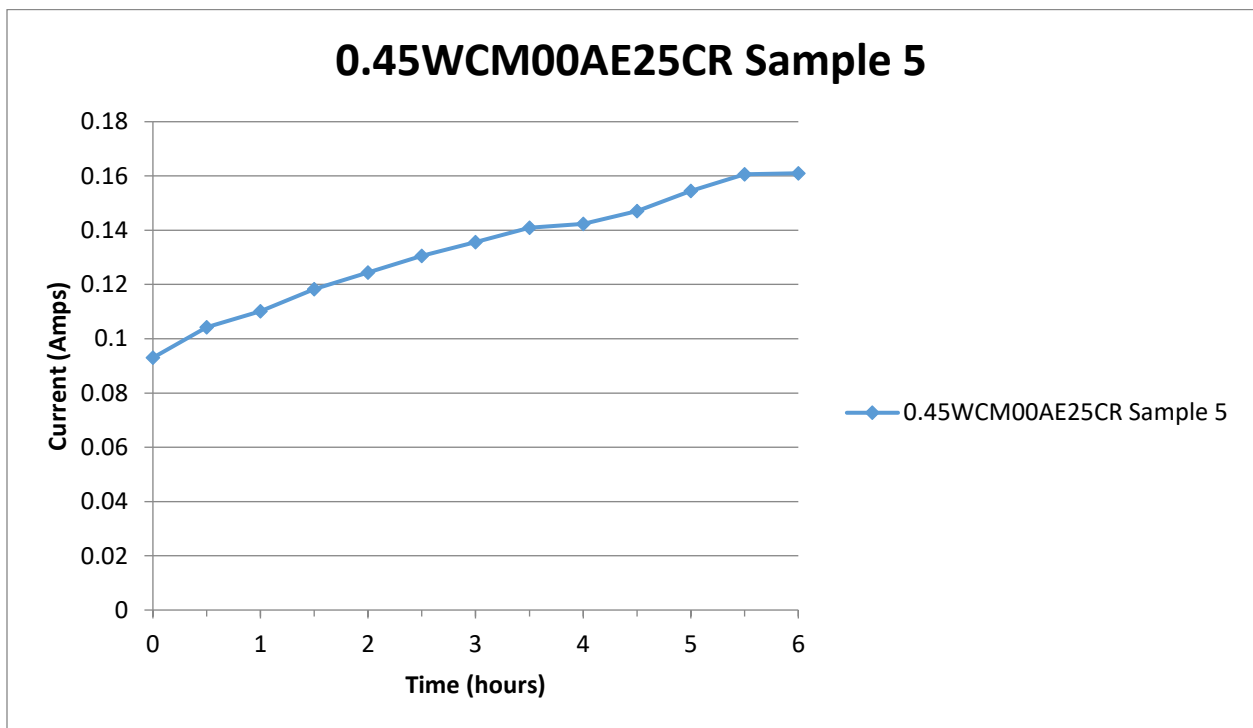


Figure 12-20 0.45WCM00AE25CR Sample 5 RCP Result

Charge Passed: 2541 Coulombs, Moderate Penetrability

Appendix E. Freeze Thaw Data

Due to equipment malfunction the batches CM1R, 00CR, and 05CR have been shifted by 30 cycles.

Table 12-45 Comprehensive Freeze Thaw Data

Batch and Sample ID	Mass (kg)	Length (mm)	Width (mm)	Depth (mm)	Fundamental Frequency (0 Cycles)	Mass after 30 Cycles	30 Cycles	Relative Dynamic Modulus	Durability Factor	Mass after 60 cycles	60 Cycles	Relative Dynamic Modulus	Durability Factor
CM1RS1	7.846	406	75	100	179.85	7.85	472.8			7.834	569.5	145.0883431	Test still running
CM1RS2	Control	406	75	100								#DIV/0!	#DIV/0!
CM1RS3	7.713	406	75	100	Inconclusive	7.781	698.3			7.702	193.6	7.686464432	0.768646443
CM1RS4	7.762	406	75	100	179.9	7.774	5509			7.762	972.3	3.114978309	0.311497831
0.45WCM00AE05CRS1	7.782	406	75	100	179.95	7.803	299.3			7.778	163	29.65935998	2.965935998
0.45WCM00AE05CRS2	7.769	406	75	100	179.9	7.78	538.5			7.76	884.6	269.8500201	Test still running
0.45WCM00AE05CRS3	7.82	406	75	100	180	7.834	707.8			7.806	787.6	123.8198571	Test still running
0.45WCM00AE00CRS1	8.025	406	75	100	179.9	8.037	127.1			8.001	141.6	124.118182	Test still running
0.45WCM00AE00CRS2	7.992	406	75	100	179.9	8.011	158.5			7.982	167.3	111.4123536	Test still running
0.45WCM00AE00CRS3	8.007	406	75	100	179.8	8.002	655.5			7.998	1071	266.9522278	Test still running
0.45WCM00AE10CRS1	7.847	406	75	100	5290	7.85	344.2	0.423360551	0.042336055	7.852	1006	3.616467923	0.723293585
0.45WCM00AE10CRS2	7.938	406	75	100	155.8	7.947	863.9	3074.624201	Test Still Running	7.945	716.3	2113.756692	Test still running
0.45WCM00AE10CRS3	7.824	406	75	100	757.3	7.826	151.2	3.986278788	0.398627879	7.827	903.4	142.3063432	Test still running
0.45WCM00AE15CRS1	7.578	406	75	100	374	7.578	879	552.3756756	Test Still Running	7.575	497.7	177.0892004	Test still running
0.45WCM00AE15CRS2	7.65	406	75	100	201.7	7.647	628.3	970.3363994	Test Still Running	7.654	652.2	1045.562004	Test still running
0.45WCM00AE15CRS3	7.5	406	75	100	768	7.511	525.6	46.83691406	4.683691406	7.512	879.2	131.054796	Test still running
0.45WCM00AE20CRS1	7.643	406	75	100	865	7.703	720	69.28397207	Test Still Running	7.704	1065	151.5887601	Test still running
0.45WCM00AE20CRS2	7.617	406	75	100	980	7.671	890	82.47605165	Test Still Running	7.673	990	102.0512287	Test still running
0.45WCM00AE20CRS3	7.562	406	75	100	860	7.625	830	93.14494321	Test Still Running	7.631	865	101.1661709	Test still running
0.45WCM00AE25CRS1	7.3	406	75	100	635	7.36	790	154.7771096	Test Still Running	7.365	1185	348.2484965	Test still running
0.45WCM00AE25CRS2	7.334	406	75	100	580	7.388	1020	309.274673	Test Still Running	7.398	1880	1050.653983	Test still running
0.45WCM00AE25CRS3	7.323	406	75	100	1080	7.383	1010	87.45713306	Test Still Running	7.395	1000	85.73388203	Test still running

Batch and Sample ID	Mass after 90 cycles	90 Cycles	Relative Dynamic Modulus	Durability Factor	Mass after 120 cycles	120 Cycles	Relative Dynamic Modulus	Durability Factor	Mass after 150 Cycles	150 Cycles	Relative Dynamic Modulus	Durability Factor
CM1RS1	7.828	966.3	417.7043743	Test Running Still	7.826	1272	498.8692852	Test Running Still	7.82	1075	516.9660138	Test Running Still
CM1RS2			#DIV/0!	#DIV/0!			#DIV/0!	#DIV/0!			#DIV/0!	#DIV/0!
CM1RS3	7.701	795.7	129.8418313	Test Running Still	7.697	759.9	1540.643596	Test Running Still	7.694	890	162.4411028	Test Running Still
CM1RS4	7.758	787.8	2.04496749	0.408993498	7.757	1025	111.1340546	Test Running Still	7.748	1151.7	4.370520775	1.74820831
0.45WCM00AE05CRS1	7.779	681.7	518.7679706	Test Running Still	7.779	672	1699.665023	Test Running Still	7.776	1067.6	1272.341511	Test Running Still
0.45WCM00AE05CRS2	7.758	988.9	337.2355411	Test Running Still	7.753	965.8	119.2011738	Test Running Still	7.753	1074	397.7746914	Test Running Still
0.45WCM00AE05CRS3	7.802	743	110.1936353	Test Running Still	7.799	786.9	99.82232379	Test Running Still	7.794	753	113.1797775	Test Running Still
0.45WCM00AE00CRS1	8.012	146.3	132.4944086	Test Running Still	8.005	814.5	3308.68689	Test Running Still	8.007	1097	7449.414742	Test Running Still
0.45WCM00AE00CRS2	7.98	919.4	3364.731901	Test Running Still	7.978	1071	4098.14254	Test Running Still	7.969	917.4	3350.109007	Test Running Still
0.45WCM00AE00CRS3	7.997	7034	11514.87787	Test Running Still	7.994	836.8	61.04701053	Test Running Still	7.986	695.2	112.4796962	Test Running Still
0.45WCM00AE10CRS1	7.852	968.6	3.352567922	1.005770377	7.847	886.3	2.807050039	1.122820016	7.851	1129	4.554875804	2.277437902
0.45WCM00AE10CRS2	7.948	697.7	2005.407059	Test Running Still	7.943	952.6	3738.404129	Test Running Still	7.95	1032	4387.57434	Test Running Still
0.45WCM00AE10CRS3	7.826	983.4	168.6259829	Test Running Still	7.821	1051.8	192.8991968	Test Running Still	7.821	750	98.08139026	Test Running Still
0.45WCM00AE15CRS1	7.572	799.6	457.0906803	Test Running Still	7.565	910	592.0243644	Test Running Still	7.576	935	625	Test Running Still
0.45WCM00AE15CRS2	7.658	347.5	296.8231854	Test Running Still	7.654	737.1	1335.491186	Test Running Still	7.652	731.7	1315.995226	Test Running Still
0.45WCM00AE15CRS3	7.516	654.4	72.60460069	Test Running Still	7.507	755.7	96.82252502	Test Running Still	7.511	765	99.22027588	Test Running Still
0.45WCM00AE20CRS1	7.709	965	124.4578837	Test Running Still	7.709	870	101.1594106	Test Running Still	7.706	870	101.1594106	Test Running Still
0.45WCM00AE20CRS2	7.676	740	57.0179092	17.10537276	7.677	810	68.3152853	Test Running Still	7.67	905	85.27957101	Test Running Still
0.45WCM00AE20CRS3	7.63	1015	139.2948891	Test Running Still	7.63	1740	409.3564089	Test Running Still	7.624	730	72.05246079	Test Running Still
0.45WCM00AE25CRS1	7.371	1055	276.0307521	Test Running Still	7.376	465	53.62390725	21.4495629	7.379	880	192.0515841	Test Running Still
0.45WCM00AE25CRS2	7.404	1065	337.1655767	Test Running Still	7.405	760	171.7003567	Test Running Still	7.406	1160	400	Test Running Still
0.45WCM00AE25CRS3	7.401	710	43.21844993	12.96553498	7.406	6645	3785.667438	Test Running Still	7.407	880	66.39231824	Test Running Still

Batch and Sample ID	Mass after 180 Cycles	180 Cycles	Relative Dynamic Modulus	Durability Factor	Mass After 210 Cycles	210 Cycles	Relative Dynamic Modulus	Durability Factor	Mass After 240 Cycles	240 Cycles	Relative Dynamic Modulus	Durability Factor
CM1RS1	7.82	1030	474.591017	Test Still Running	7.807	1045	488.5147095	Test Still Running	7.802	1220	665.8320951	Test Still Running
CM1RS2			#DIV/0!	#DIV/0!			#DIV/0!	#DIV/0!			#DIV/0!	#DIV/0!
CM1RS3	7.686	880	158.8112486	Test Still Running	7.679	1140	266.5174311	Test Still Running	7.668	850	148.1677778	Test Still Running
CM1RS4	7.749	1013	3.381219352	1.690609676	7.745	895	2.639371518	1.583622911	7.733	990	3.229422334	2.260595634
0.45WCM00AE05CRS1	7.776	1270	1800.503659	Test Still Running	7.766	925	955.146595	Test Still Running	7.756	1120	1400.30491	Test Still Running
0.45WCM00AE05CRS2	7.737	860	255.0500936	Test Still Running	7.725	1225	517.4885704	Test Still Running	7.717	950	311.2259457	Test Still Running
0.45WCM00AE05CRS3	7.776	980	191.7039382	Test Still Running	7.766	840	140.8437097	Test Still Running	7.757	1025	209.713609	Test Still Running
0.45WCM00AE00CRS1	7.993	1320	10785.90923	Test Still Running	7.986	1250	9672.281439	Test Still Running	7.972	835	4316.004113	Test Still Running
0.45WCM00AE00CRS2	7.972	915	3332.603569	Test Still Running	7.962	930	3442.76488	Test Still Running	7.955	795	2515.797749	Test Still Running
0.45WCM00AE00CRS3	7.985	710	117.3197977	Test Still Running	7.975	1110	286.7481109	Test Still Running	7.95	1015	239.7655	Test Still Running
0.45WCM00AE10CRS1	7.851	1155	4.767082022	2.860249213	7.847	1030	3.791081364	2.653756955	7.844	790	2.230195004	1.784156003
0.45WCM00AE10CRS2	7.945	775	2474.391974	Test Still Running	7.945	970.8	3882.617687	Test Still Running	7.948	645	1713.896227	Test Still Running
0.45WCM00AE10CRS3	7.817	1150	230.6002464	Test Still Running	7.81	800	111.5948262	Test Still Running	7.81	780	106.0848317	Test Still Running
0.45WCM00AE15CRS1	7.575	1035	765.8390289	Test Still Running	7.575	960	658.8692842	Test Still Running	7.57	865	534.920215	Test Still Running
0.45WCM00AE15CRS2	7.653	1325	4315.389098	Test Still Running	7.648	915	2057.929021	Test Still Running	7.65	865	1839.163835	Test Still Running
0.45WCM00AE15CRS3	7.51	1340	304.429796	Test Still Running	7.51	1065	192.2988892	Test Still Running	7.51	895	135.8074612	Test Still Running
0.45WCM00AE20CRS1	7.7	1035	143.1688329	Test Still Running	7.6854	1140	173.6910689	Test Still Running	7.68	330	14.55444552	11.64355642
0.45WCM00AE20CRS2	7.668	620	40.02498959	24.01499375	7.656	1005	105.1671179	Test Still Running	7.65	645	43.31788838	34.6543107
0.45WCM00AE20CRS3	7.625	1135	174.1786101	Test Still Running	7.614	805	87.61830719	Test Still Running	7.609	995	133.8595187	Test Still Running
0.45WCM00AE25CRS1	7.387	1495	554.2873086	Test Still Running	7.385	1110	305.5614111	Test Still Running	7.387	845	177.0785542	Test Still Running
0.45WCM00AE25CRS2	7.411	760	171.7003567	Test Still Running	7.404	1295	498.5211058	Test Still Running	7.404	660	129.4887039	Test Still Running
0.45WCM00AE25CRS3	7.412	1125	108.5069444	Test Still Running	7.412	1260	136.1111111	Test Still Running	7.407	845	61.21613512	Test Still Running

Batch and Sample ID	Mass after 270 Cycles	270 Cycles	Relative Dynamic Modulus	Durability Factor	Mass after 300 Cycles	300 Cycles	Relative Dynamic Modulus	Durability Factor	Mass After 330 Cycles	330 Cycles	Relative Dynamic Modulus	Durability Factor	Cut off Cycle	Taken Durability Factor
CM1RS1	7.798	715	228.6952518	Test Still Running	7.792	940	395.2762962	Test Still Running	7.783	1040	483.8511113	483.8511113	300	100
CM1RS2			#DIV/0!	#DIV/0!			#DIV/0!	#DIV/0!			#DIV/0!	#DIV/0!		
CM1RS3	7.663	840	144.7019848	Test Still Running	7.656	825	139.580199	Test Still Running	7.652	715	104.8402383	104.8402383	30	0.77
CM1RS4	7.728	555	1.014940123	0.811952098	7.724	950	2.973730901	2.676357811	7.717	685	1.546092944	1.546092944	30	0.311
0.45WCM00AE05CRS1	7.752	785	687.9009034	Test Still Running	7.746	805	723.3997046	Test Still Running	7.737	850	806.537227	806.537227	30	2.97
0.45WCM00AE05CRS2	7.707	790	215.2200695	Test Still Running	7.701	795	217.9529954	Test Still Running	7.694	1080	402.2315159	402.2315159	300	100
0.45WCM00AE05CRS3	7.742	1010	203.6205616	Test Still Running	7.734	945	178.2553201	Test Still Running	7.725	1165	270.9135543	270.9135543	300	100
0.45WCM00AE00CRS1	7.959	730	3298.789618	Test Still Running	7.948	620	2379.53599	Test Still Running	7.935	800	3961.766477	3961.766477	300	100
0.45WCM00AE00CRS2	7.947	530	1118.132333	Test Still Running	7.939	605	1456.97539	Test Still Running	7.93	600	1432.992666	1432.992666	300	100
0.45WCM00AE00CRS3	7.924	690	110.8033241	Test Still Running	7.903	690	110.8033241	Test Still Running	7.889	925	199.1306326	199.1306326	300	100
0.45WCM00AE10CRS1	7.844	575	1.18147448	1.063327032	7.84	910	2.959180392	2.959180392					30	0.04
0.45WCM00AE10CRS2	7.945	865	3082.458997	Test Still Running	7.944	1190	5833.900478	5833.900478					300	100
0.45WCM00AE10CRS3	7.807	860	128.9617711	Test Still Running	7.804	1160	234.6281222	234.6281222					30	0.4
0.45WCM00AE15CRS1	7.575	675	325.7349367	Test Still Running	7.571	1040	773.2563127	773.2563127					300	100
0.45WCM00AE15CRS2	7.65	635	991.1414848	Test Still Running	7.648	1470	5311.569557	5311.569557					300	100
0.45WCM00AE15CRS3	7.513	740	92.84125434	Test Still Running	7.514	1180	236.070421	236.070421					30	4.68
0.45WCM00AE20CRS1	7.673	1206	194.3848441	Test Still Running	7.661	1350	243.5764643	243.5764643					240	11.6
0.45WCM00AE20CRS2	7.643	5670	3347.44898	Test Still Running	7.627	715	53.23042482	53.23042482					90	17.1
0.45WCM00AE20CRS3	7.609	100	1.352082207	1.216873986	7.577	7500	7605.462412	7605.462412					270	1.2
0.45WCM00AE25CRS1	7.38	820	166.7555335	Test Still Running	7.378	695	119.7904396	119.7904396					120	21.4
0.45WCM00AE25CRS2	7.395	1633	792.7137337	Test Still Running	7.384	890	235.4637337	235.4637337					300	235
0.45WCM00AE25CRS3	7.406	710	43.21844993	38.89660494	7.397	795	54.18595679	54.18595679					90	13

Appendix F. Computer Codes

12.20. RCP Data Logger

(Connect "34405A", "USB0::0x0957::0x0618::TW47340036::0::INSTR", "34405 Digital Multimeters / 1.46_3.11")

(Connect "34405A 2 (40039)", "USB0::0x0957::0x0618::TW47340039::0::INSTR", "34405 Digital Multimeters / 1.46_3.11")

:CONF:CURRE:DC 1,0.001

:INIT:IMM

<Bot_Reading_1> = :FETC?

:CONF:CURRE:DC 1,0.001

:INIT:IMM

<Top_Reading_1> = :FETC?

(Wait 1800000ms)

:CONF:CURRE:DC 1,0.001

:INIT:IMM

<Top_Reading_2> = :FETC?

:CONF:CURRE:DC 1,0.001

:INIT:IMM

<Bot_Reading_2> = :FETC?

(Wait 1800000ms)

:CONF:CURRE:DC 1,0.001

:INIT:IMM

<Top_Reading_3> = :FETC?

:CONF:CURRE:DC 1,0.001

:INIT:IMM

<Bot_Reading_3> = :FETC?

(Wait 1800000ms)

:CONF:CURRE:DC 1,0.001

:INIT:IMM

<Top_Reading_4> = :FETC?

:CONF:CURR:DC 1,0.001
:INIT:IMM
<Bot_Reading_4> = :FETC?
(Wait 1800000ms)
:CONF:CURR:DC 1,0.001
:INIT:IMM
<Top_Reading_5> = :FETC?
:CONF:CURR:DC 1,0.001
:INIT:IMM
<Bot_Reading_5> = :FETC?
(Wait 1800000ms)
:CONF:CURR:DC 1,0.001
:INIT:IMM
<Top_Reading_6> = :FETC?
:CONF:CURR:DC 1,0.001
:INIT:IMM
<Bot_Reading_6> = :FETC?
(Wait 1800000ms)
:CONF:CURR:DC 1,0.001
:INIT:IMM
<Top_Reading_7> = :FETC?
:CONF:CURR:DC 1,0.001
:INIT:IMM
<Bot_Reading_7> = :FETC?
(Wait 1800000ms)
:CONF:CURR:DC 1,0.001
:INIT:IMM
<Top_Reading_8> = :FETC?
:CONF:CURR:DC 1,0.001
:INIT:IMM
<Bot_Reading_8> = :FETC?

(Wait 1800000ms)
:CONF:CURR:DC 1,0.001
:INIT:IMM
<Top_Reading_9> = :FETC?
:CONF:CURR:DC 1,0.001
:INIT:IMM
<Bot_Reading_9> = :FETC?
(Wait 1800000ms)
:CONF:CURR:DC 1,0.001
:INIT:IMM
<Top_Reading_10> = :FETC?
:CONF:CURR:DC 1,0.001
:INIT:IMM
<Bot_Reading_10> = :FETC?
(Wait 1800000ms)
:CONF:CURR:DC 1,0.001
:INIT:IMM
<Top_Reading_11> = :FETC?
:CONF:CURR:DC 1,0.001
:INIT:IMM
<Bot_Reading_11> = :FETC?
(Wait 1800000ms)
:CONF:CURR:DC 1,0.001
:INIT:IMM
<Top_Reading_12> = :FETC?
:CONF:CURR:DC 1,0.001
:INIT:IMM
<Bot_Reading_12> = :FETC?
(Wait 1800000ms)
:CONF:CURR:DC 1,0.001
:INIT:IMM

<Top_Reading_13> = :FETC?

:CONF:CURR:DC 1,0.001

:INIT:IMM

<Bot_Reading_13> = :FETC?

12.21. MATLAB Fundamental Frequency Calculator

```
% This script reads acceleration time domain data from a txt file using the
% MATLAB generated importfile function. A plot of the data in the time
% domain is generated, then an FFT is performed on that data.
% This script is written solely for research purposes in partial fulfilment
% of the Master of Science in Civil Engineering degree at Lakehead
% University. An adxl-337 accelerometer is used in conjunction with a DAQ
% system provided by Bruce Misner, an Engineering Technologist at Lakehead
% University. Variables used are::
%
% fs          :: Sampling Frequency
% Start       :: Time after beginning of sampling period to start filling
% data in xldotdot vector
% File        :: Stores Filename of data set being processed
% xldotdot    :: Acceleration data vector
% dcOffset    :: The amount of dcOffset from the DAQ
% T           :: Cut of time to end data filling of xldotdot
% N           :: Number of data points imported
% t           :: Time vector used in plotting
% ZeroPad     :: Variable to used to extend the time domain for better
% frequency resolution
% A           :: Place holder variable to use sscanf count option
% count       :: output of sscanf count option, used to control characters
% read into samp
% samp        :: String to store frequency plot title
% sampl       :: String to store time history plot title
% Xl          :: Stores frequency bins of fft function
% Xl_mag      :: Stores the magnitude of the fft bins
% Xlds       :: Zeropadded fft frequency bins converted to frequency space
% Xlss       :: Single sided plot of fft in frequency space
%
% Inputs      :: Filename
% Outputs     :: Single Sided Frequency Plot, Magnitude Plot (Bin Space),
% Time History Plot
%=====
clc, clear all, close all

fs = 20000; % Sampling Frequency (Hz)
Start = 0; % Time after sampling to start (s)
File = input('Filename: ', 's');
xldotdot = importfile2(File, 1, inf); % Load acceleration data
dcOffset = mean(xldotdot(1:20)); % Find offset
xldotdot = xldotdot - dcOffset; % Correct offset
T = numel(xldotdot) / fs; % Cutoff time (s)
N = T * fs - Start*fs; % Number of data points
```

```

% Correct for odd valued vectors %
if mod(N,2) == 0;
    t = (0:(1/fs):(T-(1/fs)))';
else
    t = (0:(1/fs):T)';
    xldotdot(numel(xldotdot)+1) = 0;
    N = N+1;
end

%Filter out noise floor
for n = 1:numel(xldotdot);
    if (abs(xldotdot(n)) < 0.022);
        xldotdot(n) = 0;
    else
        xldotdot(n) = xldotdot(n);
    end
end

%Zero Pad the data
ZeroPad = N + fs * 8;
t((N+1):ZeroPad) = ((N+1)/fs:(1/fs):(ZeroPad / fs));
xldotdot((N+1):ZeroPad) = zeros();

%Extract Plot titles from file
[A, count] = sscanf(File, '%c');
if (count == 22);
    samp = File(1:9);
elseif (count == 21);
    samp = File(1:8);
else
    samp = File(1:10);
end

%Plot Acceleration Data
sampl = strcat(samp, ' Time History');
figure
plot(t, xldotdot)
title(sampl)
xlabel('Time (s)')
ylabel('Acceleration (cm/s^2)')

% Perform FFT of data
X1 = fft(xldotdot);

%Plot Magnitude Spectrum
X1_mag = abs(X1);

figure
semilogy(X1_mag)
title('Channel 1')
xlabel('Bins')
ylabel('Magnitude')

%Generate Single Sided Frequency Plot

```

```
Npad = ZeroPad;
Xlds = abs(X1 / Npad);

Xlss = Xlds(1:Npad / 2 + 1);
Xlss(2:end - 1) = 2 * Xlss(2:end - 1);
f = (fs * (0:(Npad / 2)) / Npad)';

figure
plot(f, Xlss)
title(samp)
xlabel('Frequency (Hz)')
ylabel('Amplitude')
```